THE STABILITY OF INTERFACES IN FLUIDISED BEDS

A thesis submitted for the Degree

of DOCTOR OF PHILOSOPHY in the Faculty

of Engineering of the University of London

by

Patrick Charles UPSON, BSc (Eng); ACGI

Department of Chemical Engineering
and Chemical Technology
City and Guilds College
Imperial College
London SW7

November 1973

ABSTRACT

Theory is developed for the stability of a plane horizontal interface in a fluidised bed. It is found that the configuration with the fluidised phase uppermost is always unstable to small perturbations. The results of this analysis are used to derive a criterion for bubble stability, which is based on the relative magnitudes of the growth rate of the disturbance and the speed at which the disturbance would be swept away around the bubble. Experimental evidence is provided for this theory which predicts a much greater range of stability for bubbles in gas fluidised systems than in liquid fluidised beds. The experimental results are in qualitative agreement with the predictions of the theory.

Theory is developed for the stability of a plane vertical interface in a fluidised bed. It is found that the interface is always stable when the homogeneous phase is not fluidised (spouting), but that the interface is only stable if the upward velocity in the particle-free fluid exceeds a given limit when the homogeneous phase is well fluidised (channelling). This limiting superficial velocity is much greater in gas fluidised systems than in liquid fluidised beds. The theory is tested experimentally and the experimental results are in quantitative and qualitative agreement with the predictions of the theory.

The behaviour of liquid fluidised beds following a stepwise increase in fluidising velocity has also been studied. It is shown that the interface formed between two regions of different voidage fraction is unstable. Theory developed by Layzer for Taylor instabilities which lead to slugging adequately describes the behaviour and development of these instabilities, provided allowance is made for the effects of density difference and geometry.

TO HELEN

ACKNOWLEDGEMENTS

I would like to express my sincere thanks to Dr D L Pyle for his advice and encouragement throughout the course of this work.

In addition, I am grateful to Dr D N Sutherland for his valuable encouragement during Dr Pyle's absence, and to Mr W Meneer and Mr J D Roche for their technical advice and assistance on the subject of photography.

I would like to thank the Science Research Council for providing the necessary financial support.

Finally, I would like to thank all my friends for making my stay at Imperial College more enjoyable, and to acknowledge the debt to my wife, who has given every encouragement and support throughout my studies.

P C UPSON

CONTENTS

		Page No
ABSTRACT		
INTRODUCTION		
CHAPTER 1:	A REVIEW OF THE STABILITY OF FLUIDISED BEDS	1
	1.1 Equations of Motion for the Homogeneous Phase	1
	1.2 Solution of the Equations of Motion	6
	1.3 Bubble Stability in Fluidised Systems	15
	1.4 Maximum and Minimum Stable Bubble Size	19
	1.5 Bubble Stability in Viscous Fluids (Liquids)	21
CHAPTER 2:	THE STABILITY OF A PLANE HORIZONTAL INTERFACE IN A FLUIDISED BED	23
SECTION 2A:	THEORY	23
	2A.1 Equations of Motion	23
	2A.2 General Solution to the Equations of Motion	29
	2A.3 Boundary Conditions	30
	2A.3.1 Boundary Conditions; Fluidised Bed Uppermost	31
	2A.3.2 Boundary Conditions; Support Fluid Uppermost	38
	2A.4 Solution Using the Proposed Sets of Boundary Conditions	41
	2A.4.1 Solution; Fluidised Phase Uppermost	41
	2A.4.2 Solution; Support Fluid Uppermost	41
	2A.4.3 Physical Parameters	42
SECTION 2B:	PREDICTIONS FROM THE THEORY	43
	2B.1 Support Fluid Uppermost	43
	2B.2 Fluidised Phase Uppermost	43

		Page No
SECTION 2C:	COMPARISON WITH THE STABILITY OF THE HOMOGENEOUS PHASE	61
SECTION 2D:	DIMENSIONAL ANALYSIS	65
CHAPTER 3:	BUBBLE STABILITY	70
	3.1 A Theory for Bubble Splitting	70
	3.2 Comparison with Other Theories	72
	3.3 Experimental Study of Bubble Splitting	76
	3.4 Results and Discussion	79
CHAPTER 4:	STABILITY OF VERTICAL CHANNELS IN FLUIDISED BEDS	89
	4.1 Introduction	89
	4.2 Equations of Motion for Channelling and their Solution	92
	4.3 Boundary Conditions and the Solution Using these Boundary Conditions	94
	4.4 Predictions from the Theory	96
	4.5 Experimental Study of Channelling Behaviour	103
CHAPTER 5:	THE BEHAVIOUR OF LIQUID FLUIDISED BEDS FOLLOWING STEP-WISE CHANGES IN FLOW RATE	108
	5.1 Introduction	108
	5.2 Theory	109
	5.3 Experimental	113
	5.4 Observations, Results and Comparison with the Theory	113
	5.5 Conclusions	121
CHAPTER 6:	CONCLUSIONS AND SUGGESTIONS FOR FURTHER WORK	123
APPENDIX 1:	GENERAL SOLUTION TO THE EQUATIONS OF MOTION	125
APPENDIX 2:	SOLUTION USING THE PROPOSED SETS OF BOUNDARY CONDITIONS	127

Page No

A2.1 Horizontal Interface Between the Phases 127

A2.2 Vertical Interface Between the Phases 136

APPENDIX 3: COMPARISON WITH THE STABILITY OF THE STATE OF HOMOGENEOUS FLUIDISATION 139

APPENDIX 4: FREQUENCY OF TWO-DIMENSIONAL BUBBLE FORMATION FROM AN ORIFICE 143

NOTATION 144

REFERENCES 147

LIST OF TABLES

		Page No
Table 1:	Features of the Proposed Equations of Motion	5
Table 2:	Features of the Proposed Solution of the Unsteady Equations of Motion	14
Table 3:	Features of the Sets of Boundary Conditions Investigated	40
Table 4:	Stability of Various Fluidised Systems	60
Table 5:	Comparison with the Stability of the State of Uniform Fluidisation	64
Table 6:	Comparison of the Criteria Proposed for the Prediction of the Stability of Fluidised Systems	69
Table 7:	a Bubble Stability for Glass/Air Systems	
	b Physical Parameters of the Sand/Air System	78
Table 8:	Limiting Values of the Superficial Channel Velocity, above which the Channel Wall is Stable	102
Table 9:	Frequency of Bubble Formation for 100 Micron Diameter Particles Fluidised with Air	108

LIST OF FIGURES

		Page No
Figure 1:	Wavelike Disturbance on a Plane Horizontal Surface	32
Figure 2:	Growth Rate of a Surface Disturbance as a Function of Wave Number. Boundary Condition Set 1	44
Figure 3:	Growth Rate of a Surface Disturbance as a Function of Wave Number. Boundary Condition Set 2.	45
Figure 4:	Growth Rate of a Surface Disturbance as a Function of Wave Number. Boundary Condition Set 3	46
Figure 5:	Growth Rate of a Surface Disturbance as a Function of Wave Number. Boundary Condition Set 4	47
Figure 6:	Growth Rate of a Surface Disturbance as a Function of Wave Number. Boundary Condition Set 5	48
Figure 7:	Growth Rate of a Surface Disturbance as a Function of Wave Number. Boundary Condition Set 6	49
Figure 8:	Growth Rate of a Surface Disturbance as a Function of Wave Number. 1010 Micron Diameter Glass/Water	52
Figure 9:	Growth Rate of a Surface Disturbance as a Function of Wave Number. 1280 Micron Diameter Lead/Water	53
Figure 10:	Growth Rate of a Surface Disturbance as a Function of Wave Number. 100 Micron Diameter Glass/Air	54
Figure 11:	Growth Rate of a Surface Disturbance as a Function of Wave Number, 210 Micron Diameter Glass/Air	55
Figure 12:	Growth Rate of a Surface Disturbance ás a Function of Wave Number. 280 Micron Diameter Glass/Air	56
Figure 13:	Growth Rate of a Surface Disturbance as a Function of Wave Number. 490 Micron Diameter Glass/Air	57
Figure 14:	Stable Bubble Diameters; Comparison of Regions of Stability for Gas- and Liquid-Fluidised Systems, Using Boundary Condition Set 2	73
Figure 15:	Stable Bubble Diameters; Comparison of Regions of Stability for Gas- and Liquid-Fluidised Systems, Using Boundary Condition Set 6	74
Figure 16:	Fingering in a Bubble in a Gas Fluidised Bed	80
Figure 17:	Splitting Caused by Fingering in a Gas Fluidised Bed	81
Figure 18:	Behaviour of a Bubble in a Water Fluidised Bed	82
Figure 19:	Behaviour of a Bubble in a Water Fluidised Bed	83
Figure 20:	Behaviour of a Bubble in a Water Fluidised Bed	84

Page No

Figure 21: Experimental Values of the Frequency of Bubble Splitting 86

Figure 22: Channel Initiator and Wavelike Disturbance on a Plane Vertical Boundary 93

Figure 23: Growth Rate of a Surface Disturbance on a Vertical Boundary as a Function of Wave Number. Boundary Condition Set 2 98

Figure 24: Growth Rate of a Surface Disturbance on a Vertical Boundary as a Function of Wave Number. Boundary Condition Set 6 99

Figure 25: Behaviour of an Unstable Channel in a Gas Fluidised Bed 104

Figure 26: Behaviour of a Stable Channel in Gas and Liquid Fluidised Beds 106

Figure 27: Formation and Growth of Voidage Fraction Disturbance in a Liquid Fluidised Bed Following a Step Increase in Liquid Flow Rate 115

Figure 28: Growth of Voidage Fraction Disturbance: Comparison of Experimental and Theoretical Froude Numbers. 100 Micron Diameter Glass/Water 117

Figure 29: Growth of Voidage Fraction Disturbance: Comparison of Experimental and Theoretical Froude Numbers. 280 Micron Diameter Glass/Water 118

Figure 30: Growth of Voidage Fraction Disturbance: Comparison of Experimental and Theoretical Froude Numbers. 490 Micron Diameter Glass/Water. 119

Figure 31: Slug Velocity: Comparison of Time Averaged Results and Results from Cine Photography 121

INTRODUCTION

Fluidisation is now used industrially in many different chemical and metallurgical processes and, although the number of applications is still increasing, our understanding of the phenomena involved is still inadequate. For example, in the case of a fluidised chemical reactor, it appears that the size and frequency of bubbles have some effect on the temperature, gas contacting and conversion, but as yet, no theoretical approach has been developed which adequately describes from first principles the way in which bubbles grow from small disturbances or the manner in which other factors, such as bubble splitting, limit the size of bubbles in a large fluidised bed. It is clear that the questions of bubble formation and splitting involve problems of hydrodynamical stability.

This work was undertaken to extend previous investigations into the effect of the physical parameters involved on the stability of fluidised beds and in particular, to consider the behaviour of different configurations of the interface between the fluidising fluid and fluidised phase. The purpose of these analyses is to discuss the differences between the states of bubbling and non-bubbling fluidisation, and to predict the way in which well observed phenomena, such as channel formation or bubble splitting, initiate or limit bubbling in fluidised beds.

Before discussing the formulation and analysis of the situations in this work it is appropriate to review briefly earlier studies of the stability of fluidised beds and other problems in hydrodynamic stability which bear upon the present work.

CHAPTER 1: A REVIEW OF THE STABILITY OF FLUIDISED BEDS

1.1 Equations of Motion for the Homogeneous Phase

In the past decade a great deal of interest has been shown in the stability of the state of uniform fluidisation with reference to the behaviour of the fluidised system and in particular to bubble formation. A number of theoretical analyses have been presented (van Deemter and van der Laan (1961); Hinze (1962); Jackson (1963); Pigford and Baron (1965); Murray (1965,1966); Anderson and Jackson (1967, 1968, 1969); Molerus (1967); Ruckenstein and Tzeculescu (1967) and Jones (1970)), the results of which, although agreeing qualitatively, show a distinct lack of quantitative agreement. An examination of these analyses shows that this is due to differences in the linearisation techniques employed and a general disagreement over the terms to be included in the momentum equations.

The general form of the momentum equations is not in dispute, and consists of equations of motion for two interacting continua, one corresponding to the interstitial fluid and the other to the particle phase. For each phase, the equation of motion is defined by a balance between the acceleration and momentum of that phase, gravitational forces, viscous and pressure stress forces and the forces of interaction between the two phases (which include such terms as viscous drag, bouyancy and additional mass acceleration). This leads to equations which are comparable to typical hydrodynamic equations of motion (ie Navier-Stokes) but with additional terms to account for the interaction between the two phases.

The main differences of opinion occur in the choice of the fluid-particle interaction forces and on the importance of the additional

mass acceleration and particulate shearing stress terms.

In principle, the equations of motion of a system of particles suspended in a fluid could be written in terms of the initial state of motion, the boundary conditions, the Navier-Stokes equation, to be satisfied at each point of the fluid, and Newtonian equations of motion for each particle. However, a typical fluidised system contains too many particles for this to be a practical possibility, so that a simplification must be made for the particle phase to be described in terms comparable to the continuum mechanics of a single fluid.

It is therefore convenient to replace the point mechanical variables by smoothed variables obtained by averaging over regions large compared with the interparticulate spacing but small in comparison to the complete system. The particle and fluid phases are thus defined by all the authors referred to above as if they were interpenetrating continua.

In one of the earliest attempts to formulate equations of motion of this type for fluidised systems, van Deemter and van der Laan developed formal, unsteady continuity and motion equations but did not propose specific forms for the fluid-particle interaction, or the fluid and particle shear stress forces. Hinze completed this work by suggesting specific forms for these terms, but his work does differ radically from all the others mentioned as he postulates a combined shear stress force based on a velocity, W, averaged over the whole system.

So that $W = \varepsilon U + (1 - \varepsilon)V$

Where U, V are the fluid and particle velocities and ϵ is the voidage fraction of the system. Hinze also includes an additional mass force in the equations of motion for the fluid, but omits the equal and opposite force in the equations for the particle phase. As Murray (1965) points out, this cannot be correct as it contradicts Newton's third law.

The first published set of unsteady equations of motion for the homogeneous phase of a fluidised bed, together with solutions used to estimate the stability of the bed was suggested by Jackson (1963). These describing equations however, have limited applicability due to the omission of the particulate shear stress forces, which, as Jackson (1970) himself points out, Schugerl et al (1961) have shown to be significant in gas fluidised systems.

This omission in Jackson's equations of motion was corrected by Pigford and Baron (1965) who also solved these equations to show the effect of the particle phase viscosity (ie particulate shear stress forces) on the stability of the bed.

Murray (1965) proposed a much more complete form of the unsteady continuum equations, adding energy balances to the momentum balances, in which he included the particulate shear stress and compressibility effects. He derived new approximations for the prediction of the particle phase shear and bulk viscosities. These equations were then used in a study of the stability of the homogeneous phase, the propagation of surface waves, and to bubble motion (1965a). Murray (1966) later improved his earlier momentum equations, deriving a new form for the fluid particle interaction forces. He also argued that the particle collision (pressure) forces, although probably insignificant,

can be interpreted as a bulk viscosity term, thus reducing the number of unknowns and eliminating the need to estimate the size of the particle pressure forces.

The most complete set of equations that have been proposed to date are due to Anderson and Jackson (1967). All the other workers have assumed that the unsteady equations of motion may be written in terms of variables which are smoothed averages, taken over an area large compared to the interparticulate spacing but small in comparison to the complete system. Anderson and Jackson formally derived their equations of motion from the corresponding equations for the variables at each point in the system, by taking local averages of these equations and translating them into a set of equations in terms of the smoothed, local averaged variables.

They show that all the other derived sets of equations referred to above reduce to special cases of their equations. A summary of the more important features of the equations as proposed is shown in Table 1.

However, Anderson and Jackson, in presenting such a complete set of motion equations, introduce further difficulties, since, as Murray (1966) also pointed out, a complete set of equations must include several terms of unknown magnitude and importance. These include, for example, the local mean pressure in the particle phase, the virtual (additional) mass acceleration and the drag forces on the particle phase. Thus, although the equations derived by Anderson and Jackson apparently describe the system completely, the fact that the unknown coefficients have to be approximated to somewhat reduces the advantages which this set of equations should hold over the earlier approximations.

TABLE 1

Features of the Proposed Equations of Motion

Terms in equations of motion / Authors	Particulate Stress	Fluid Stress	Virtual Mass	Fluid-Particle Interaction
van Deemter & van der Laan	Included but not specifically defined		Included but not specifically defined	
Hinze	No individual particle or fluid stresses, but a combined one, based on a velocity averaged over the whole system		- ve in fluid phase only	Included, but not specifically defined
Jackson	zero	Pressure stress only	+ ve in particle phase - ve in fluid phase	$\beta(\epsilon)\ (U_i - V_i)$
Pigford & Baron	Viscous stress only	Pressure stress only	Not included	$\frac{\mu}{K}(U_i - V_i)$
Murray (1966)	Viscous stress only	Pressure and viscous stress	+ ve in particle phase - ve in fluid phase	$A(U_i - V_i)$
Anderson & Jackson (1967)	Pressure, viscous and 'Reynold's' (turbulent) stresses	Pressure, viscous and 'Reynold's' (turbulent) stresses	+ ve in particle phase - ve in fluid phase	$\beta(\epsilon)\ (U_i - V_i)$
This work	Viscous stress only	Pressure and viscous stresses	+ ve in particle phase - ve in fluid phase	$\beta(\epsilon)\ (U_i - V_i)$

Where, U_i, V_i = fluid and particle velocities.

NB The virtual mass terms and coefficients in the fluid-particle interaction force ($\beta(\epsilon)$, $\frac{\mu}{K}$, A) are defined in different ways by each author.

1.2 Solution of the Equations of Motion

The simplest solution of all these sets of equations is the steady state solution, representing uniform fluidisation. Under these conditions the local (averaged) particle velocity is everywhere zero, the local (averaged) fluid velocity is constant and acts only in the vertical direction, and the voidage is constant throughout the system.

This simplification satisfies the continuity equations and reduces the equations of motion to a balance between the drag forces on the particles and their bouyant weight, together with a balance between the drag forces, the fluid pressure forces and gravitational forces, which can be used to define the pressure drop in a fluidised system.

The stability of this state of uniform fluidisation to small disturbances can then be determined by normal perturbation techniques. That is, a small disturbance is imposed on the steady state solution by perturbing the variables, and the behaviour of this disturbance is used to predict the stability of the system. If the disturbed variable grows with time, the system is assumed unstable, if it decays with time, the system is assumed stable.

Consider any variable, say U, to be composed of a steady value, U_o, which satisfies the steady state solution, and a continuous perturbation variable, $\hat{U}$, which is small in comparison with U_o.

ie $U = U_o + \hat{U}$

Casting all the variables into this form, substitution into the continuity equations and equations of motion, and subtraction of the steady state solutions, gives the equations governing the perturbation variables.

As these variables are, by definition, small in comparison with the steady state solutions, all terms of second or higher order in perturbation variables can be neglected.

Thus, the non-linear equations of motion may be reduced to linear, partial differential equations in terms of the perturbation variables.

A plane wave solution of these linearised equations of motion is sought, and an exponential time dependence which is common to all variables is assumed, so that a typical variable has the form:

$U = A \exp(Kx + Ky + nt)$

Where A = a constant associated with that variable.

K = the wave number of the solution, where the disturbance wavelength, $\lambda = 2\pi/K$

and n = the growth rate, where positive values of n correspond to the unstable solution, and negative values of n correspond to the stable solution.

Casting all the perturbation variables into this form and substituting into the governing equations, gives a set of simultaneous, linear equations; the non-trivial solution of which is that the determinant of the matrix of coefficients vanishes. Another, simpler method of solution is by the elimination of variables from the set of simultaneous equations; this method was used in all the previous work mentioned here.

In this way, a relationship between the growth rate, n, wave number, K, and the physical system parameters is achieved; if this solution reveals no positive (or zero) growth rate for any positive wave number, all disturbances will decay with time, hence the system is

stable. Any positive growth rate for positive wave numbers will show an unstable system.

Jackson (1963) used the above method to solve his equations of motion, and concluded that the uniform state of fluidisation is always unstable. By comparing the growth rate, at a given dimensionless wave number, for the different fluidised systems investigated by Wilhelm and Kwauk (1948), he showed that all fluidised systems are unstable (+ve growth rate) but that the growth rate was smaller in water fluidised systems than in gas fluidised systems. However, this solution gives an increasing growth rate with wave number (decreasing wavelength) which would indicate that as the disturbance wavelength approaches zero, the growth rate approaches infinity which is clearly untenable, as this would provoke explosive situations. It must be noted that, as the disturbance wavelength approaches the particle diameter (from above) the solution might be expected to break down, as the assumption that the particle phase is a continuous fluid will no longer apply. Pigford and Baron (1965) show that this behaviour at large wave numbers is due to Jackson's omission of particle stress terms. Using a similar solution to Jackson with improved equations of motion, Pigford and Baron show that the effect of particle viscosity is to reduce the growth rate at large wave number, in such a way as to give zero growth rate as the wavelength tends to zero.

Thus, for any given system, there is a maximum growth rate and a corresponding dominant wavelength. (ie In any physical system, which will produce disturbances over the whole range of wavelengths, that disturbance which grows most rapidly will become the dominant one). However, at the time, the available data on the viscosity

of the particulate phase was limited and Pigford and Baron did not have enough accurate data to calculate the growth rate for any specific systems.

Murray (1965), again using this method of solution, showed that all systems are unstable to internal disturbances, and that surface waves are quickly damped out, but made no attempt to calculate the growth rates for specific systems.

Molerus (1967) used the equations of motion derived by Hinze (1962) to provide stability charts for fluidised systems. He linearised the equations in the normal manner, and used the method of elimination of variables from the differential equations at this stage to produce one second order, linear, partial differential equation for the perturbed voidage variable, $\epsilon(X, t)$.

By seeking the typical plane wave solution for this variable, but with a general time dependence, $T(t)$, this equation was transformed into the standard form of Mathieu's differential equation, from which Molerus was able to produce stability charts for any given system. These charts do compare qualitatively with known experimental behaviour, but, once again, it would appear that more data on Molerus' unknown coefficients is needed before quantitative results could be obtained.

Using equations similar to those proposed by Pigford and Baron (the fluid-particle interaction force is replaced by an expression for the drag force on an isolated sphere in flow through a pipe), Ruckenstein and Tzeculescu (1967) used an analogue computer to solve the non-linear equations of motion.

The equations of motion were transformed into one non-linear differential equation in terms of the voidage variable. The unknown parameters were selected to give a solution which was a periodical function of time. Although their results show that all fluidised systems are unstable to some degree, they do not make comparisons with experimental results as, once again, some of the assumed values of their unknown parameters are uncertain.

Anderson and Jackson's (1968) solution of their equations of motion follows the general method outlined here. They determined the effect of the uncertain system parameters (particle phase shear and bulk viscosity, particle collision pressure, virtual mass coefficient and drag coefficient for water fluidised systems and particle shear and bulk viscosity for air fluidised systems), on the relationship between the disturbance wave number and growth rate.

Their theoretical results agree qualitatively with those of other authors: that is, that all fluidised systems are unstable, and gas fluidised systems more so than water fluidised systems; the particle phase viscosity decreases the growth rate at large wave number, so that there exists a dominant disturbance. Their analysis also shows that the interparticulate pressure tends to decrease the growth rate, but is not capable of inducing a maximum in the growth rate - wave number relationship on its own.

To test their analysis experimentally, Anderson and Jackson (1969) investigated the rate of growth, propagation velocity and dominant wavelength of naturally occurring voidage disturbances in water fluidised beds using a light transmission technique. They obtained encouraging agreement between theory and experiment, bearing in mind

the uncertainty in the values of some of the parameters used in their theoretical analysis, for although in individual cases the accuracy of agreement between theory and experiment was not high, the general variation in observed properties was correctly accounted for.

Murray's (1966) equations of motion were solved in a similar way to that described above by Jones (1970) (denoted by Jones (1) in Table 2). He found that a fluidised bed was generally unstable to disturbances, but that under certain conditions, such as gas fluidisation of very fine particles, stable solutions were possible. He considered the effect of the system parameters on the growth rate of disturbances and found that one, the particulate stress, had a stabilising effect. This, of course, concurs with the findings of other workers that the particulate stress force decreases the growth rate as the wave number increases. Jones also approached the problem of stability in a rather different way (denoted by Jones (2) in Table 2); by considering a force balance on an individual particle, he obtained a non-linear differential equation in terms of the particle displacement and was thus able to determine the effect of the non-linearity of this equation on the particle oscillating frequency. He found that the non-linearity increased with decreasing particle size in gas fluidisation, and thus explained the qualitative aspects of the bubbling frequency of fluidised beds: that is, the variation with particle diameter and fluidising gas velocity.

Although the oscillation frequency given by this approach compared well with bubble frequencies recorded experimentally, Jones did not attempt to map out the stability limits of a system in terms of its parameters, as the accuracy of some of the parameters used was no

greater than an order of magnitude.

By solving his non-linear differential equation of particle motion on an analogue computer, Jones was also able to show that an instability could be triggered off either by increasing the damping coefficient, or by increasing the amplitude of particle oscillation, and he therefore associated this behaviour with the eventual onset of bubbling in a fluidised system.

The results of all these stability analyses, the one reported here being no exception, have the same limited application. The greatest danger inherent in the application of the linearised equations, used in one form or another in the work mentioned, is to infer conclusions about the final behaviour of a disturbed system - which necessarily includes non-linear effects - from an analysis which holds true only for infinitesimally small disturbances. This also implies that comparison between theoretical results and experimental results can be accurately made only during the initial growth, whilst the disturbance is still infinitesimally small, and, outside this range can be no more than tentative.

Table 2 summarises the main features of these proposed solutions. It can be seen that the predictions of all the authors agree qualitatively with the known experimental behaviour of fluidised systems. The only authors to achieve even poor quantitative agreement were Anderson and Jackson, whose experimental results were recorded for small disturbances in water fluidised beds.

It must be noted that this type of theory is very difficult to test experimentally. As pointed out above, the analysis is only valid for

infinitesimally small disturbances, whereas, in any experimental system the disturbances recorded are necessarily of finite size. There is no guarantee that disturbances of finite size continue to grow at the same rate as they did when infintesimally small, in any fluidised system.

In general, with, it would seem, only a few exceptions, the homogeneous phase of a fluidised system is unstable to small disturbances in the particle density. The growth rate of these disturbances being an order of magnitude larger in air fluidised systems than in the equivalent water fluidised system.

TABLE 2

Features of the Proposed Solutions of the Unsteady Equations of Motion

Author	Method of Linearisation	Stability of Fluidised Systems	Effect of Particle Stress Forces	Comparison with Experiments
Jackson (1963)	Perturbation techniques	All fluidised systems always unstable	Not included	Qualitative agreement
Pigford & Baron (1965)	Perturbation techniques	All fluidised systems always unstable	Decreases growth rate as wave number increases	Not made, as accurate data on all coefficients was not available
Murray (1965)	Perturbation techniques	All fluidised systems always unstable	Not calculated	Not made
Molerus (1967)	Perturbation techniques	Stability depends on system parameters. Some systems stable, some unstable.	Not included as such	Qualitative agreement
Ruckenstein & Tzeculescu (1967)	Not linearised	All fluidised systems always unstable	Not calculated	Qualitative agreement for gas fluidisation. No comparison made for water fluidisation
Anderson & Jackson (1968)(1969)	Perturbation techniques	All fluidised systems always unstable	Decreases growth rate as wave number increases	Qualitative agreement with poor quantitative agreement for water fluidised beds
Jones (1) (1970)	Perturbation techniques	Generally unstable Some cases, such as fine particles fluidised with air are always stable	Stabilising effect	Qualitative agreement
Jones (2) (1970)	Not linearised	All fluidised systems always unstable	Decreasing force could trigger off instability	Qualitative agreement Quantitative agreement for bubble frequencies of gas fluidised systems.

1.3 Bubble Stability in Fluidised Systems

Observation of the motion of bubbles in both air and water fluidised systems (Rowe (1971); Clift and Grace (1972)) suggests that bubbles are unstable to disturbances on the bubble roof. These disturbances are seen to grow rapidly downwards into the bubble so that some actually split the bubble in two.

The study of the stability of the homogeneous phase of a fluidised system reveals only the initial behaviour of small disturbances. It is generally assumed that these disturbances in the density of the particulate phase continue to grow, eventually becoming, in aggregatively fluidised systems, large enough to appear as bubbles, or voids. However, as the theoretical studies discussed in section 1.2 hold only for infinitesimally small disturbances, no information can be obtained from them about the behaviour of the final, fully-grown bubble.

The theories which have been derived for the motion of a bubble in a fluidised bed (Davidson (1961); Jackson (1963a); Murray (1965a)) are summarised by Jackson (1969), and Rowe (1971). Jackson and Murray started from the steady state version of the equations reported in section 1.1, whilst Davidson assumed that Darcy's law also related the pressure gradient and relative velocities in a fluidised system at low Reynolds number. The distribution of gas flow through the bubble was derived, which, for an assumed particle motion, maintains the bubble surface in its assumed form (circular, in 2-dimensions). The gas percolation across the interface adjusts itself so as to exactly balance the particle momentum. Thus, the gas flow distribution for a stable (circular) bubble has been derived, but no attempt has been

made to predict the rate of growth of instabilities on the bubble surface.

The problem of bubble stability can therefore be approached by analysing the stability to small disturbances of the bubble surface which exists as an interface between a particle free fluid and a fluid-particle suspension. In a complete consideration of the stability of the bubble surface, the curvature of the surface and the velocity and voidage profiles in all phases in the region of this surface must be considered. However, this would lead to a very complex analysis, the solution of which would still only be approximate as many of the parameters would be uncertain. It is therefore thought that as much useful information on the stability of bubbles in fluidised systems could be obtained from the study of a simpler model; for example, for a bubble large in comparison with the horizontal scale of the solution, the roof of the bubble could be approximated to a plane horizontal interface.

The problem of the stability of an initial horizontal interface between two superposed fluids is well known and is generally referred to as the Taylor stability problem, after Taylor's initial work in this field (1950). He studied the behaviour of two inviscid fluids of infinite extent, meeting at a plane horizontal interface. The solution of the linearised equations of motion for both fluids, following a sinusoidal perturbation in space of this interface, was studied and the system found to be unstable when the acceleration force is directed from the more dense to the less dense medium; the rate of growth of the disturbance being proportional to $\sqrt{\frac{\rho_2 - \rho_1}{\rho_2 + \rho_1}}$

Where ρ = density

1 = less dense fluid

2 = more dense fluid

This work was extended by Bellman and Pennington (1954) to include the influences of viscosity and surface tension on the solution, and they showed that both of these variables exert a stabilising influence on initial disturbances of small wavelength. They demonstrated that the role of viscosity is to decrease the rate of growth of the disturbance over the corresponding inviscid solution although the instability is never eliminated completely; they also found that, besides decreasing the growth rate of the disturbance, surface tension forces can completely eliminate the growth of disturbances with a wave length smaller than some critical value.

This analysis was extended to the problem of the stability of a plane horizontal interface in a fluidised bed by Rice and Wilhelm (1958). To facilitate this, they made the approximation that the interacting fluid and particle phases in the bed could be described as a single Newtonian fluid with mean density and viscosity, obeying the Navier-Stokes equations. They linearised their describing equations by assuming the non-linear terms to be negligible, but did also show that linearisation by perturbation techniques gave similar results under certain conditions, viz zero slip velocity between the two phases. Unfortunately, at the time of their analysis little information was available on the viscosity of the bed phase, which has a most important effect on the solution, so that their results could only be tentatively applied to explaining the differences between bubbling and non-bubbling systems.

By treating the particles and interstitial fluid as one phase and the particle free fluid as another discrete phase, Rice and Wilhelm effectively neglected the percolation of fluid across the boundary between these two regions. It therefore follows that their solution is valid only where the momentum of the fluid percolating across the boundary is negligible.

Since this early analysis, considerable advances have been made towards setting up the describing equations for the motion of both the fluid and particle bed phases (see section 1.1 above), and the present work was therefore undertaken to investigate the problem of stability of an interface in a fluidised bed, by extending the Rice and Wilhelm analysis to incorporate two interacting bed phases. A similar, unpublished analysis by Clift, Grace and Weber (1973) has recently been brought to notice. Starting from a similar set of equations of motion (yet again, there are small differences in the choice of particle stress and fluid-particle interaction terms) and linearising in a manner similar to that described in section 1.2, they arrive at a solution to these equations not too far removed from the one presented here. The reaction of a given system to a small perturbation at a plane horizontal boundary is then found by substituting this solution into an appropriate set of boundary conditions, and the growth rate of the imposed perturbation used to predict the incidence of bubble splitting in fluidised situations.

In general terms, their work shows that, if the momentum of the interstitial fluid is neglected, Rice and Wilhelm's solution is correct for gas fluidisation, but only approximately so for systems fluidised by liquids. The results of their work and the differences

between their analysis and the one presented here will be discussed in later sections.

This type of analysis of the stability of a plane horizontal interface in a fluidised bed to small sinusoidal disturbances can be applied to the stability of a bubble roof with the following limitations:

1 When the equations of motion are linearised by perturbation techniques the limitations of this technique must apply.

2 For the bubble roof to be approximated to by a flat plane, the bubble radius must be large in comparison with the wavelength of the imposed disturbance.

Provided these conditions are applicable, the analysis can be used to give a guide to the effect of the system parameters on the stability of bubbles in fluidised beds and the limitations on bubble growth thus imposed.

1.4 Maximum and Minimum Stable Bubble Size

Various workers have suggested that upper and lower limits on the bubble size do exist in practice.

Davidson, Harrison and de Kock (1961) based their theory of maximum bubble diameter on the rather tenuous assumption that the bubble disintegrates by particles being dragged in through the wake. This led to the conclusion that the bubble is stable until the fluid circulation velocity inside the bubble exceeds the particle free fall velocity, at which point the void should fill with particles entrained from the wake. The only observations of this mode of bubble instability are by Davidson, Harrison and de Kock themselves, and, as Clift and Grace (1972) observed, this should only occur when

the method of injection imparts the wake with sufficient momentum for it to rise to the bubble roof.

However, on the basis of this assumption, Davidson et al were able to predict a maximum stable bubble diameter which is large for gas fluidised beds and relatively small for liquid fluidised beds. In other words, the theory suggests that most liquid fluidised systems appear to be particulate in nature because the largest possible stable bubble is so small that it is not visible.

For example: Glass beads of diameter 510 microns have as the maximum diameter, 0.2 cm when fluidised with water

and 250.0 cm when fluidised with air.

Although the model used appears very doubtful, the theory leads to an ordering of the stability of fluidised systems which agrees qualitatively both with the experimental evidence and also with Wilhelm and Kwauk's earlier classification. It appears that correct ordering of the stability of fluidised systems arises since the criterion proposed by Davidson et al, D/d_p, $\left(= \frac{\text{the max stable bubble diameter}}{\text{particle diameter}}\right)$, is proportional to the Froude number, $(Fr = U_o^2/d_p g)$, and the solid-fluid density ratio $\frac{(\rho_s - \rho_F)}{\rho_F}$ the constant of proportionality depending on the parameters of the system studied.

Wilhelm and Kwauk (1948) have shown that the Froude number is a reasonable measure of bed stability, and Romero and Johanson (1962) show that a combination of Fr, $\frac{(\rho_s - \rho_F)}{\rho_F}$ and a Reynold's number

gives an even better indication of stability than Fr alone (see section 2D)

Godard and Richardson (1969) investigated the possibility of a minimum stable bubble size. They found, by measurement of the collapse rate of small injected bubbles in a particulately fluidised bed, that such a minimum stable size does exist. Typically, for spherical acrylic resin particles, with surface mean diameter = 126 microns; density = 1.18 g/cc, fluidised with air at twice the minimum fluidising velocity, the minimum stable bubble volume is 0.08 cc (or, for a spherical bubble, the minimum stable diameter = 0.5 cm = 40 x particle diameter). Their results show that this minimum bubble size tends to increase as the background velocity decreases towards the minimum fluidising velocity, but for conclusive proof, determination of actual values and of the dependence on other bed variables, more experimental work in this field is necessary.

1.5 Bubble Stability in Viscous Fluids (Liquids)

Gas bubbles in liquids also exhibit a tendency towards instability as the bubble size increases: large individual bubbles deform and then fragment into smaller bubbles. According to Levich (1962), a rising bubble flattens out, pulsates and forms a thin film at the centre. The sudden rupture of this film fragments the bubble. Levich calculated, by balancing the dynamic pressure within the bubble with the capillary pressure (surface tension forces), the critical radius, a_{cr}, at which break up begins. Thus:

$$a_{cr} = \sqrt[3]{\frac{3.0}{k_f}} \quad \frac{\sigma_T}{U_b^2 \sqrt[3]{\rho' \rho^2}} \qquad \text{----------} \quad (1.1)$$

Where ρ = liquid density

ρ' = gas density

U_b = bubble velocity

k_f = numerical coefficient = 0.5

σ_T = surface tension

For a typical bubble of air in water, a_{cr} = 1.8 cm. It would be very misleading to compare the break-up of bubbles in fluidised beds with that of gas bubbles in liquids, especially as the mechanism in the latter case is wholly dependent on the liquid surface tension at the bubble boundary, a variable which is non-existent in the case of fluidised beds. A fluidised system has no actual surface tension because there is no discrete boundary between separate fluids; the boundary is merely the limit of the region of particles suspended in one continuous fluid.

However, using the principle of corresponding states, Furukawa and Ohmae (1958) have described an 'effective' surface tension at the boundary of bubbles in water fluidised beds, by comparison with the behaviour of bubbles in liquids of known surface tension. Their results for glass particles of diameter 300 to 400 microns, when used in equation (1.1) lead to a critical radius of order 1 cm for a system of these particles fluidised with water. This compares with a maximum diameter of 2-3 cm predicted by Davidson, Harrison and de Kock (1961) (see section 1.5), but comparison with experimental results would seem unprofitable, since Davidson et al base their maximum diameter on a doubtful model and bubble break-up in liquids is dependent on a force which is not present in fluidised situations, and takes place in a manner not observed in bubble break-up in fluidised beds.

CHAPTER 2: THE STABILITY OF A PLANE HORIZONTAL INTERFACE IN A FLUIDISED BED

SECTION 2A: THEORY

2A.1 Equations of Motion

As explained above, Rice and Wilhelm (1958) treated the fluidised system as a single fluid phase. A more correct treatment would be to consider the homogeneous phase of the fluidised bed not as one single fluid, but as two interacting continua: the 'particle phase' and the interstitial fluid phase. It is therefore necessary to define the equations of motion for these two phases. In sections 1.1 and 1.2, previous work in this field has been discussed, and in the light of the information available from this previous work, for the present analysis, a rather simple set of equations based on the original equations derived by Jackson (1963) and including particle stress and fluid-particle interaction terms similar to those proposed by Murray (1966), Anderson and Jackson (1967) and Jones (1970)* is employed in preference to the more complete set used by Anderson and Jackson (1967, 1968, 1969). The equations then include those physical terms which the other authors show to be the most important and are simple enough to lead to readily manageable mathematical analysis.

Following the general method of analysis used by Rice and Wilhelm, the study is undertaken of the stability of a horizontal plane surface in the fluidised bed to small wave-like disturbances. The equations of motion must therefore be written for three fluid phases: the homogeneous particle-free fluid phase, referred to by Rice and Wilhelm and hereafter as the 'support fluid'; and the two interacting phases in the fluidised region. All three phases are

*see page 23a.

The particle stress forces (equations 2A.4 and 2A.7) have the form suggested by Murray (1966) and Anderson and Jackson (1968, 1969). The components of this force are given by $\frac{\partial \sigma_{ik}}{\partial x_i}$ where σ_{ik} is the particle stress given by the above workers as

$$\sigma_{ik} = - \delta_{ik} P_i + \mu_p \left[\frac{\partial V_i}{\partial x_k} + \frac{\partial V_k}{\partial x_i} - \frac{2}{3} \delta_{ik} \operatorname{div} \underline{V} \right]$$

Equations 2A.4 and 2A.7 are derived by differentiating the normal stress ($i = k$) and the tangential stress ($i \neq k$) respectively, and the same definition of stress is used later in defining the boundary conditions at the interface (ie equations 2A.45 and 2A.46)

For the particle phase, $P = 0$, and thus,

$$\sigma_y = \sigma_{ii} = \mu_p \left[\frac{\partial V_x}{\partial x} + \frac{\partial V_x}{\partial x} - \frac{2}{3} \frac{\partial V_x}{\partial x} - \frac{2}{3} \frac{\partial V_y}{\partial y} \right]$$

$$\frac{\partial \sigma_y}{\partial y} = \mu_p \left[\frac{4}{3} \frac{\partial^2 V_x}{\partial x \partial y} - \frac{2}{3} \frac{\partial^2 V_y}{\partial y^2} \right].$$

Similarly, for the tangential stress, $\sigma_x = \sigma_{ik}$, $i \neq k$ and

$$\frac{\partial \sigma_x}{\partial x} = \mu_p \left[\frac{\partial^2 V_x}{\partial x \partial y} + \frac{\partial^2 V_y}{\partial x^2} \right]$$

as used in equations 2A.4 and 2A.7

assumed to be incompressible. Considering a plane disturbance, then, there are nine such equations in all, for a two-dimensional system. These equations of motion are:-

Continuity:

Particle phase:

$$-\frac{d\epsilon}{dt}+\frac{d[(1-\epsilon)V_x]}{dx}+\frac{d[(1-\epsilon)V_y]}{dy}=0 \qquad (2A.1)$$

Interstitial fluid:

$$\frac{d\epsilon}{dt}+\frac{d(\epsilon U_x)}{dx}+\frac{d(\epsilon U_y)}{dy}=0 \qquad (2A.2)$$

Support fluid:

$$\frac{dW_x}{dx}+\frac{dW_y}{dy}=0 \qquad (2A.3)$$

Momentum in x Direction:

Particle phase:

$$(1-\epsilon)\rho_p\left[\frac{dV_x}{dt}+V_x\frac{dV_x}{dx}+V_y\frac{dV_x}{dy}\right]-\epsilon\rho_F\left[\frac{dU_x}{dt}+U_x\frac{dU_x}{dx}+\frac{dU_x}{dy}\right]-$$

$$-\frac{\beta(U_x-V_x)}{(1-\epsilon)}+\mu_p\left[\frac{d^2V_x}{dxdy}+\frac{d^2V_y}{dx^2}\right]=0 \qquad (2A.4)$$

Interstitial fluid:

$$\epsilon\rho_F\left[\frac{dU_x}{dt}+U_x\frac{dU_x}{dx}+U_y\frac{dU_x}{dy}\right]+\frac{dP_2}{dx}+\beta(U_x-V_x)=0 \qquad (2A.5)$$

Support fluid:

$$\rho_F\left[\frac{dW_x}{dt}+W_x\frac{dW_x}{dx}+W_y\frac{dW_x}{dy}\right]+\frac{dP_3}{dx}-\mu_F\left[\frac{d^2W_x}{dx^2}+\frac{d^2W_x}{dy^2}\right]+F_x=0 \qquad (2A.6)$$

Momentum in y Direction:

Particle phase:

$$(1-\epsilon)\rho_P \left[\frac{dV_y}{dt} + V_x\frac{dV_y}{dx} + V_y\frac{dV_y}{dy} \right] - \epsilon\rho_F \left[\frac{dU_y}{dt} + U_x\frac{dU_y}{dx} + U_y\frac{dU_y}{dy} \right] -$$

$$- \frac{\beta(U_y-V_y)}{(1-\epsilon)} + \mu_p \left[\frac{4}{3}\frac{d^2V_x}{dxdy} - \frac{2}{3}\frac{d^2V_y}{dy^2} \right] + [(1-\epsilon)\rho_P - \epsilon\rho_F]g = 0 \text{ - - - } \quad (2A.7)$$

Interstitial fluid:

$$\epsilon\rho_F \left[\frac{dU_y}{dt} + U_x\frac{dU_y}{dx} + U_y\frac{dU_y}{dy} \right] + \frac{dP_2}{dy} + \beta(U_y-V_y) + \epsilon\rho_F g = 0 \text{ - - - - } \quad (2A.8)$$

Support fluid:

$$\rho_F \left[\frac{dW_y}{dt} + W_x\frac{dW_y}{dx} + W_y\frac{dW_y}{dy} \right] + \frac{dP_3}{dy} - \mu_F \left[\frac{d^2W_y}{dx^2} + \frac{d^2W_y}{dy^2} \right] + \rho_F g + F_y = 0$$

$$\text{- - - - } \quad (2A.9)$$

Where U is the velocity of the fluidising fluid

V is the velocity of the particle phase

W is the velocity of the support fluid

Subscripts x, y represent the horizontal and vertical directions

F, P represent the fluid and particle phase parameters

2, 3 represent the interstitial and support fluid

and the drag coefficient $\beta(\epsilon) = \dfrac{18\mu_F\, W(\epsilon)\,(1-\epsilon)}{d_p^2}$

with $W(\epsilon) = \epsilon^{-N}$

The exponent, N, is dependent on the Reynold's number as given by Richardson and Zaki (1958). In the following calculations, N is taken to be 4.7, the value for low Reynold's numbers.

These equations may be linearised in the manner described in section 1.2 by casting the variables in the form $U = \bar{U} + \hat{U}$

Where $\hat{U}$ is the perturbation variable

$\bar{U}$ is the steady state solution

with the following steady state solutions:

$$\bar{\epsilon} = \epsilon_o \quad \text{(2A.10a)}$$

$$\bar{V}_{x,y} = 0 \quad \text{(2A.10b)}$$

$$\bar{U}_x = 0 \quad \text{(2A.10c)}$$

$$\bar{U}_y = \frac{U_o}{\epsilon_o} \quad \text{(2A.10d)}$$

$$\bar{W}_x = 0 \quad \text{(2A.10e)}$$

$$\bar{W}_y = U_o \quad \text{(2A.10f)}$$

Where U_o = minimum fluidising velocity

ϵ_o = voidage fraction at minimum fluidisation

and the homogeneous phase is assumed to be at the conditions of minimum fluidisation. Linearisation of equations (2A.1) to (2A.9) by this method gives, where all variables are now perturbation variables:

$$-\frac{d\epsilon}{dt} + (1-\epsilon_o)\frac{dV_x}{dx} + (1-\epsilon_o)\frac{dV_y}{dy} = 0 \quad \text{(2A.11)}$$

$$\frac{d\epsilon}{dt} + \frac{U_o}{\epsilon_o}\frac{d\epsilon}{dy} + \epsilon_o\frac{dU_x}{dx} + \epsilon_o\frac{dU_y}{dy} = 0 \quad \text{(2A.12)}$$

$$\frac{dW_x}{dx} + \frac{dW_y}{dy} = 0 \quad \text{(2A.13)}$$

$$(1-\epsilon_o)\rho_P\frac{dV_x}{dt} - \epsilon_o\rho_F\left[\frac{dU_x}{dt} + \frac{U_o}{\epsilon_o}\frac{dU_x}{dy}\right] - \frac{18W(\epsilon_o)\mu_F}{d_p^2}(U_x - V_x) +$$

$$+ \mu_P\left[\frac{d^2V_x}{dxdy} + \frac{d^2V_y}{dx^2}\right] = 0 \quad \text{(2A.14)}$$

$$\epsilon_o\rho_F\left[\frac{dU_x}{dt} + \frac{U_o}{\epsilon_o}\frac{dU_x}{dy}\right] + \frac{dP_2}{dx} + \frac{18W(\epsilon_o)(1-\epsilon_o)\mu_F}{d_p^2}(U_x - V_x) = 0 \quad \text{(2A.15)}$$

$$\rho_F \left[\frac{dW_x}{dt} + U_o \frac{dW_x}{dy} \right] + \frac{dP_3}{dx} - \mu_F \left[\frac{d^2W_x}{dx^2} + \frac{d^2W_x}{dy^2} \right] = 0 \quad \text{- - -} \quad (2A.16)$$

$$(1-\epsilon_o)\rho_P \frac{dV_y}{dt} - \epsilon_o \rho_F \left[\frac{dU_y}{dt} + \frac{U_o}{\epsilon_o} \frac{dU_y}{dy} \right] - \frac{18W(\epsilon_o)^{\mu}_F}{d_p^2} \left[U_y - V_y - \frac{4.7U_o\epsilon}{\epsilon_o^2} \right] +$$

$$+ \mu_P \left[\frac{4}{3} \frac{d^2V_x}{dxdy} - \frac{2}{3} \frac{d^2V_y}{dy^2} \right] - g(\rho_P + \rho_F)\epsilon = 0 \quad \text{- - - - - - - -} \quad (2A.17)$$

$$\epsilon_o \rho_F \left[\frac{dU_y}{dt} + \frac{U_o}{\epsilon_o} \frac{dU_y}{dy} \right] + \frac{dP_2}{dy} + \frac{18W(\epsilon_o)^{\mu}_F}{d_p^2} \left[(U_y - V_y)(1-\epsilon_o) + \right.$$

$$\left. + (3.7 - \frac{4.7}{\epsilon_o}) \frac{U_o\epsilon}{\epsilon_o} \right] + \epsilon\rho_F g = 0 \quad \text{- - - - - - - - - - - - - - - -} \quad (2A.18)$$

$$\rho_F \left[\frac{dW_y}{dt} + U_o \frac{dW_y}{dy} \right] + \frac{dP_3}{dy} - \mu_F \left[\frac{d^2W_y}{dx^2} + \frac{d^2W_y}{dy^2} \right] = 0 \quad \text{- - - -} \quad (2A.19)$$

To cast these equations into a convenient dimensionless form, the following characteristic dimensions are chosen:

Length = $[d_p]$

Time = $\left[\frac{d_p}{U_o} \right]$

Pressure = $[\rho_P d_p g]$ - (2A.20)

Substitution of (2A.20) into (2A.11) to (2A.19) gives, where all the variables are now dimensionless, perturbation variables:

$$-\frac{d\epsilon}{dt} + (1-\epsilon_o) \frac{dV_x}{dx} + (1-\epsilon_o) \frac{dV_y}{dy} = 0 \quad \text{- - - - - - - - - - - - -} \quad (2A.21)$$

$$\frac{d\epsilon}{dt} + \frac{1}{\epsilon_o}\frac{d\epsilon}{dy} + \epsilon_o \frac{dU_x}{dx} + \epsilon_o \frac{dU_y}{dy} = 0 \qquad \text{(2A.22)}$$

$$\frac{dW_x}{dx} + \frac{dW_y}{dy} = 0 \qquad \text{(2A.23)}$$

$$(1-\epsilon_o)\frac{dV_x}{dt} - \epsilon_o\rho\left[\frac{dU_x}{dt} + \frac{1}{\epsilon_o}\frac{dU_x}{dy}\right] - \frac{18W(\epsilon_o)}{R_{ep}}(U_x-V_x) +$$

$$+ \frac{\mu}{Rep}\left[\frac{d^2V_x}{dxdy} + \frac{d^2V_y}{dx^2}\right] = 0 \qquad \text{(2A.24)}$$

$$\epsilon_o\rho\left[\frac{dU_x}{dt} + \frac{1}{\epsilon_o}\frac{dU_x}{dy}\right] + \frac{1}{Fr}\frac{dP_2}{dx} + \frac{18W(\epsilon_o)(1-\epsilon_o)}{R_{ep}}(U_x-V_x) = 0 \qquad \text{(2A.25)}$$

$$\rho\left[\frac{dW_x}{dt} + \frac{dW_x}{dy}\right] + \frac{1}{Fr}\frac{dP_3}{dx} - \frac{1}{R_{ep}}\left[\frac{d^2W_x}{dx^2} + \frac{d^2W_x}{dy^2}\right] = 0 \qquad \text{(2A.26)}$$

$$(1-\epsilon_o)\frac{dV_y}{dt} - \epsilon_o\rho\left[\frac{dU_y}{dt} + \frac{1}{\epsilon_o}\frac{dU_y}{dy}\right] - \frac{18W(\epsilon_o)}{R_{ep}}\left[U_y - V_y - \frac{4.7\epsilon}{\epsilon_o^2}\right] +$$

$$+ \frac{\mu}{Rep}\left[\frac{4}{3}\frac{d^2V_x}{dxdy} - \frac{2}{3}\frac{d^2V_y}{dy^2}\right] - \frac{(1+\rho)}{Fr}\epsilon = 0 \qquad \text{(2A.27)}$$

$$\epsilon_o\rho\left[\frac{dU_y}{dt} + \frac{1}{\epsilon_o}\frac{dU_y}{dy}\right] + \frac{1}{Fr}\frac{dP_2}{dy} + \frac{18W(\epsilon_o)}{R_{ep}}\left[(U_y-V_y)(1-\epsilon_o) +\right.$$

$$\left. + (3.7 - \frac{4.7}{\epsilon_o})\frac{\epsilon}{\epsilon_o}\right] + \frac{\rho\epsilon}{Fr} = 0 \qquad \text{(2A.28)}$$

$$\rho\left[\frac{dW_y}{dt} + \frac{dW_y}{dy}\right] + \frac{1}{Fr}\frac{dP_3}{dy} - \frac{1}{R_{ep}}\left[\frac{d^2W_y}{dx^2} + \frac{d^2W_y}{dy^2}\right] = 0 \qquad \text{(2A.29)}$$

Where the dimensionless groups are:

$R_{ep} = \frac{\rho_P d_p U_o}{\mu_F}$ - a type of Reynold's number

$Fr = \frac{U_o^2}{g d_p}$ - a Froude number

$\rho = \frac{\rho_F}{\rho_P}$

$\mu = \frac{\mu_P}{\mu_F}$

and it is also convenient to define a second Reynold's number

$Re_F = \frac{\rho_F d_P U_o}{\mu_F} = \rho R_{ep}$

2A.2 General Solution to the Equations of Motion

The solution of the set 2A.21 to 2A.29 to an arbitrary initial disturbance may be found by the methods of Fourier analysis, and accordingly a solution is sought to a small initial sinusoidal disturbance of the interface with wave number K. The variables are thus assumed to have a wave-like spatial variation with a common time dependence of the form e^{nt}, the sign and magnitude of n (the growth rate) then determine the quantitative and qualitative features of the resulting solution. If n is positive the resulting solution is unstable, any disturbance being magnified at the rate e^{nt}. Negative values of n correspond to solutions in which any disturbance is damped out.

A particular solution to the equations 2A.21 to 2A.29 is then:

$\epsilon = A \exp(-Ky + nt) \cos Kx$ - - - - - - - - - - - - - - - - - (2A.30)

$V_x = B \exp(-Ky + nt) \sin Kx$ - - - - - - - - - - - - - - - - - (2A.31)

$$V_y = B \exp(- K_y + nt) \cos kx - \frac{n}{K(1-\epsilon_o)} A \exp(- Ky + nt) \cos Kx$$

- - - - - - - (2A.32)

$$U_x = C \exp(- Ky + nt) \sin Kx + D \exp(-Ky + nt) \sin Kx - - - \quad (2A.33)$$

$$U_y = C \exp(- Ky + nt) \cos Kx + D \exp(- Ky + nt) \cos Kx +$$

$$+ \frac{(\epsilon_o n - K)}{\epsilon_o^2 K} A \exp(- Ky + nt) \cos Kx \quad - - - - - - - - - - \quad (2A.34)$$

$$P_2 = Fr \frac{n}{K} D \exp(- Ky + nt) \cos Kx \quad - - - - - - - - - - - - - \quad (2A.35)$$

$$W_x = E \exp(m_3 y + nt) \sin Kx + F \exp(Ky + nt) \sin Kx \quad - - - - \quad (2A.36)$$

$$Wy = \frac{- K}{m_3} E \exp(m_3 y + nt) \cos Kx - F \exp(Ky + nt) \cos Kx \quad - - \quad (2A.37)$$

$$P_3 = F_{r.}\rho \frac{(n + K)}{K} F \exp(Ky + nt) \cos Kx \quad - - - - - - - - - - \quad (2A.38)$$

Where m_3 is defined by:

$$m_3^2 - Re_F m_3 - Re_F n - K^2 = 0 \quad - - - - - - - - - - - - - - - \quad (2A.39)$$

and is, by definition, positive

Details of the derivation of the particular solution, equations (2A.30) to (2A.38) from a general solution are given in Appendix I.

2A.3 Boundary Conditions

A consistent set of interfacial boundary conditions must be imposed to relate the growth rate, n, of the disturbance on the plane horizontal interface to the wave number, K, and the physical parameters of the system.

As the solution governing the behaviour of the system parameters to a wave-like disturbance at the interface (equations 2A.30 to 2A.39) contains six unknowns (the constants A to F) six consistent and independent boundary conditions are required for the complete solution to obtain the growth rate.

The boundary is defined at $y = 0$, the perturbed boundary being $y = \eta\,(x,\ t)$. (See Figure 1 for definition of the co-ordinate system). By definition, the boundary is the limit of the particle phase, thus, the rate of change of the boundary with time, is

$$\frac{d\eta}{dt} = V_y \qquad (2A.40)$$

Integration of (2A.40) gives:

$$\eta = \frac{V_y}{n} = \frac{B}{n}\ \exp(-\ Ky + nt)\ \cos Kx - \frac{1}{K(1-\varepsilon_o)}\ A\ \exp(-Ky + nt)\ \cos Kx \qquad (2A.41)$$

for $V_y = 0$ at $t = 0$

The boundary conditions are then derived by taking material balances across the (slightly) deformed surface and by equating normal and tangential stresses on either side of the surface.

There are two possible configurations of the system with a horizontal boundary:

2A.3.1 Fluidised Phase Uppermost; eg roof of a bubble or base of the bed.

a Material Balance

Taking a material balance normal to the (slightly deformed) interface gives (cast into perturbation and

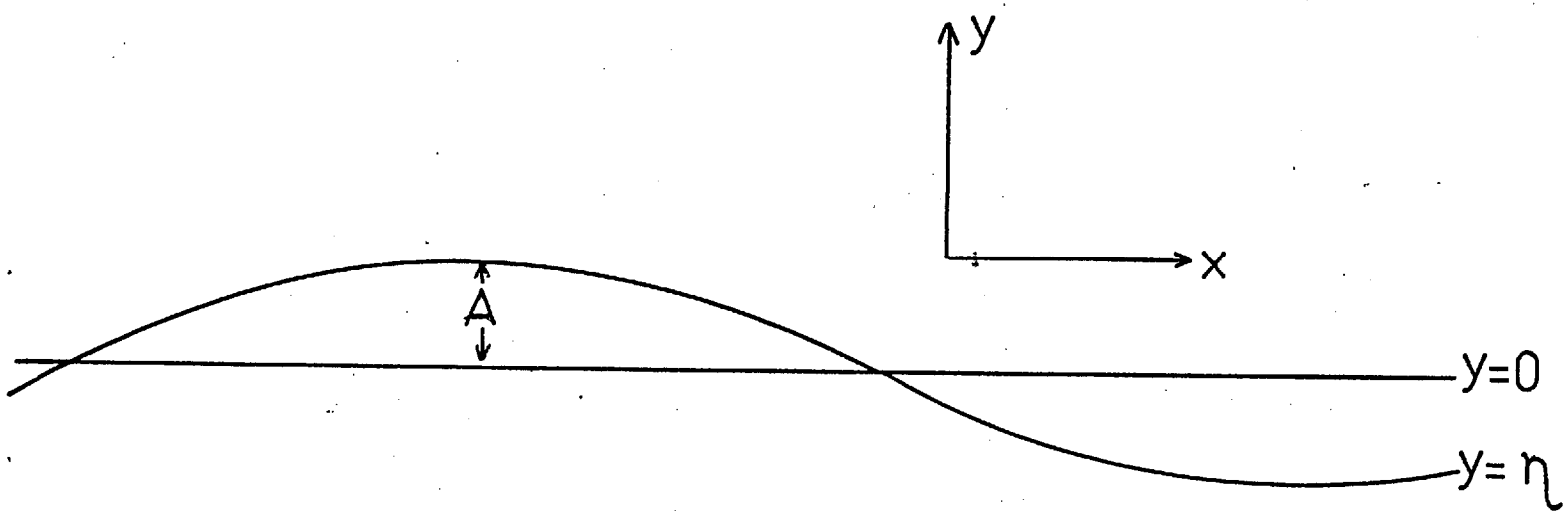

Figure 1: Wavelike disturbance on a plane horizontal surface

dimensionless form, as in section 2A.1):

$$W_y = \epsilon_o U_y + \frac{\epsilon}{\epsilon_o} + V_y (1 - \epsilon_o) \qquad \text{- - - - - - - -} \qquad (2A.42)$$

A simplified approximation of this is to treat the interface as a fixed boundary. That is, at any instant in time the particle phase, by definition, cannot move across the boundary. Taking material balances across this fixed boundary then leads to (again in perturbation and dimensionless form):

$$W_y = \epsilon_o U_y + \frac{\epsilon}{\epsilon_o} \qquad \text{- - - - - - - - - - - - - - - -} \qquad (2A.42a)$$

$$\text{and } W_x = \epsilon_o U_x \qquad \text{- - - - - - - - - - - - - - - -} \qquad (2A.43)$$

Pyle and Rose (1965) also used the simple form of the boundary conditions, equation (2A.43) to determine the gas flow inside a bubble in a fluidised bed; it is employed throughout this analysis, although other possibilities do exist.

b Stress Boundary Condition

Continuity of the normal and tangential stresses at the interface gives:-

$$\sigma_{SF} = \sigma_F + \sigma_P \qquad \text{- - - - - - - - - - - - - - - -} \qquad (2A.44)$$

Where σ = normal or tangential stress

subscripts SF represents the support fluid

F represents the interstitial fluid

P represents the particle phase

Employing a definition of stress analogous to that used by Murray (1966), Anderson and Jackson (1967) and Jones (1970) gives, for the support fluid:

Tangential stress: $$\sigma_{SF} = \mu_F \left[\frac{dW_x}{dy} + \frac{dW_y}{dx} \right] \quad - - - \quad (2A.45)$$

Normal stress: $$\sigma_{SF} = P_3 + \frac{4}{3} \mu_F \frac{dW_y}{dy} - \frac{2}{3} \mu_F \frac{dW_x}{dx}$$

$$- - - \quad (2A.46)$$

with corresponding expressions for the other two phases. Thus (2A.44) gives, in perturbed and dimensionless form:-

$$\frac{dW_x}{dy} + \frac{dW_y}{dx} = \frac{dU_x}{dy} + \frac{dU_y}{dx} + \mu \left[\frac{dV_x}{dy} + \frac{dV_y}{dx} \right] \quad - - - \quad (2A.47)$$

$$\frac{R_{ep}}{Fr} P_3 + \frac{4}{3} \frac{dW_y}{dy} - \frac{2}{3} \frac{dW_x}{dx} = \frac{R_{ep}}{Fr} P_2 + \frac{4}{3} \frac{dW_y}{dy} - \frac{2}{3} \frac{dU_x}{dx} +$$

$$+ \mu \left[\frac{4}{3} \frac{dV_y}{dy} - \frac{2}{3} \frac{dV_x}{dx} \right] \quad - - - - - - - - - - - - - - - \quad (2A.48)$$

In (2A.48) the interparticulate pressure is taken, as in the equations of motion, to be zero.

Also, from hydrostatic considerations

P_3 at $y = \eta$ = P_3 at $y = 0 - \rho\eta$

and P_2 at $y = \eta$ = P_2 at $y = 0 - \epsilon_o \rho \eta$

To obtain the other two necessary boundary conditions an assumption must be made about the distribution of stress across the boundary. This gives rise to a number of possibilities whose implications are discussed below.

The simplest assumption is that the stress is shared equally by the two fluidised bed phases; so that, for both normal and tangential stresses, $\sigma_F = \sigma_P$ (2A.49).

A variation of this assumption, which has more physical reasoning behind it, is that (2A.44) can be replaced, for both normal and tangential stresses by

$\sigma_{SF} = \sigma_P = \sigma_F$ (2A.50).

This follows from observing the system on a microscopic scale: a 'packet' of support fluid may be opposed at the boundary by a corresponding 'packet' of either interstitial fluid or of the particle phase. Thus, if the stress is directly transmitted between the two opposing fluids, (2A.50) will be correct. However, the equations of motion are derived for variables averaged over a distance large in comparison with the particle spacing, so that this assumption may not be consistent with the equations chosen.

Another assumption similar to (2A.49) is that the stress is shared by the two fluidised phases in the ratio of their volumes:

$\epsilon_o \sigma_F = (1-\epsilon_o)\, \sigma_P$ for normal and tangential stresses

- - - - - - - (2A.51)

Equations (2A.49). (2A.50) and (2A.51) have a similar form:

(2A.49) with (2A.44) gives $\sigma_{SF} = 2\sigma_F = 2\sigma_P$

(2A.50) $\sigma_{SF} = \sigma_F = \sigma_P$

(2A.51) with (2A.44) gives $\sigma_{SF} = \frac{1}{(1-\epsilon_o)}\, \sigma_F =$

$= \frac{1}{\epsilon_o}\, \sigma_P$ where $\epsilon_o \simeq 0.4$

In the present calculations, equation (2A.50) is employed throughout, having checked that the other two give results of similar order.

As the tangential stresses are proportional to the velocity gradient, (2A.50) implies that the velocity gradients in the fluids are in the inverse ratio of the respective viscosities. Two other possible assumptions are then:

a that the velocity gradients in the two fluidised bed fluids are equal, giving rise to:

$$\frac{dU_x}{dy} + \frac{dU_y}{dx} = \frac{dV_x}{dy} + \frac{dV_y}{dx} \qquad \text{- - - - - - - - (2A.52)}$$

$$\text{and } \frac{4}{3}\frac{dU_y}{dy} - \frac{2}{3}\frac{dU_x}{dx} = \frac{4}{3}\frac{dV_y}{dy} - \frac{2}{3}\frac{dV_x}{dx} \qquad \text{- - - - (2A.53)}$$

and

b that the interstitial velocity gradients are negligible (zero).

This assumption was made by Clift, Grace, and Weber (1973) and is also implied by Rice and Wilhelm.

In (2A.47) and (2A.48), this is equivalent to assuming that the velocity gradients in the interstitial fluid phase are negligible in comparison to those in the other phases. Thus, the terms involving velocity gradients of the interstitial fluid are neglected. Equations (2A.47) and (2A.48) are simplified by setting:

$$\frac{\partial u_x}{\partial y} + \frac{\partial u_y}{\partial x} = 0 \qquad \text{.....(2A.54)}$$

$$\text{and} \quad \frac{4}{3}\frac{\partial u_y}{\partial y} - \frac{2}{3}\frac{\partial u_y}{\partial x} = 0 \qquad \text{.....(2A.55)}$$

As no conclusive evidence can be presented either for or against these assumptions, different consistent combinations of the proposed boundary conditions are solved in this work to find the dependence of the solution on these boundary conditions. There are therefore several possible consistent sets of boundary conditions; those investigated here are, as summarised in Table 3:-

Set 1: This set is derived from the full material balance allowing interfacial movement, and from the assumption that the stress is directly transmitted between the phases (equation 2A.50). This latter assumption also implies that the velocity gradients in the particle phase are $(\frac{1}{\mu})$ x those in the interstitial fluid; where, for water fluidised systems, $\mu = O[10^2 \text{ to } 10^3]$, and for air fluidised systems, $\mu = O[10^4 \text{ to } 10^6]$.

Set 2: This set is similar to Set 1, but with the full material balance replaced by the approximate material balance taken over a fixed boundary. The effect of this approximation on the solution can thus be investigated.

If the stress boundary conditions are employed simultaneously with the assumption that normal and tangential velocity gradients in the two fluidised bed phases are equal (equations (2A.52) and (2A.53)), this unfortunately leads to an indefinite result, (two rows of the determinant, M (see section 2A.4), are equal). Thus the effect of the boundary conditions was determined separately in sets 3 and 4:

Set 3: This set is similar to set 2, but with the velocity gradients in the tangential stress terms equal.

Set 4: This set is similar to set 2, but with the velocity gradients in the normal stress terms equal.

Set 5: This set is similar to set 1, but with the velocity gradients

in the normal stress terms equal. That is, sets 4 and 5 are used to investigate the effect of the approximate mass balance on the solution in this case.

Set 6: Again, neglecting the velocity gradients in the interstitial fluid gives an indefinite result by this method of solution, but as this is the assumption made by Clift, Grace and Weber (1973), their solution has been re-calculated for the physical systems investigated here.

In their solution, Clift, Grace and Weber simplified the equations of motion by neglecting the interstitial fluid momentum and assuming that the voidage is constant, so that only four constants were necessary. Thus, only four consistent boundary conditions were needed for the complete solution. *

2A.3.2 Support Fluid Uppermost; eg top of the bed

The boundary conditions are as in 2A.3.1 for the configuration; fluidised bed phases uppermost, with the definition of normal stress which is equivalent to (2A.46) in dimensionless terms:-

$$\sigma'_{SF} = -\frac{R_{EF}}{Fr} P_3 + \frac{4}{3}\frac{dW_y}{dy} - \frac{2}{3}\frac{dW_x}{dx} \qquad \text{- - - - - - - -} \quad (2A.46a)$$

Where σ'_{SF} is a dimensionless stress.

The only difference between these two configurations is the change in the direction of the acceleration force (eg gravity, g, and hence Fr) with respect to the chosen system of co-ordinates. That is, with the stress as defined in (2A.46), y is positive in the opposite direction to that in which the gravitational force acts for the configuration,

*Full details of boundary conditions for sets 2 and 6 are given in Table 3a, page 40a.

fluidised phases uppermost, and in the same direction for the configuration support fluid uppermost.

TABLE 3

Features of the Sets of Boundary Conditions Investigated

Boundary Conditions	Material Balance	Assumptions and Equations Employed in Deriving the Stress Boundary Conditions
Set 1	Full mass balance over moving interface. Equations: (2A.42) and (2A.43)	Normal and tangential stress directly transmitted across the boundary. From observations on microscopic scale. Equation: (2A.50)
Set 2	Approximate mass balance over fixed interface. Equations: (2A.42a) and (2A.43)	Normal and tangential stress directly transmitted across the boundary. From observations on microscopic scale. Equation: (2A.50)
Set 3	Approximate mass balance over fixed interface. Equations: (2A.42a) and (2A.43)	Normal stress directly transmitted across the boundary. From observations on microscopic scale. Equation (2A.50) Tangential stress: velocity gradients equal. Equations: (2A.47) with (2A.52)
Set 4	Approximate mass balance over fixed interface Equations: (2A.42a) and (2A.43)	Tangential stress directly transmitted across the boundary. From observations on microscopic scale. Equation (2A.50). Normal stress: velocity gradients equal. Equations: (2A.48) with (2A.53)
Set 5	Full mass balance over moving interface. Equations: (2A.42) and (2A.43)	Tangential stress directly transmitted across the boundary. From observations on microscopic scale. Equation (2A.50). Normal stress: velocity gradients equal. Equations: (2A.48 with (2A.53)
Set 6	Full mass balance over moving interface. Equations: (2A.42) and (2A.43)	Interstitial fluid velocity gradients zero. Normal and tangential stresses are continuous across the interface. Equations: (2A.47), (2A.48) with (2A.54) and (2A.55)

Table 3a

Boundary Condition	Set 2	Set 6
Mass balance (i)	$W_y = \varepsilon_o U_y + \frac{\varepsilon}{\varepsilon_o}$	$W_y = \varepsilon_o U_y + \frac{\varepsilon}{\varepsilon_o} + V_y (1 - \varepsilon_o)$
Mass balance (ii)	$W_x = \varepsilon_o U_x$	$W_x = \varepsilon_o U_x$
Tangential stress balance (i)	$\frac{\partial W_x}{\partial y} + \frac{\partial W_y}{\partial x} = \mu \left[\frac{\partial V_x}{\partial y} + \frac{\partial V_y}{\partial x} \right]$	$\frac{\partial W_x}{\partial y} + \frac{\partial W_y}{\partial x} = \mu \left[\frac{\partial V_x}{\partial y} + \frac{\partial V_y}{\partial x} \right]$
Tangential stress balance (ii)	$\frac{\partial W_x}{\partial y} + \frac{\partial W_y}{\partial x} = \frac{\partial U_x}{\partial y} + \frac{\partial U_y}{\partial x}$	-
Normal stress balance (i)	$\frac{Re_p}{Fr} P_3 - \frac{Re_F \eta}{Fr} + \frac{4}{3} \frac{\partial W_y}{\partial y} - \frac{2}{3} \frac{\partial W_x}{\partial x}$ $= \frac{4}{3} \mu \frac{\partial V_y}{\partial y} - \frac{2}{3} \mu \frac{\partial V_x}{\partial x}$	$\frac{Re_p}{Fr} P_3 - \frac{Re_F \eta}{Fr} + \frac{4}{3} \frac{\partial W_y}{\partial y} - \frac{2}{3} \frac{\partial W_x}{\partial x}$ $= \frac{Re_p}{Fr} P_2 - \frac{Re_F}{Fr} \varepsilon_o + \frac{4}{3} \mu \frac{\partial V_y}{\partial y} - \frac{2}{3} \mu \frac{\partial V_x}{\partial x}$
Normal stress balance (ii)	$\frac{Re_p}{Fr} P_3 - \frac{Re_F \eta}{Fr} + \frac{4}{3} \frac{\partial W_y}{\partial y} - \frac{2}{3} \frac{\partial W_x}{\partial x}$ $= \frac{Re_p}{Fr} P_2 - \frac{Re_F}{Fr} \varepsilon_o + \frac{4}{3} \frac{\partial U_y}{\partial y} - \frac{2}{3} \frac{\partial U_x}{\partial x}$	-

2A.4 Solution Using the Proposed Sets of Boundary Conditions

2A.4.1 Fluidised Phase Uppermost

Full details of all the algebra involved is given in Appendix 2.

Substitution of the assumed solution of the equations of motion (2A.30) to (2A.39) into the boundary conditions gives the matrix equation:

$$[M] \times [A\ B\ C\ D\ E\ F]^T = 0 \qquad \text{- - - - - - - - - - - - - (2A.56)}$$

Where [M] is a 6 x 6 matrix of coefficients.

The matrix, M, is given in Appendix 2 for all the sets of boundary conditions used.

The non-trivial solution to (2A.56) is given by:

$$\det [M] = 0 \qquad \text{- - - - - - - - - - - - - - - - - - - (2A.57)}$$

Which leads to $n^3(a) + n^2 (b + c) + n (d + e) + f = 0$

$$\text{- - - - - (2A.58)}$$

where the coefficients a to f are also given in Appendix 2, for all the sets of boundary conditions used.

The solution to equation (2A.58) together with (2A.39) can then be determined by a fairly straightforward method using a digital computer.

2A.4.2 Support Fluid Uppermost

Substitution into the boundary conditions for the configuration, supprt fluid uppermost, gives the same general form of solution and equation (2A.58) becomes:

$$n^3(a) + n^2(- b + c) + n (- d + e) + f = 0 \qquad \text{- - - - (2A.58a)}$$

2A.4.3 Physical Parameters

To make the solution of equations (2A.58) and (2A.39) possible, the physical parameters of each system must be known. Values for ρ_F, ρ_P, dp and μ_F are readily available for systems of interest; values for the minimum fluidising velocity, U_o, when not available, were found experimentally in the normal manner.

ϵ_o is taken to be 0.4 for all systems. This is, of course, an approximation, but will not introduce large errors: Wilhelm and Kwauk (1948) show that ϵ_o is between 0.37 and 0.41 for all the water fluidised systems investigated here, and most gas fluidised beds have a voidage fraction at incipient fluidisation of around 0.4 - 0.45.

The viscosity of the particle phase, μ_P has been taken from the work of Schugerl et al (1961); Schugerl (1971), Hetzler and Williams (1969) and Hagyard and Sacerdote (1966).

Schugerl gave values of μ_P as a function of fluidising velocity for many air fluidised systems, and showed that μ_P settles down to a (fairly) constant value in a well fluidised system (fluidising velocity > 2 U_o). Hetzler and Williams correlated the average bed viscosities for many water fluidised systems. Hagyard and Sacerdote determined the effect of the system density on μ_P.

SECTION 2B: PREDICTIONS FROM THE THEORY

2B.1 Support Fluid Uppermost

The solution for this configuration (that is, equations (2A.58a) and (2A.39) has no positive roots of n for positive K, for any of the six sets of boundary conditions proposed. This configuration is therefore always stable, and any plane wave disturbance on such a boundary will be damped out. This agrees with the findings of Murray (1965) (see section 1.2) who predicted that disturbances on the upper surface of the bed (ie this configuration) were always damped out.

2B.2 Fluidised Phase Uppermost

The solution for this configuration, (that is, equations (2A.58) and (2A.39) has one positive root of n for positive K, for each of the six sets of boundary conditions proposed. Thus, this configuration is always unstable. There is, of course, no surface tension force to exert a stabilising influence, as in the case of the gas/liquid systems investigated by Bellman and Pennington (1954).

In the following work, attention is confined only to this one positive root.

Figures 2, 3, 4, 5 6 and 7 show the solution in the form of a graph of n vrs K for several known physical systems for each proposed set of boundary conditions. (For systems fluidised by water, the experimental values of Wilhelm and Kwauk (1948) are taken; for systems fluidised by air, the experimental systems presented in section 3, (Table 7), are taken).

It can be seen from Figures 5 and 6 that the two sets of boundary conditions in which the velocity gradients in the two fluidised bed phases are assumed equal in the normal stress terms give a similar

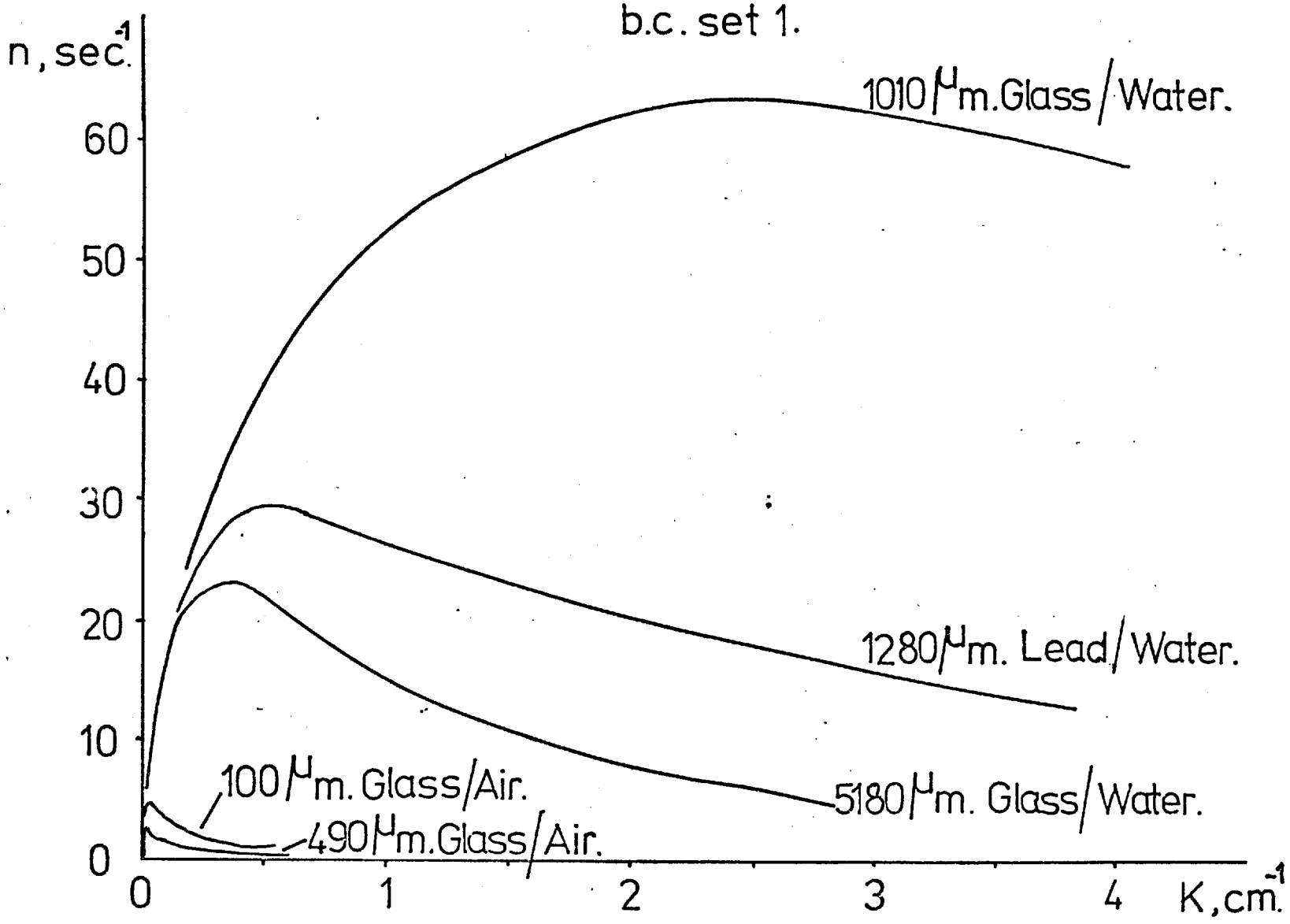

Figure 2: Growth rate of a surface disturbance as a function of wave number

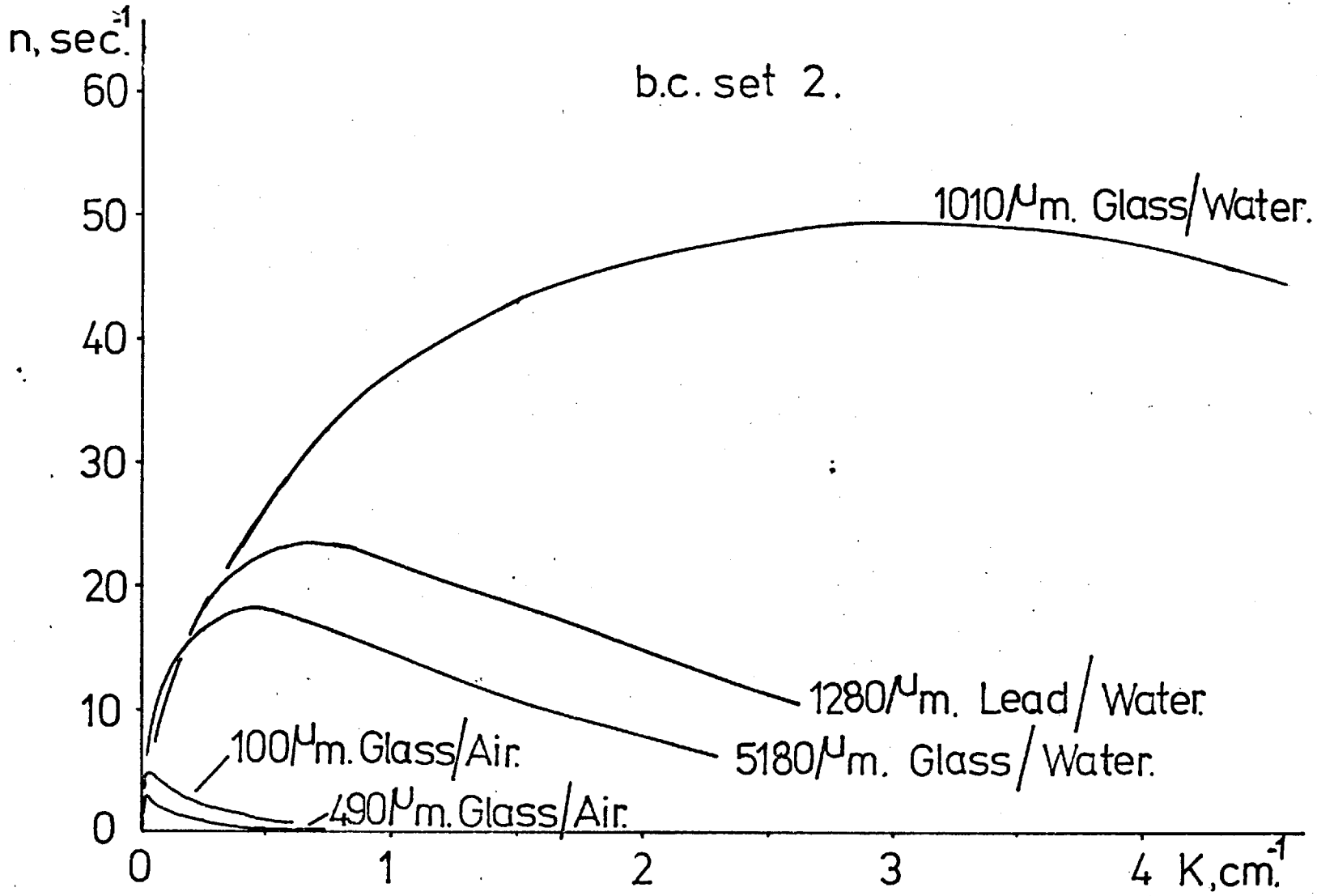

Figure 3: Growth rate of a surface disturbance as a function of wave number

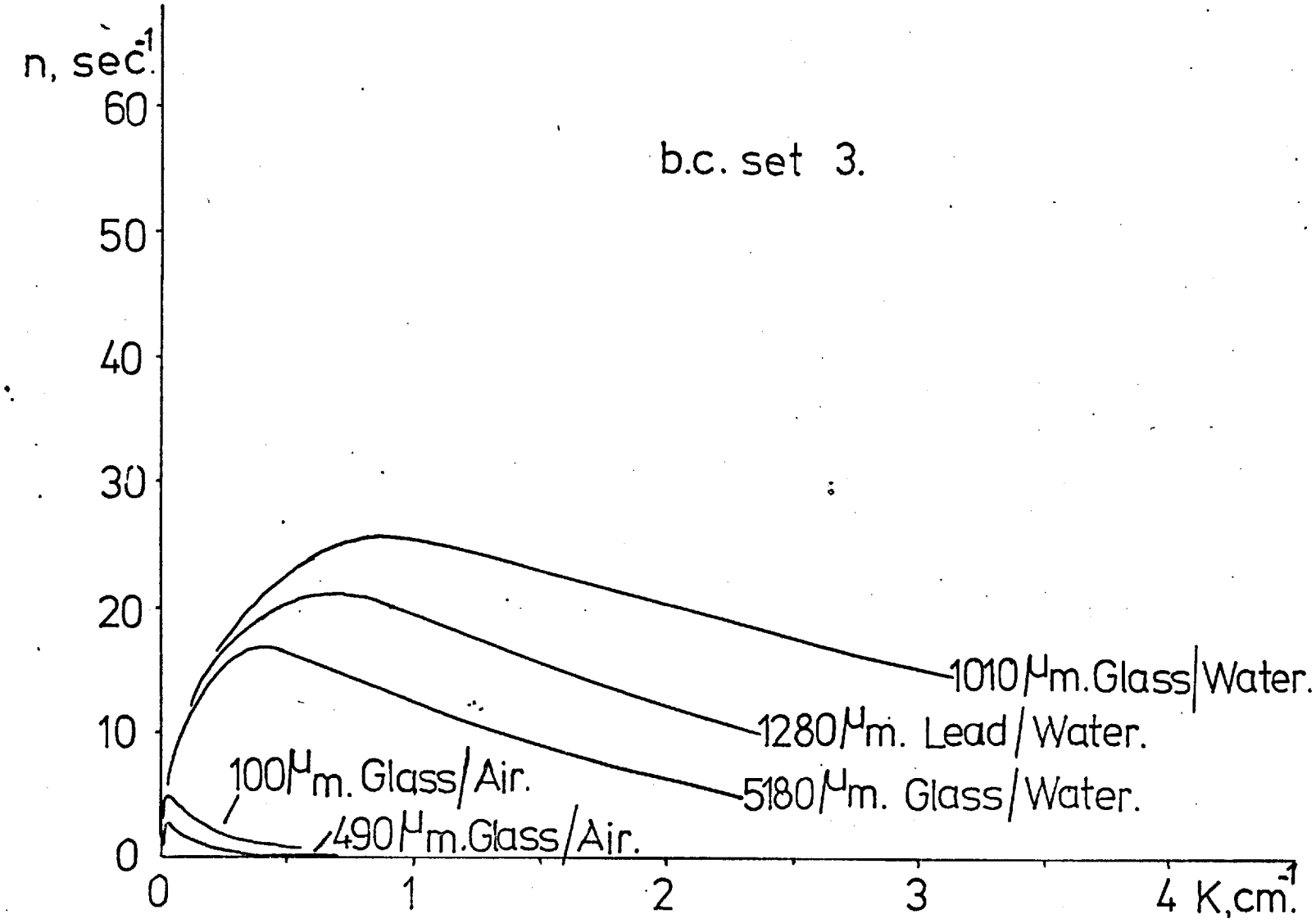

Figure 4: Growth rate of a surface disturbance as a function of wave number

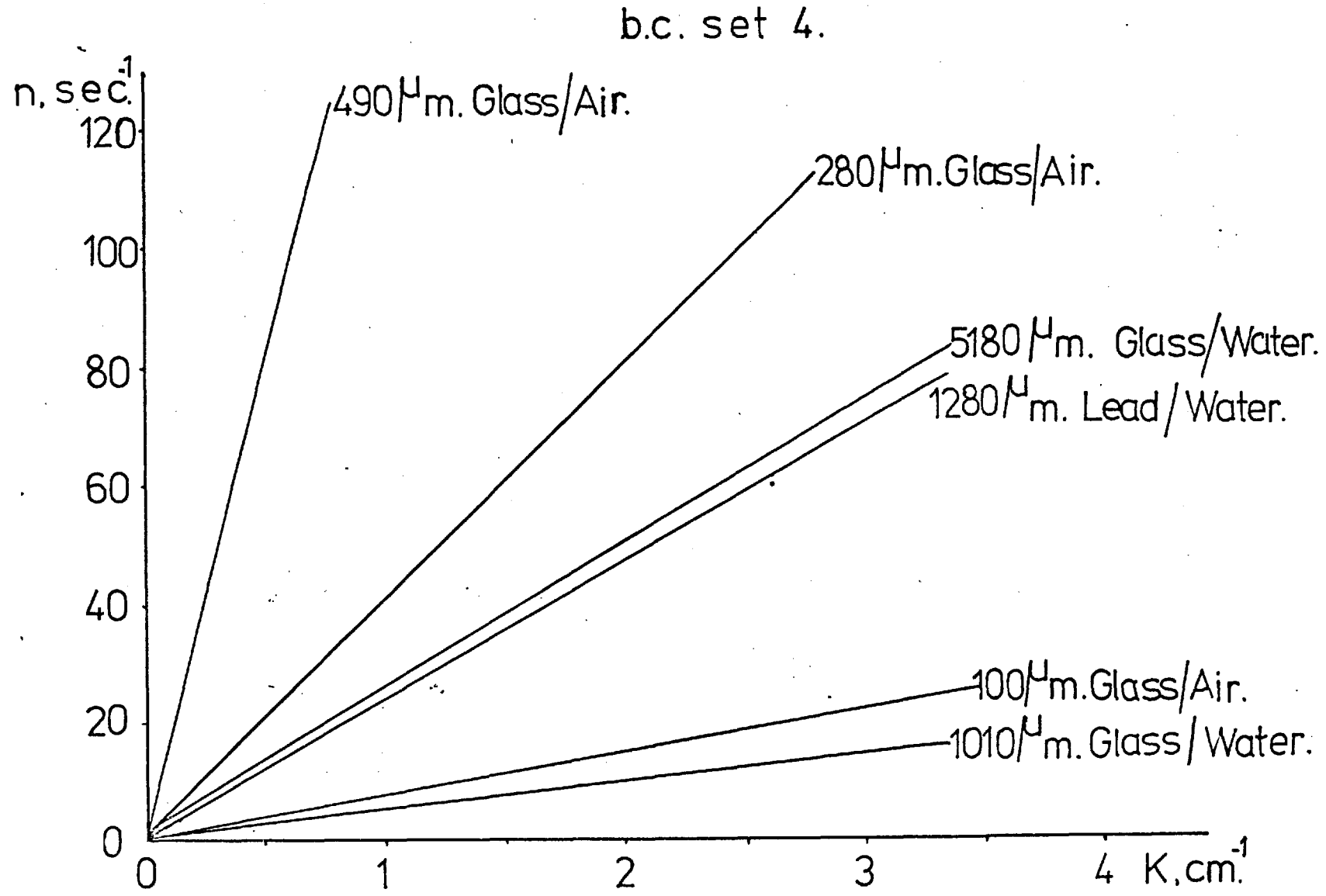

Figure 5: Growth rate of surface disturbance as a function of wave number

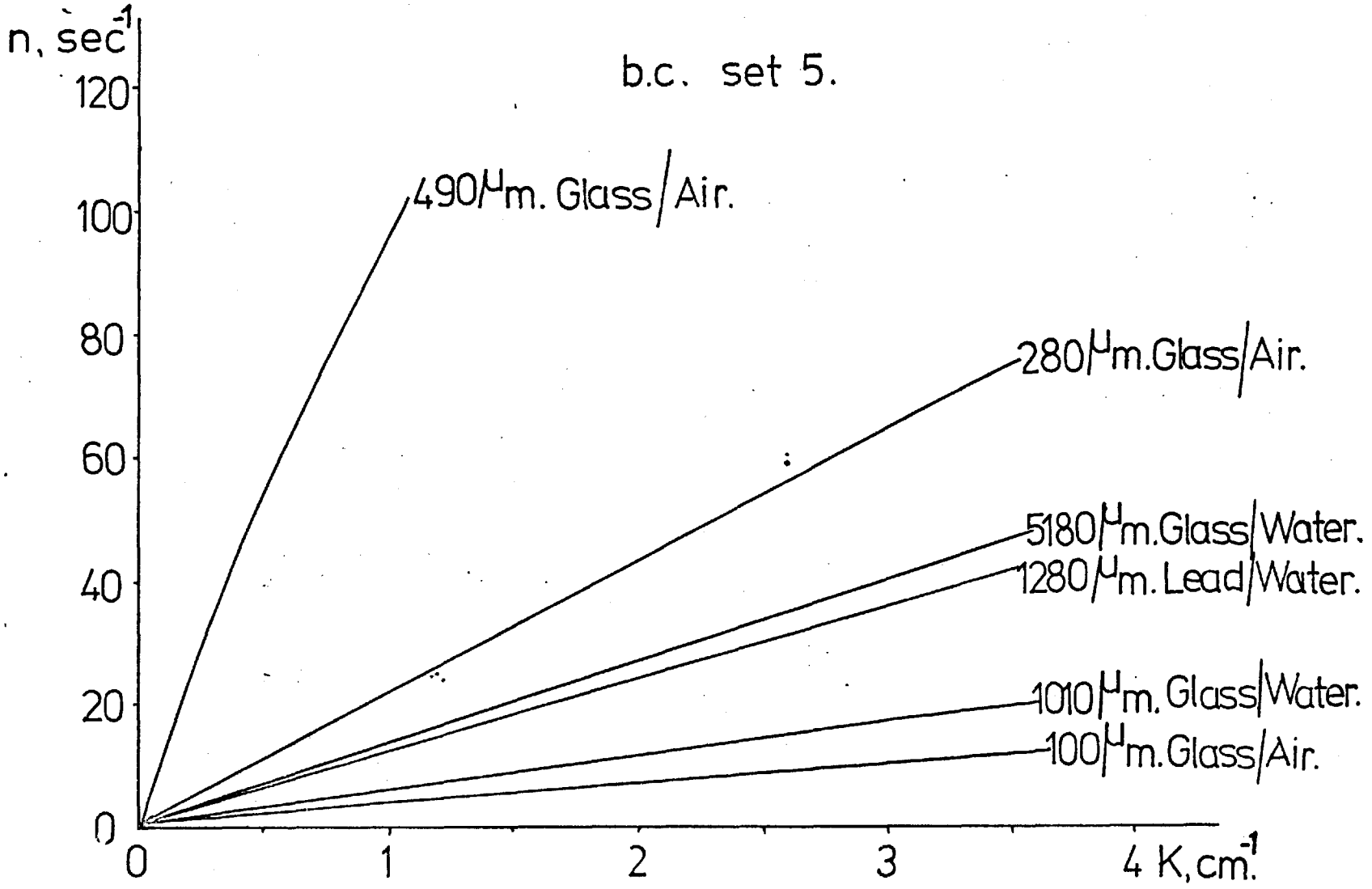

Figure 6: Growth rate of a surface disturbance as a function of wave number

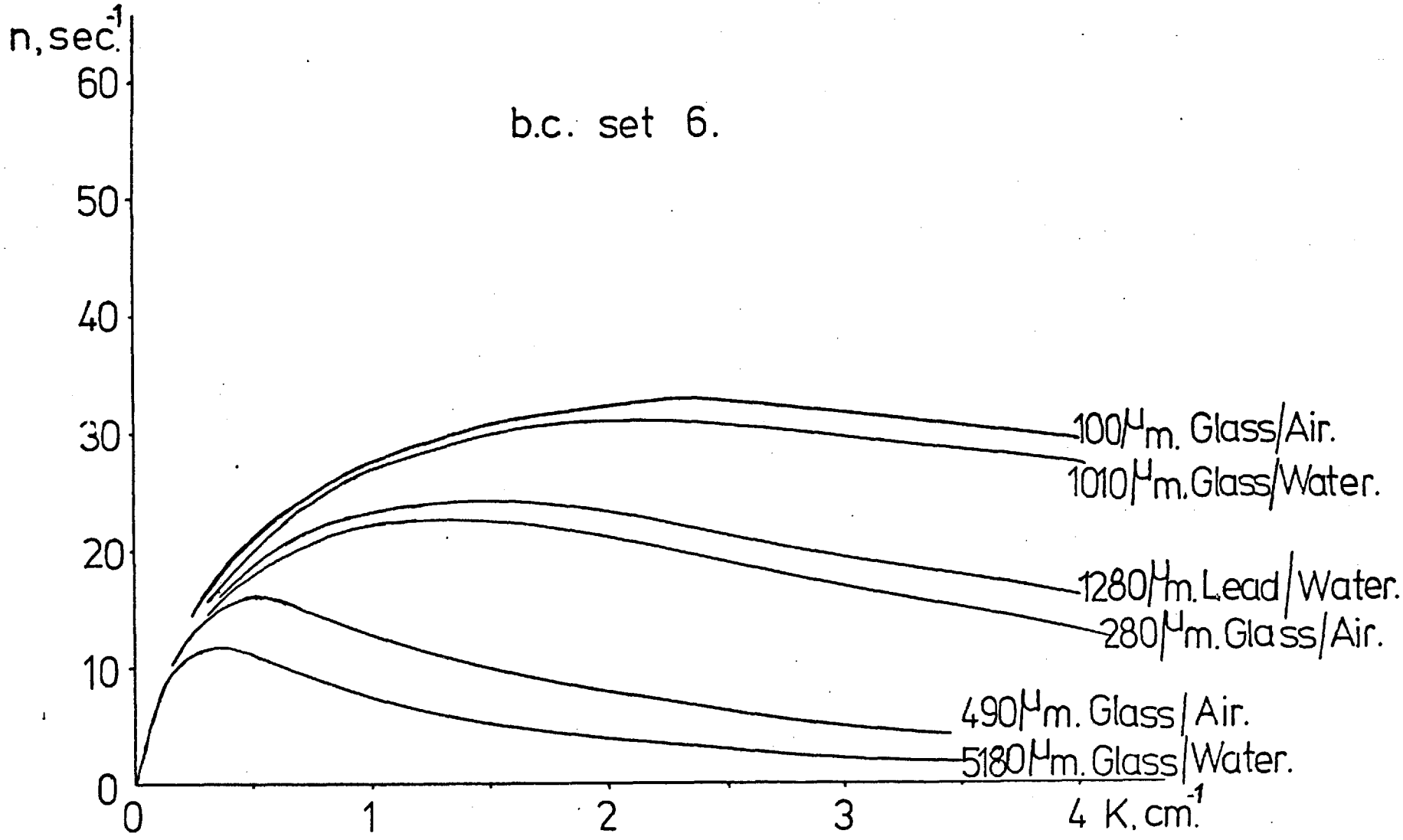

Figure 7: Growth rate of a surface disturbance as a function of wave number

solution to that due to Jackson (1963). His analysis of the stability of homogeneous fluidisation showed that the growth rate increased monotonically with wave number. The reason for this in Jackson's work (see section 1.2) was the omission of the particle phase viscous (stress) forces. It can be seen in Appendix 2 that the dominant coefficients in the solution equations for these two boundary condition sets have the viscosity ratio, μ, and thus the particle phase viscosity, μ_p, as a common factor, so that these two sets of boundary conditions also produce a solution which is independent of the particle phase viscosity.

However, there would seem to be no physical explanation for this solution; the assumption that the velocity gradients in the particle and interstitial fluid phases are equal in the normal direction, in no way implies that the particle phase viscosity is zero. These sets of boundary conditions could be inconsistent, but again there seems to be no physical justification to suppose that this is true.

Figures 2, 3, 4 and 7, the solutions for the other sets of boundary conditions, show that, for these four sets, the general form of the solution n versus K is similar for the whole range of physical properties investigated. It can be seen that, as Rice and Wilhelm found, there is a maximum in the n versus K curve at n_{max}, corresponding to the most rapidly growing, or 'the most dangerous' wavelength, λ.

Table 4 lists the calculated values of n_{max} and the corresponding 'most dangerous' wavelength λ, for a range of different fluidised systems for each of these four sets of boundary conditions.

Figures 2, 3 and 4, and the corresponding columns in Table 4, show that the sets of boundary conditions 1, 2 and 3 give very similar solutions. The difference between these boundary conditions is given in section 2A.3 and summarised in Table 3, but in summary; Set 1 was derived from the full material balance and the assumption that the stresses are directly transmitted between the phases. Set 2 differs from set 1 in as much as the approximate material balance is used, ie sets 1 and 2 may be used to study the effect of this approximation on the solution. Set 3 differs from set 2 in as much as the velocity gradients in the two fluidised phases are assumed equal in the tangential stress terms, ie sets 2 and 3 may be used to study the effect of this assumption on the solution.

Obviously, from the results, neither of these two assumptions have a great effect on the solution, and thus from here on only the solutions using boundary condition sets 2 and 6 will be discussed. (Sets 1 and 3 being very similar to 2 and 4 and 5 yielding results independent of the particle phase viscosity).

Figures 8 to 13 show that, although the solutions using boundary condition sets 2 and 6 are of similar order for water fluidisation, set 6 leads to a much larger maximum growth rate for air fluidisation than does set 2. This is quite consistent with the assumptions made in deriving these two sets of boundary conditions. Set 6 (which gives a solution directly comparable to that of Rice and Wilhelm, and Clift, Grace and Weber) involves the assumption that the momentum of the gas percolating across the interface is zero and that the velocity gradients in the interstitial fluid are small in comparison with those in the particle phase. Set 2 implies that the momentum of the gas

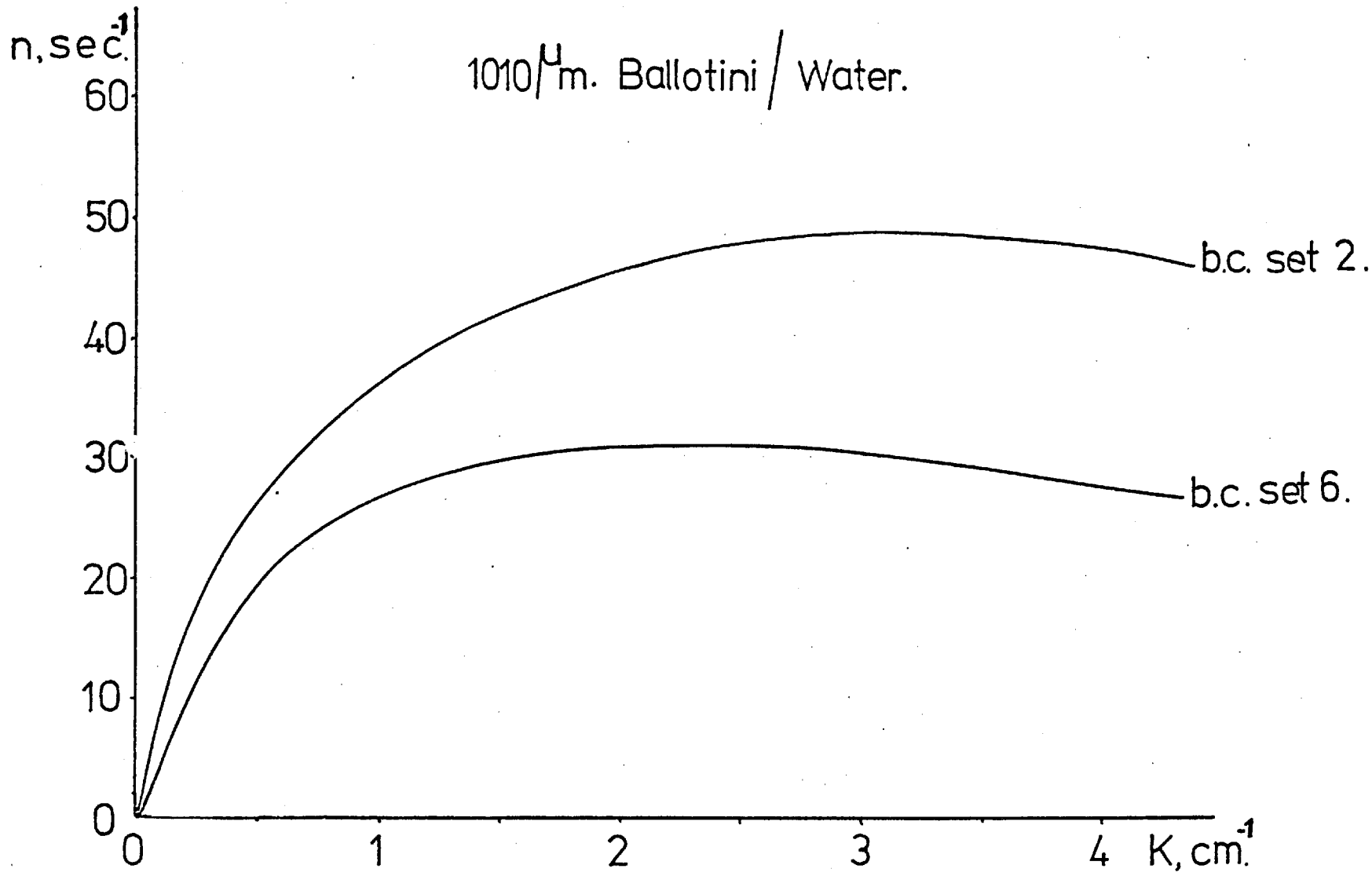

Figure 8: Growth rate of a surface disturbance as a function of wave number

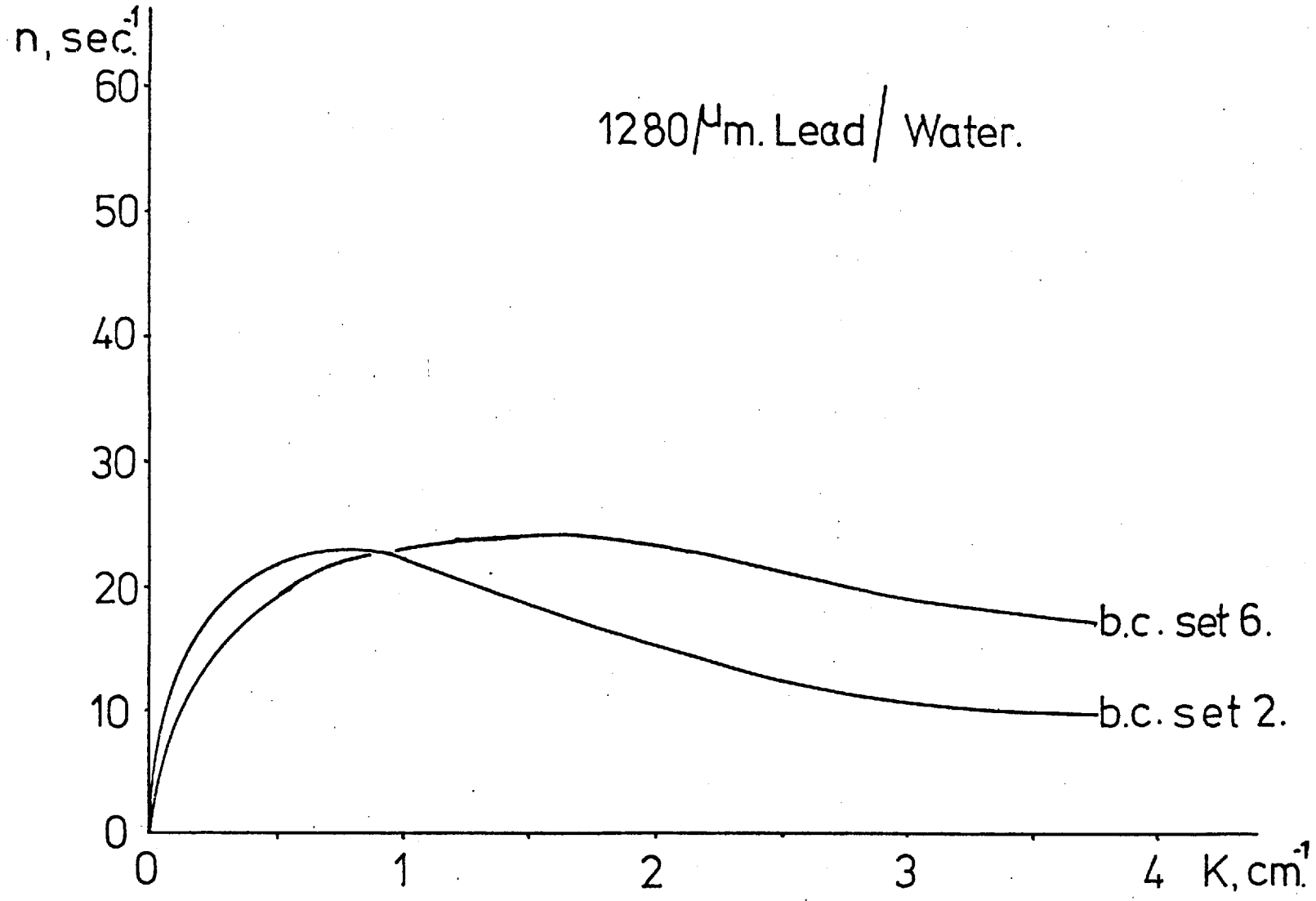

Figure 9: Growth rate of a surface disturbance as a function of wave number

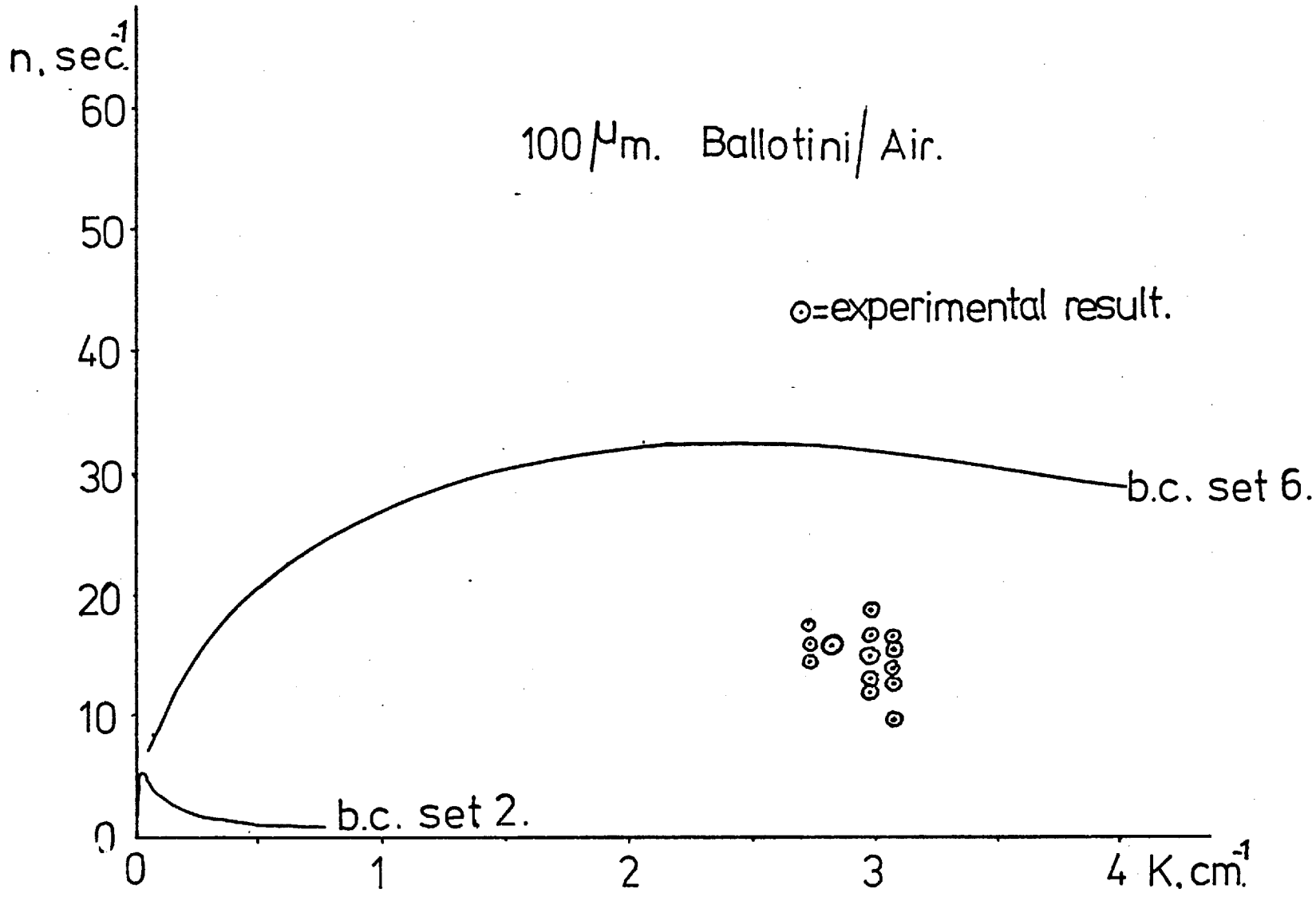

Figure 10: Growth rate of a surface disturbance as a function of wave number

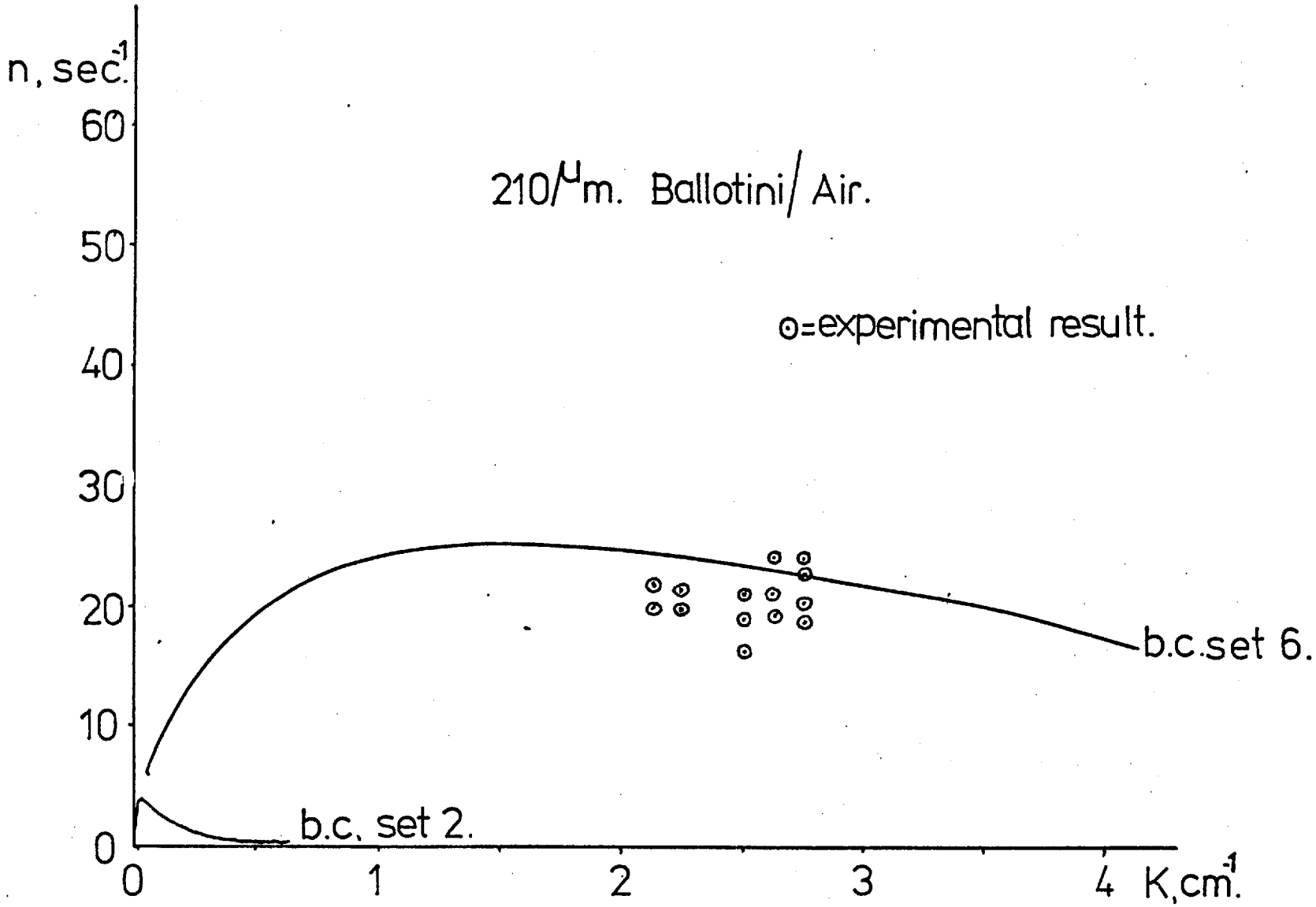

Figure 11: Growth rate of a surface disturbance as a function of wave number

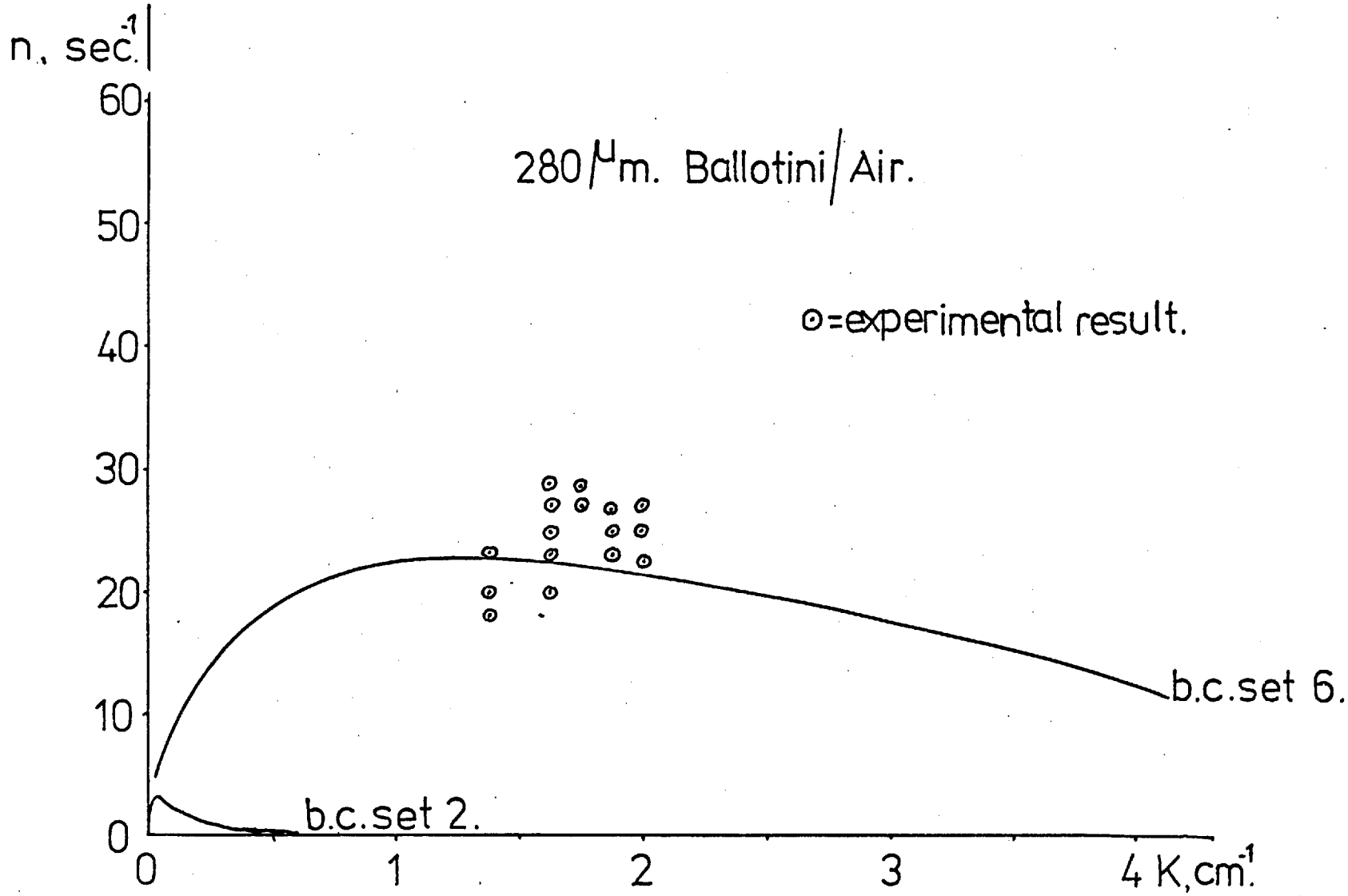

Figure 12: Growth rate of a surface disturbance as a function of wave number

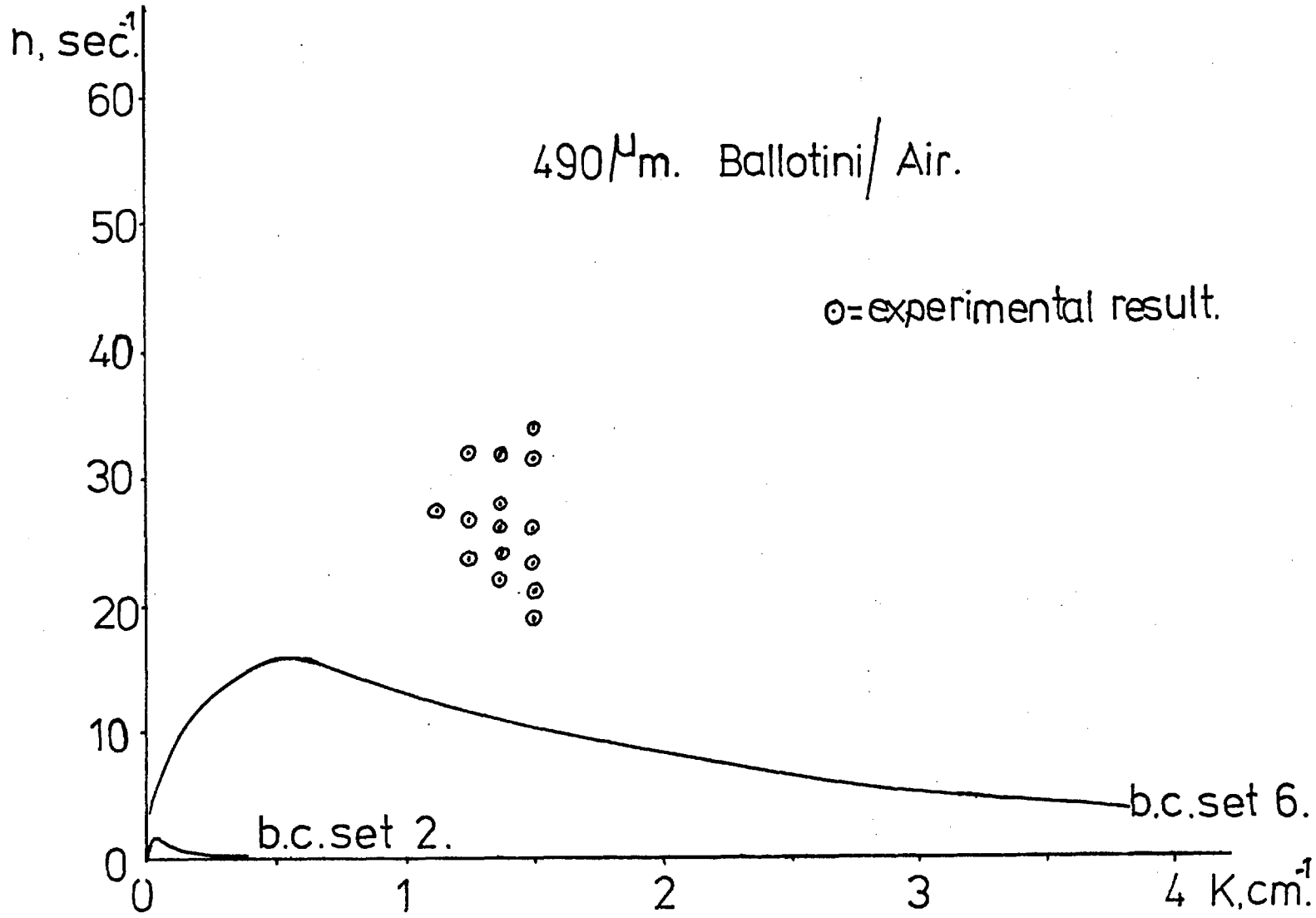

Figure 13: Growth rate of a surface disturbance as a function of wave number

percolating across the interface is large (ie the velocity gradients in the interstitial fluid are μx those in the particle phase, where μ is large, (see 2A.3).

It is to be expected that the higher the momentum of the fluid percolating across the interface, the more stable that interface will be, as this increases the drag force on the particles: Jones (1970) showed that increasing the drag force on particles in a fluidised bed leads to a decrease in particle oscillation (ie greater stability).

Thus, for air fluidised systems, which have much larger density and viscosity ratios than water fluidised systems, it is to be expected that boundary condition set 2, with the higher momentum in the interstitial fluid than in set 6, should be more stable.

Clift, Grace and Weber did attempt to calculate the effect of including the interstitial fluid momentum in their solution, and claim to have proved that the effect is negligible. However, this more complete calculation necessitated the use of an extra boundary condition. Clift et al overcame this problem by using their general continuity boundary condition twice, with different values for the uncertain constant. Their set of boundary conditions are therefore not consistent or independent, so that their claim that the inclusion of the interstitial fluid momentum terms has negligible effect on the solution has not been proved.

It is probable that neither set of boundary conditions is completely correct: under certain conditions either one may appear more reasonable, but the true situation almost certainly lies somewhere between the two extremes of large and zero interstitial fluid momentum.

In Table 4, the use of boundary condition set 2 predicts an increasing growth rate (ie instability) with decreasing Froude number, or in more concrete terms, that liquid fluidised beds are more unstable in the situation investigated here, than gas fluidised beds. This is, of course, an opposite trend to the results found by analysis of the stability of the state of homogeneous fluidisation, (see section 1) and of the correlation of the degree of stability proposed by Wilhelm and Kwauk (1948). These results are not however inconsistent. It is possible that the homogeneous phase in a liquid fluidised system is more stable to disturbances, while a horizontal interface between this phase and the support fluid is less stable than in gas fluidised systems. In other words, it could be argued that one possible reason for the general absence of bubbles in liquid fluidised beds lies precisely in the instability of any interface, for example, the bubble boundary, to small disturbances.

Although this same argument cannot be applied to the solution with boundary condition set 6, as this solution gives growth rates of similar order for both air and water fluidised systems, it will be shown later (in section 3) that, if these boundary conditions apply, bubbles in water fluidised systems are still less stable to disturbances than are bubbles in air fluidised beds.

TABLE 4

Stability of Various Fluidised Systems

Diameter of Particles dp Microns	System	R_{eF}	Fr	Boundary Condition Set 1		Boundary Condition Set 2		Boundary Condition Set 3		Boundary Condition Set 6	
				n_{max} sec^{-1}	λ cm	n_{max} sec^{-1}	λ cm	n_{max} sec^{-1}	λ cm	n_{max} sec^{-1}	λ cm
490	Glass/Air	8.65	18.7	2.46	790	3.13	1050	2.26	890	17.0	12.4
370	Glass/Air	2.61	3.79	3.14	628	4.04	628	3.02	628	20.0	7.0
280	Glass/Air	1.24	2.05	3.66	314	4.54	314	3.54	314	23.0	5.3
210	Glass/Air	0.68	1.47	4.08	314	5.09	314	3.98	314	26.0	4.3
100	Glass/Air	0.088	0.23	5.12	209	6.42	209	5.07	209	32.0	3.1
5180	Glass/Water	222	0.036	18.24	15.7	23.2	15.7	16.7	15.7	11.5	17.9
4580	Socony Beads/Water	96.6	0.009	22.6	10.5	28.7	12.6	21.5	10.5	-	-
1280	Lead/Water	51.7	0.130	23.2	9.0	29.6	10.5	20.9	10.5	28.0	4.2
3360	Socony Beads/Water	57.1	0.0088	26.9	7.0	34.2	9.0	25.6	7.0	-	-
1010	Glass/Water	9.0	0.0080	49.3	2.1	62.7	2.1	47.1	2.1	31.0	2.5

SECTION 2C: COMPARISON WITH THE STABILITY OF THE HOMOGENEOUS PHASE

Anderson and Jackson (1967; 1968; 1969) studied the stability of the state of homogeneous fluidisation to small internal disturbances. Their analysis has been discussed in sections 1.1 and 1.2 but, in summary, they derived equations of motion for the particulate and interstitial fluid phases in terms of variables which are smoothed local averages, taken over an area that is large in comparison to the interparticulate spacing, but small in comparison to the whole system; they linearised these equations by the usual perturbation techniques.

They assumed a complex, wave-like solution for the perturbed variables of the form:

$$\epsilon = A \exp(- ikx - iky + nt) \qquad \text{(2C.1)}$$

where n = a complex growth rate; $n = \xi - i\eta$ (2C.2)

k = the wave number of the disturbance

and $i = \sqrt{-1}$

Elimination of variables between the equations of motion and substitution of the above solution leads to a relationship between the growth rate, n, wave number, K, and the physical system parameters. This relationship applies only for the state of homogeneous fluidisation, ie a long way from the boundary between the homogeneous phase and the support fluid.

To compare the solution given in section 2A, for the stability of the boundary between the homogeneous phase and the support fluid, with that of Anderson and Jackson for the homogeneous phase in general, the support fluid must be assigned the physical parameters of the homogeneous phase. This, of course, involves the simplifying assumption that the homogeneous phase below the (now hypothetical) boundary can be described as one fluid

with mean density and viscosity, while above the boundary it is described as two interacting phases.

A complete analysis is given in Appendix 3.

For comparison with the solution of Anderson and Jackson, the present work is repeated with their form of general solution to the equations of motion (equation (2C.1)). For this to be possible, an assumption must be made: the solution proposed in Appendix 3 to the equations of motion is valid only at $x = 0$. However it is sinusoidal in x, and thus repeated at distances of one wavelength. It is therefore assumed that the solution at $x = 0$ is valid for all x; the error of this approximation will increase as the wavelength increases, so that the solution will be invalid for disturbances of large wavelength.

This comparison has only been attempted with boundary condition set 2, as defined in section 2A.3 and Table 3. The method of solution is completely analogous to that used in the simpler case given in section 2A.2 and Appendix 1, and is therefore not repeated.

However, the final solution by digital computer proved more difficult, owing to the presence of the complex coefficients introduced, and a complete solution was not made. The equations were solved, using a minimisation routine, only for the root with the largest positive real value of n. It is not possible to state, as in the simpler case that this is the only positive root.

Table 5 shows some of the results of Anderson and Jackson for fluidisation with air and water, with the results from this analysis for approximately corresponding systems. For air fluidised systems, Anderson and Jackson

calculated their solution for three values of the bed (particle phase) viscosity 8, 16 and 32 poise, which correspond approximately to beds of glass particles of 210, 370 and 490 microns diameter.

For the system fluidised by water, they calculated the growth rate for a given experimental system of glass particles of 2000 microns diameter, setting the parameter μ_b = 70 poise. This figure would seem to be too large (for example, Anderson and Bryden (1965) show that shear viscosities of water fluidised beds are between 10 and 20 poise) even though Anderson and Jackson also include the bulk viscosity in their parameter. The results from this analysis are therefore calculated for μ_b = 20 poise.

It can be seen that the results of the two analyses do not compare well. However, it must be remembered that there are many differences between the two analyses. That is, they are based on slightly different equations of motion; it is shown in section 1.2 that similar analyses based on equations of motion differing slightly from those of Anderson and Jackson give dissimilar results. There are also many simplifying assumptions involved in the analysis presented here, such as, that the solution at x = 0 is also valid for all x; that the system can be represented as one homogeneous fluidised phase below two interacting phases; and that the stress is transmitted equally to each phase across the boundary. It would therefore be reasonable to expect results of only the same order of magnitude.

This analysis does, however, confirm that, for boundary condition set 2, the homogeneous phase itself is much more stable in water fluidised beds than in air fluidised beds, whilst the boundary between this phase and the particle free support fluid, (with the support fluid underneath) is much less stable.

TABLE 5

Comparison With the Stability of the State of Uniform Fluidisation

Description of System of Anderson & Jackson (1967, 1968)	Solution of Anderson & Jackson			Description of Equivalent System Solved Here	Solution of this Work		
	ξ max sec^{-1}	η at ξ max sec^{-1}	K at ξ max cm^{-1}		ξ max sec^{-1}	η at ξ max sec^{-1}	K at ξ max cm^{-1}
2000 micron diameter glass particles/water μ_b = 70 poise	0.38	6.6	1.2	2000 micron diameter glass particles/water μ_b = 20 poise	0.27	20.7	5.3
Glass particles/air μ_b = 8 poise	52.0	84.0	3.5	210 micron diameter Glass particles/air μ_b = 8 poise	18.6	27.3	12.9
Glass particles/air μ_b = 16 poise	39.0	64.0	2.2	370 micron diameter Glass particles/air μ_b = 16 poise	79.0	25.0	6.1
Glass particles/air μ_b = 32 poise	25.0	45.0	1.5	490 micron diameter Glass particles/air μ_b = 32 poise	130.0	15.0	7.5

SECTION 2D: DIMENSIONAL ANALYSIS

A number of investigations have been made (Wilhelm and Kwauk (1948); Romero and Johanson (1962); Doitchev (1973)) into the use of dimensional analysis in order to propose a criterion to distinguish between particulate and aggregative fluidisation.

Wilhelm and Kwauk proposed the use of the dimensionless Froude number, $Fr\left[= \frac{U_o^2}{gd_p}\right]$, for this criterion, such that:-

$Fr > 1.0$ - aggregative fluidisation (bubbling)

$Fr < 1.0$ - particulate fluidisation (non-bubbling)

- - - - - - - - (2D.1)

However, Wilhelm and Kwauk gave no theoretical justification for the use of this group nor for the limit set: Wilhelm and Kwauk found that the experimental systems which they investigated could be characterised in this way, and their classification remains a most useful guide to the type of fluidising behaviour to be expected.

By casting the solution due to Rice and Wilhelm (1958) into dimensionless form, Romero and Johanson (1962) defined the dimensionless groups on which the stability of a fluidised system depends. The simple solution (model 1 of Rice and Wilhelm) exposed the groups Fr, R_{eF}, $(\frac{1-\rho}{\rho})$; (and π a length ratio) and Romero and Johanson claimed that a linear combination of these groups gave a better criterion for ordering fluidised systems in terms of stability than did Fr alone. viz:

$Fr\ R_{eF}\ (\frac{1-\rho}{\rho}) > 100$ aggregative fluidisation

$Fr\ R_{eF}\ (\frac{1-\rho}{\rho}) < 100$ particulate fluidisation

- - - - - - - - - - (2D.2)

Once again, no justification was given for the combination of groups used in this criterion, other than that these three groups were those defined by the solution of Rice and Wilhelm. The limit set for the criterion was determined by calculating its value for many systems of known behaviour.

Doitchev (1973), by calculating the amount of energy required to transport the fluid in excess of that required for minimum fluidisation,

a with bubbling, and

b without bubbling, was able to predict that:

when $N_f > 143$ - aggregative fluidisation

$N_f < 143$ - particulate fluidisation

- - - - - - - - - - - - - (2D.3)

Where $N_f = \sqrt{\frac{g d_p^3}{\mu_F^2} (\rho_p - \rho_F) (\rho_p(1-\epsilon_o) + \rho_F (\epsilon_o))}$ - - - - - - - - - (2D.4)

Now, as $(\rho_p - \rho_F)$ and $(\rho_p (1-\epsilon_o) + \rho_F \epsilon_o)$ are of the same order, it can be seen that, approximately:-

$$N_f = R_{eF} \cdot \left(\frac{1-\rho}{\rho}\right) \cdot Fr^{-\frac{1}{2}}$$

Thus, Doitchev seems to have improved the criterion due to Romero and Johanson, equation (2D.2), by theoretically justifying a combination of the dimensionless groups proposed and also theoretically justifying their limit. However, Table 3 shows that the criterion due to Doitchev, equation (2D.3), does not in fact order the given fluidised systems as well as that due to Romero and Johanson. In fact, nearly all the systems studied here lie above the critical value. This is due to an assumption which Doitchev made. To calculate the critical value, N_{fcrit} it is necessary to assume a value for the average bubble size, d_b, since N_{fcrit} depends on the ratio

$\frac{\text{Bubble diameter}}{\text{particle diameter}}$, $(\frac{d_b}{d_p})$ and the voidage at incipient fluidisation, ϵ_o.

Then, the assumption $\frac{d_b}{d_p} = 1.0$ and $\epsilon_o = 0.4$ leads to $N_{fcrit} = 143$.

However, values of $\frac{d_b}{d_p} >> 1.0$ (thus $N_{fcrit} >> 143$) could still give a particulately fluidised system, so that the designated critical value, $N_f = 143$ seems to be somewhat below the correct limit.

Using a similar method to Romero and Johanson on the present analysis, reveals the dimensionless groups $(\frac{1-\rho}{\rho})$, Fr, R_{eF} and μ (and π, a length ratio). A linear combination of these groups should provide a more powerful ordering system than that of Romero and Johanson, as the additional group, μ, shows similar trends to the other groups (ie for a given system, μ is proportional to the density group (Hagyard and Sacerdote (1966)); is large for air fluidised systems and small for water fluidised systems) and also decreases with particle diameter for a given fluidising fluid, and should thus broaden the range of the criterion.

It might therefore be expected that the inclusion of the viscosity group would improve the criterion, especially for those systems close to the limit between aggregative and particulate fluidisation.

The linear combination of these groups gives, approximately:-

$\mu . (\frac{1-\rho}{\rho}) . R_{eF} . Fr > 2 \times 10^5$ - aggregative fluidisation

$\mu . (\frac{1-\rho}{\rho}) . R_{eF} . Fr < 2 \times 10^5$ - particulate fluidisation

-------- (2D.5)

Again, there is no justification for the combination of groups used here, and the limit set for the criterion was determined by calculating its value for many systems of known behaviour.

Table 6 shows a comparison between these four criteria for known physical systems. It can be seen that Wilhelm and Kwauk's original classification, in terms of Froude number alone, gives a correct ordering of the systems in terms of stability. The added refinements which follow from this analysis and that of Rice and Wilhelm does not lead to any significant improvement in the prediction of the type of fluidising behaviour to be expected. However, it should be remembered that the linear combination of groups proposed here and by Romero and Johanson are merely the simplest combinations possible. Further theoretical studies would be necessary to determine a combination of these groups which has physical justification, and this may then lead to a better criterion.

TABLE 6

Comparison of the Criteria Proposed for the Prediction of the Stability of Fluidised Systems

System	Wilhelm & Kwauk (1958) Fr	Romero & Johanson (1962) $(\frac{1-\rho}{\rho}).Fr.R_{eF}$	Doitchev (1973) $(\frac{1-\rho}{\rho})R_{eF}.Fr^{-\frac{1}{2}}$	This Work $(\frac{1-\rho}{\rho}).R_{eF}.Fr.\mu$	Observed Nature
1010 micron diam Glass/water	0.0080	0.117	164	50.0	Particulate*
3360 micron diam Socony beads/water	0.0088	0.292	354	876	Particulate*
4580 micron diam Socony beads/water	0.0099	0.520	527	2.81×10^3	Particulate*
5180 micron diam glass/water	0.036	12.0	1760	1.03×10^5	Particulate*
55 micron diam Glass/air	0.046	1.88	189	2.21×10^4	Transitional**
1280 micron diam Lead/water	0.130	65.7	1400	2.82×10^5	Transitional*
100 micron diam Glass/air	0.230	50.5	455	1.31×10^6	Aggregative**
210 micron diam Glass/air	1.47	2.5×10^3	1400	1.26×10^8	Aggregative**
280 micron diam Glass/air	2.05	6.4×10^3	2160	4.33×10^8	Aggregative**
370 micron diam Glass/air	3.79	2.5×10^4	3390	2.7×10^9	Aggregative**
490 micron diam Glass/air	18.7	4.0×10^5	5000	8.8×10^{10}	Aggregative**

*Data from Wilhelm and Kwauk (1958)

**Data from experimental measurements

CHAPTER 3: BUBBLE STABILITY

3.1 A Theory for Bubble Splitting

As it stands, the theory developed in section 2 cannot be expected to yield much information about bubble stability. The analysis holds good only for a plane horizontal surface, with no relative motion between the phases. On the other hand, in a complete consideration of the stability of a bubble roof, the curvature of the equilibrium surface and the velocity and voidage profiles in all phases in the region of this surface must be considered. Rather than attempt a description of this complex situation the results obtained in the solution in section 2 are used to establish a qualitative theory for bubble stability.

Observation of the mechanism of bubble splitting in fluidised beds suggests that some estimate of the likelihood of bubble splitting could be based on a comparison between the speed at which the disturbance develops and the speed at which it would be swept away around the bubble surface. As Rowe (1971) observes 'the upper boundary commonly develops downward pointing cusps which frequently grow rapidly into long fingers ... (which) run around the edge to be lost eventually near the wake ... but some grow so fast relative to their lateral movement that they divide the bubble'.

In order to apply the earlier theory to the bubble boundary it is necessary for the bubble roof to be assumed flat - that is, for the wavelength of the disturbance to be small with respect to the curvature of the bubble roof. Clearly this will be only rarely true as, too, will be the assumption that the disturbance is so large relative to the particle dimensions that the continuum assumption remains valid.

In the solution obtained in section 2A, a disturbance of initial amplitude A' has the subsequent form $\eta = A' \exp(-ky + nt) \cos Kx$ ---- (3.1)

which with $y = 0$ has the maximum value $\eta_{max} = A' e^{nt}$ ---- (3.2)

The time for this disturbance to grow to $\eta = d_b/2$, say, is thus

$$\tau_1 = \frac{1}{n} \log_e \left[\frac{d_b}{2A'} \right] \qquad \text{---------- (3.3)}$$

The solution to the perturbation equations is, of course, a standing wave. However, the particles moving around the surface of the bubble are essentially falling under gravity (see, eg Hargreaves and Pyle (1972)) and to an approximation it might be expected that the disturbance will be swept around the bubble with the particleswhilst it is growing. Of course, in practice there would be an interaction between these two movements, but here it is assumed that they may be superposed. The time for the particle to move a distance $d_{b/2}$ is thus of order:-

$$\tau_2 = \sqrt{d_b/g} \qquad \text{---------- (3.4)}$$

and it can thus be postulated that if $\tau_2 >> \tau_1$ splitting would occur, and vice versa.

Setting $\Upsilon = \tau_2/\tau_1 = n \sqrt{d_b/g}/\log_e (d_{b/2A'})$ ---------- (3.5)

then if $\Upsilon >> 1$, the bubble tends to split, and

if $\Upsilon << 1$, the bubble should be relatively stable.

An approximate condition for the transition between relative stability and instability is thus $\Upsilon = 1$, and equation (3.5) gives, for the critical bubble diameter:-

$$\sqrt{\frac{d_{b\ crit}}{g}} = \frac{1}{n} \log_e \left[\frac{d_{b\ crit}}{2A'} \right] \qquad \text{---------- (3.6)}$$

It seems reasonable to assume that the stability of different systems may be compared on the basis of initial disturbances which are proportional to the particle diameter. The solution to equation (3.6) is shown in Figures 14 and 15. Figure 14 is calculated from equation (3.6) using values of n from the solution of boundary condition set 2 (large interstitial fluid momentum). Figure 15 is calculated from equation (3.6) using values of n from the solution of boundary condition set 6 (zero interstitial fluid momentum).

The region of stability corresponds to that underneath the curve, which is not monotonic in d_b. Thus, for a given range of initial disturbances, there appear to be both a minimum and maximum possible stable bubble diameter. From Figures 14 and 15 it can be deduced that the region of stability of gas fluidised systems is much larger than that of liquid fluidised systems. For example, for initial disturbances of, say 50 d_p, water-fluidised systems would be completely unstable, whilst gas-fluidised systems remain very stable. It can be seen that the choice of boundary condition set has little effect on the solution to equation (3.6).

On the basis of the present simplified analysis, then, the non-existence of bubbles in liquid-fluidised beds, and their relative stability in gas-fluidised beds can be explained, at least in qualitative terms. Moreoever, it does not appear as if bubble diameters should be seriously limited by the splitting mechanisms proposed here.

3.2 Comparison with Other Theories

The results of the analysis presented here predict the existence of both a maximum and minimum stable bubble diameter. The relation of this prediction to the maximum and minimum stable bubble diameters

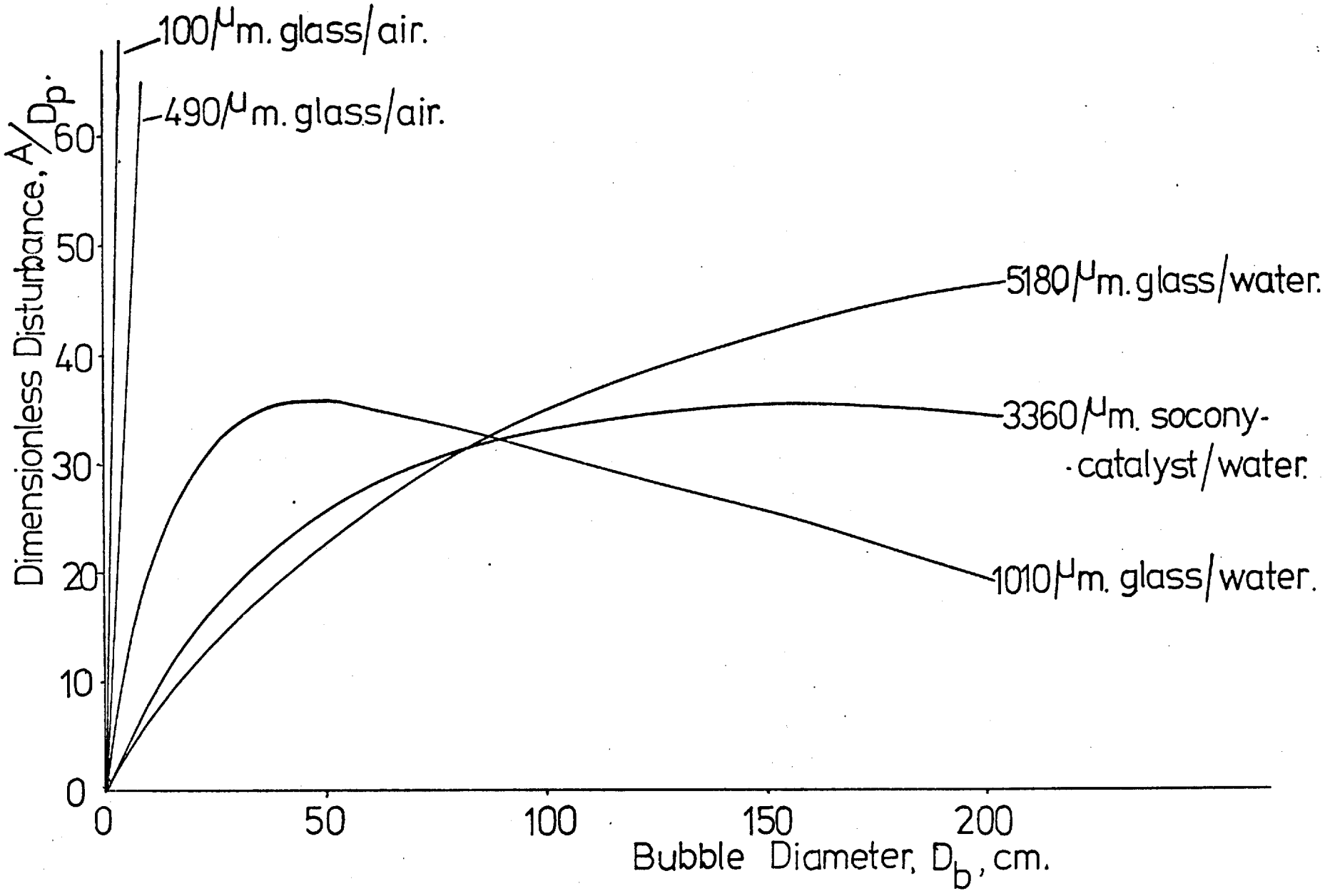

Figure 14: Stable bubble diameters; comparison of regions of stability for gas and liquid fluidised systems: boundary condition set 2

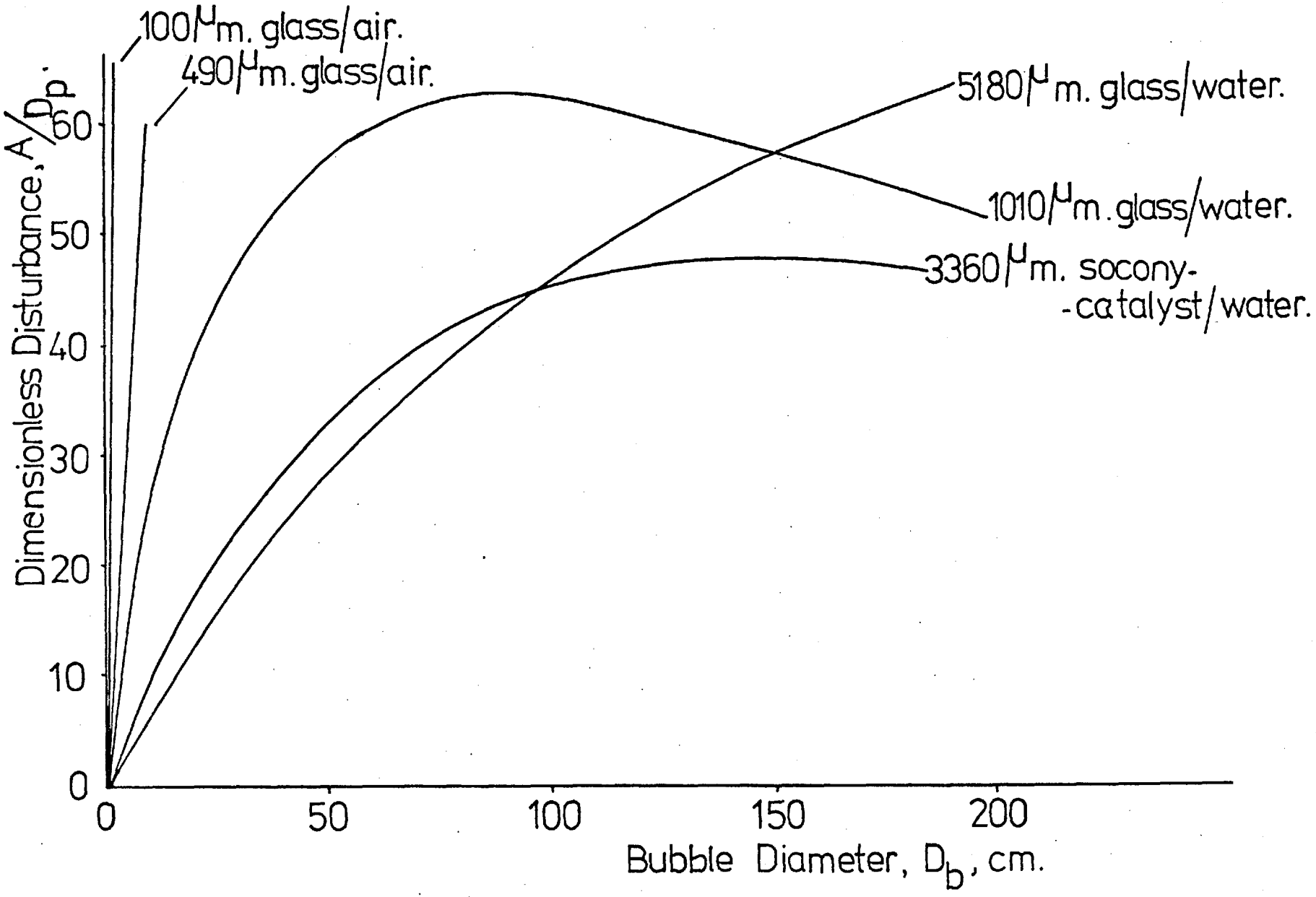

Figure 15: Stable bubble diameters; comparison of regions of stability for gas and liquid fluidised systems: boundary condition set 6

predicted by Davidsonet al (1961) and Godard and Richardson (1969) (see section 1.4) is considered. The present work reveals, for the maximum stable diameter, the limit above which splitting from the roof is likely, while the work of Davidson et al proposes a limit above which another form of instability (never yet observed under natural conditions) should occur. Similarly, a bubble larger than the Godard and Richardson minimum stable diameter may still be susceptible to splitting, and in fact may continue to divide by this process until it becomes, under the Godard and Richardson criterion, too small to exist.

Comparison of the size of maximum and minimum bubble diameters predicted here with those of the other workers is of limited applicability, as both depend explicitly on the amplitude of the initial disturbance, A'. Calculation of a specific maximum or minimum bubble diameter for any given system would thus involve artificially specifying the size of the initial disturbance.

Clift, Grace and Weber (1973) also attempted to use the results of their analysis of the stability of a horizontal interface to predict the likelihood of bubble splitting. They use, as their two time scales:

$\tau_1 = \frac{1}{n}$, or the time for the disturbance to grow by a factor e

$$\tau_2 = \sqrt{\frac{d_b}{2g}} \quad \log_e\left(\frac{1}{\tan(\theta/2)}\right)$$

Where θ is the angle from the bubble nose at which the disturbance originates.

Using a similar criterion of $\tau_1/\tau_2 = 1$ they drew a stability chart of τ_1, τ_2 vrs λ, the disturbance wavelength with the bubble diameter as a parameter. This then predicts the wavelength of the disturbance which causes splitting (small λ; disturbances are swept aside; large λ, bubble tends to split); whereas the present analysis assumes that the 'most dangerous' wavelength will always be dominant and is thus used as the basis for comparison and calculation. The conclusions then differ in as much as Clift et al predict that all bubbles are unstable, at some disturbance wavelength, whereas the present analysis assumes that the disturbance wavelength is constant for a given physical system, the bubble stability then depending on its diameter.

Measurements of the disturbance wavelength reported here (Table 7) for different systems show that the wavelength appears fairly constant for any given system and this provides some support for the assumption made in this analysis.

It must be pointed out that neither analysis can be used to obtain quantitative results for bubble stability without further information on the initial amplitude of the disturbance.

3.3 Experimental Study of Bubble Splitting

The movement and splitting characteristics of bubbles in a two-dimensional air-fluidised bed were observed and measured. The bed had the dimensions 30 cm x 120 cm x 1.5 cm and had a porous plastic (Vyon) distributor. Results were obtained for the closely graded particle systems recorded in Table 7.

The bubbles were observed using cine-photography at a frame speed of up to 64 frames/sec using angled back-illumination. The film was

analysed frame by frame on a frame analyser to find the frequencies of bubble splitting as a function of bubble size, and also to measure the growth rates and wavelengths of the observed disturbances.

For each system studied, approximately 13,000 bubbles were observed, and the growth rate and wavelength measurements recorded for approximately 30 bubbles of diameter between 3 and 15 cm.

The movement and splitting characteristics of injected bubbles of water in a two-dimensional water-fluidised bed were also observed by the same technique. The bed had the same dimensions as that used for air-fluidisation and had a fine filter-cloth distributor. A simple method of injection was employed: namely, an injection tube was inserted, flush with the bed wall and connected to a manually operated valve. No attempt was made to meter the injected volume. Unfortunately, no measurements of growth rates could be obtained, so that the results presented here are qualitative only.

TABLE 7

a Bubble Stability for Glass/Air Systems

Particle Diameter d_p, microns	Minimum Superficial Fluidising Velocity U_o, cm/sec	Measured Growth Rate sec^{-1}	Measured Disturbance Wavelength, cm
490	30.0	26.0	4.0
280	7.5	29.5	3.8
210	5.5	22.2	2.8
100	1.5	16.5	2.2

b Physical Parameters of the Non-Spherical Sand/Air System

Particle Diameter Microns	599	500	422	353	251
Wt % Retained at Diameter	4.4	37.6	53.7	4.3	0.0

Surface mean diameter = 440 microns

Minimum superficial fluidising velocity = 23.5 cm/sec

3.4 Results and Discussion

Figure 16 shows a typical bubble in a gas fluidised bed in the process of splitting. The sequence of photographs illustrates quite clearly how the growing fingers of particles are swept around the surface of the bubble. In Figure 17a one such finger is seen to finally split off a small section of the original bubble. It is also possible to estimate a mean wavelength, λ, for the disturbance: Figure 17b shows a clear waveform on the roof of the bubble and measurements of these characteristic wavelengths and growth rates are found to be approximately constant for each particle size and, independent of bubble diameter. Table 7 records these values; the figures given being the arithmetic mean of approximately 30 experimental measurements. These results are also shown in Figures 10 to 13, where the spread of the experimental measurements can be seen.

Figures 18, 19 and 20 show the behaviour of water bubbles injected into a water fluidised bed of 490, 280 and 100 micron diameter glass particles, respectively. Although no measurements of growth rates could be obtained, the photographs illustrate quite clearly that bubbles in liquid fluidised beds do indeed split from the roof rather than by collapse started from the wake (Davidson et al (1961)). This observation is borne out by Clift and Grace (1972) who observed that bubbles injected into a water fluidised bed of 1300 micron diameter lead shot, split only from the roof. Figure 20 also shows a wave-like disturbance of the roof, so that it does seem likely that there will be a characteristic disturbance wavelength and growth rate associated with water fluidised beds.

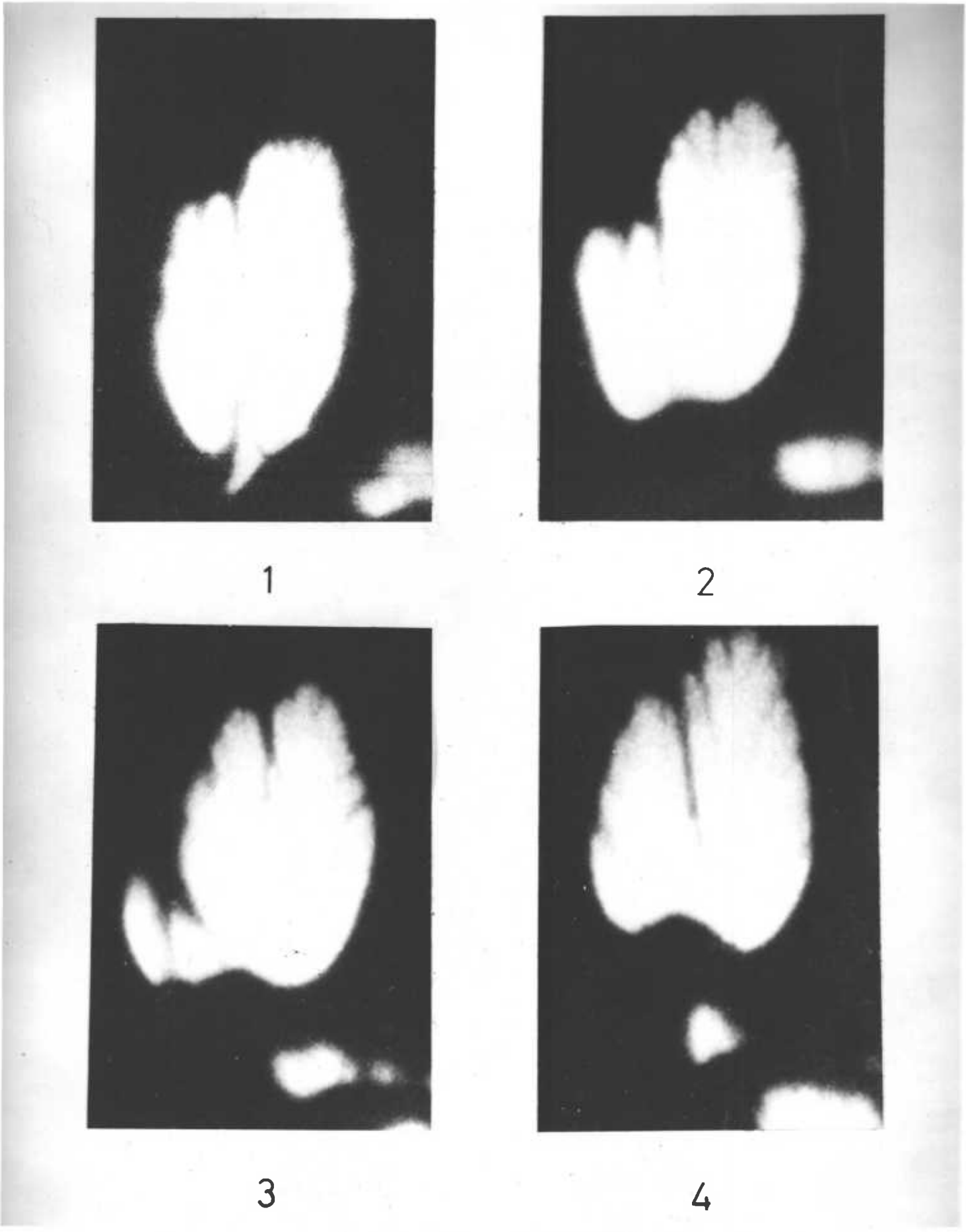

Figure 16: Fingering in a bubble in a gas fluidised bed

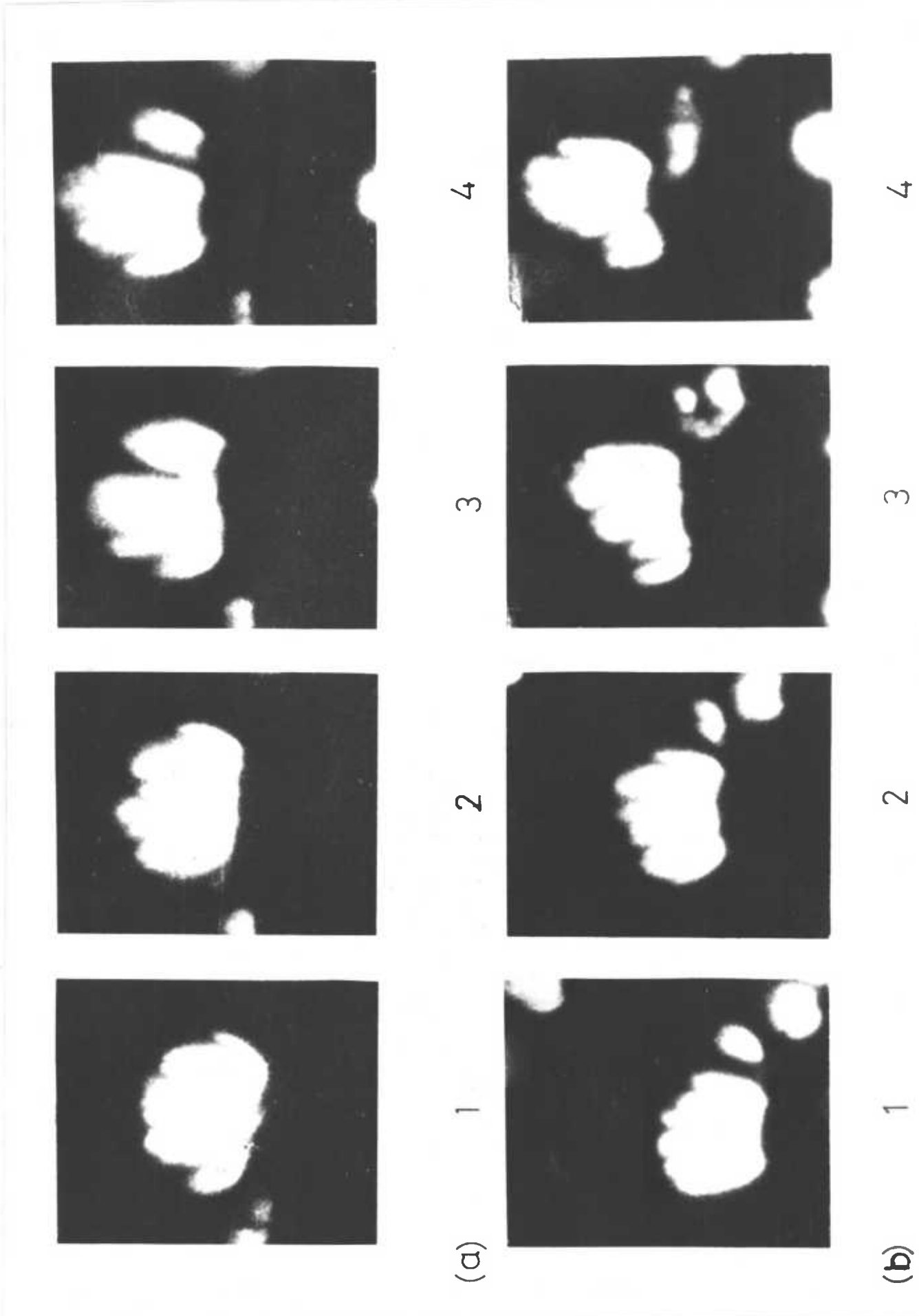

Figure 17: Splitting caused by fingering in a gas fluidised bed

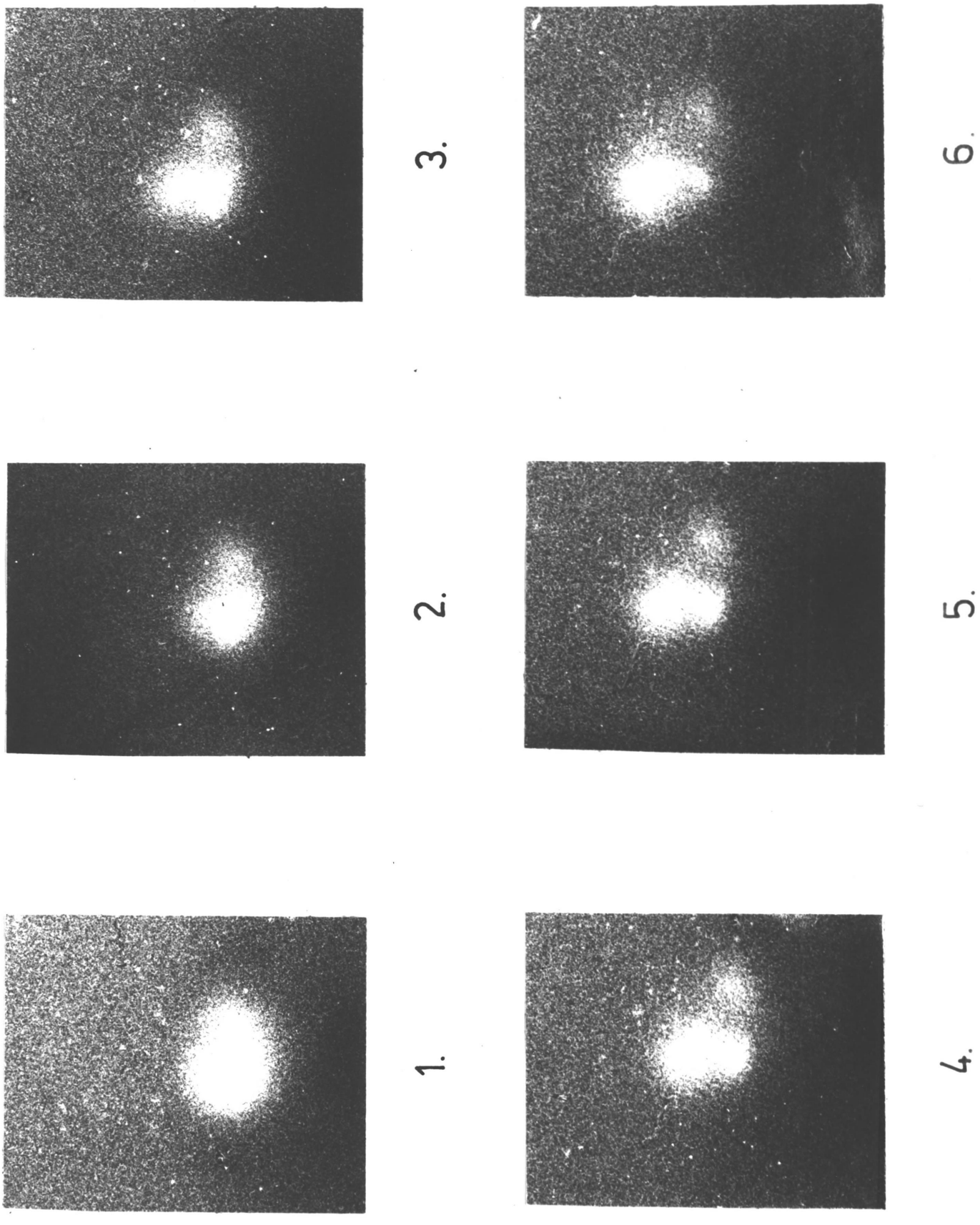

Figure 18: Behaviour of a bubble in a water fluidised bed

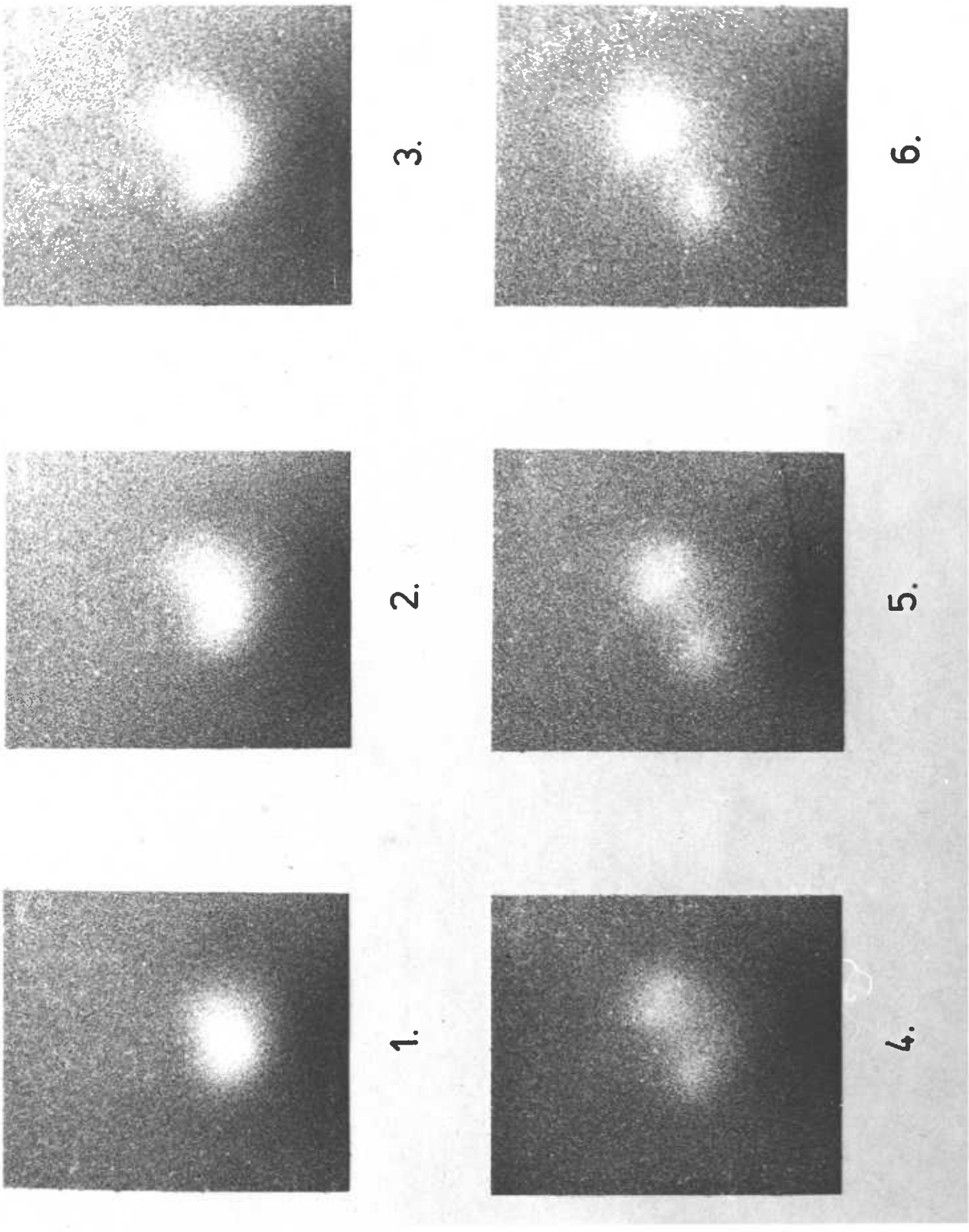

Figure 19: Behaviour of a bubble in a water fluidised bed

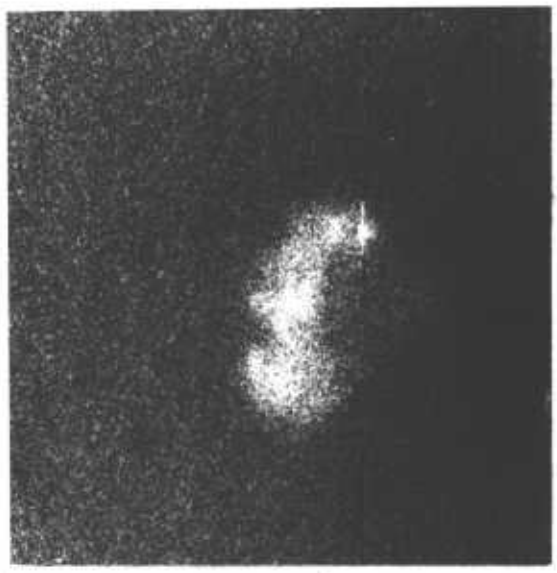

3.

2.

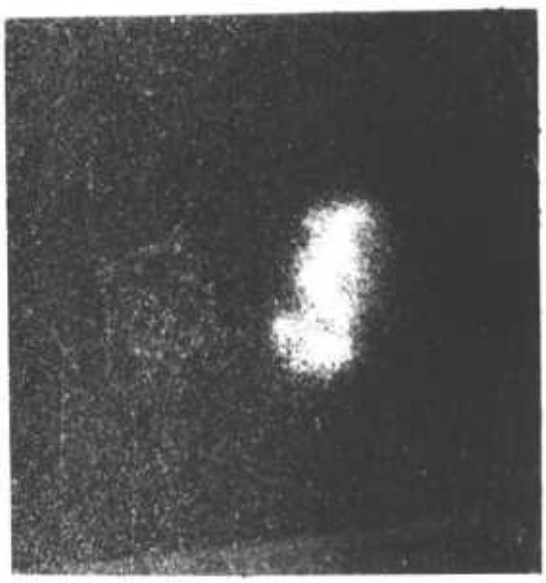

1.

Figure 20: Behaviour of a bubble in a water fluidised bed

The measured values of the disturbance growth rates and dominant wavelengths can be compared with theoretical values between Tables 7 and 4, or, better, in Figures 10, 11, 12 and 13. The values do not agree quantitatively although trends are similar in both cases; it may be that the experimental results represent a sub-harmonic of the theoretical predictions. The experimental results would seem to add weight to the suggestion that the correct boundary conditions lie somewhere in between the assumption of zero or large interstitial momentum (ie set 6 or set 2). It must again be emphasised that the theory is in any case only true for infinitesimal disturbances. The experimental results, on the other hand, refer to the characteristics of finite amplitude disturbances.

Measurements of the frequency of bubble splitting as a function of size are presented in Figure 21. For clearer representation, the results are shown as smoothed curves rather than in histogram form. The given experimental curves are the result of analysis of approximately 4000 frames of cine film for each system. Their form is independent of fluidising velocity, this is not shown, but for each system the results consist of the sum of the results at several fluidising velocities (up to 4x the minimum fluidising velocity), each of which show the same characteristic form.

The theoretical boundary between stability and instability is not sharp, for the criterion that $\Upsilon = 1$ should divide the two regions is at best an approximate one. For a system with a wide range of initial disturbances it is to be expected that the theoretical line in Figure 21 will be S-shaped, and the experimental results do in fact have the expected form.

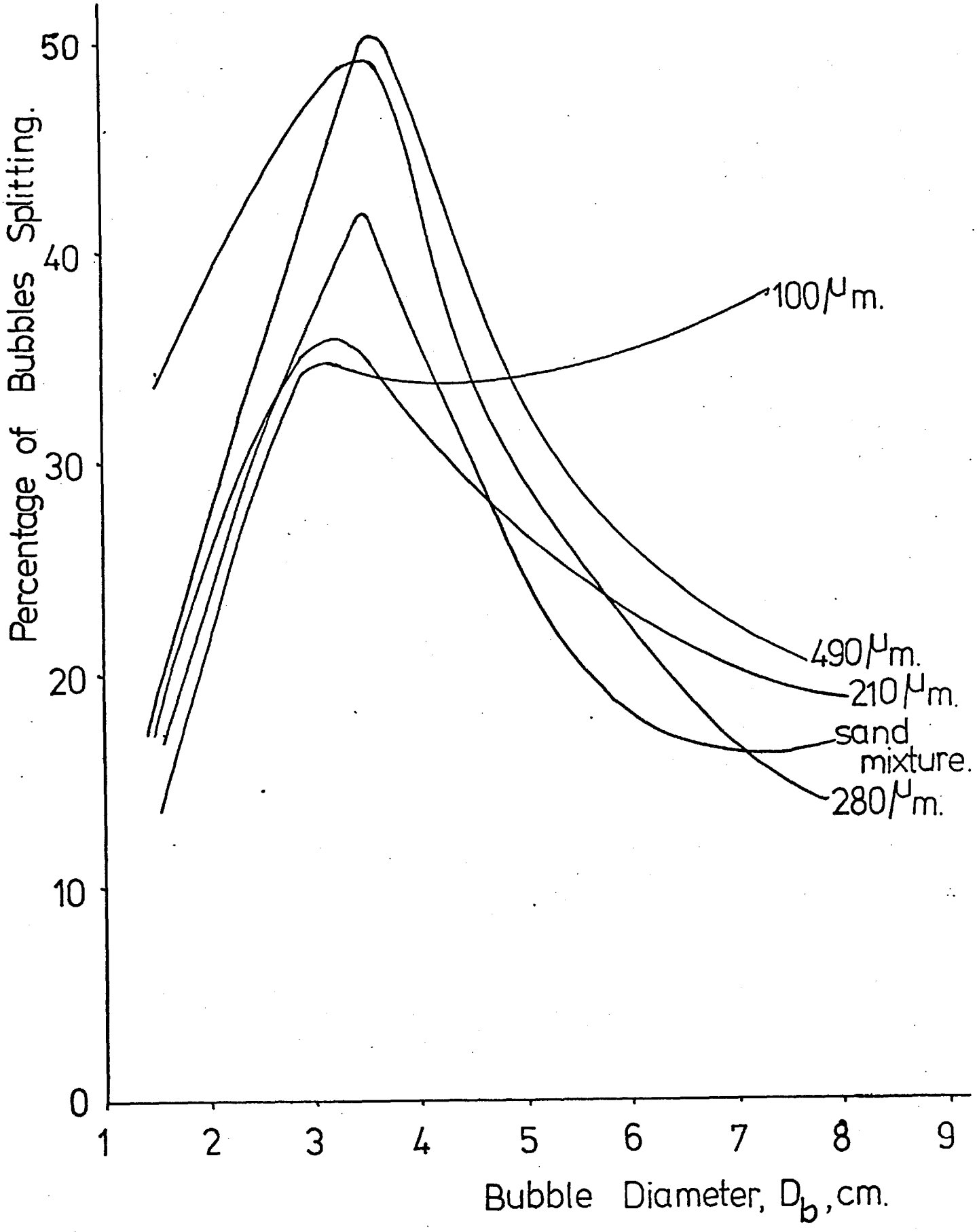

Figure 21: Experimental values of the frequency of bubble splitting, in air fluidised systems

The initial turning down of the curve is due to the effect of rapid coalescence of the smaller bubbles. These, being extremely numerous, coalesce so quickly that their life span is too short for splitting to be important. Also, the assumption of two-dimensional motion will be less nearly correct for small bubbles whose diameter is comparable to the bed thickness. Splitting in a plane other than one parallel to the viewing plane would not be observed. Rowe (1971) points out that, in three-dimensional bubbles, splitting can indeed occur at any angle to the vertical axis, whilst in two-dimensional bubbles, it occurs only in a direction normal to the plane of the bubble.

Coalescence also appears to be important both for small particle systems and at larger bubble diameters. In both cases, coalescence was seen to be a very violent process, often inducing splitting immediately afterwards, so that the splitting frequency is apparently more dependent on the frequency and scale of the coalescence rather than on the growth of disturbances as proposed here.

The trend of the results with respect to the minimum bubble diameter is very encouraging. It can be seen from Figure 21 that the minimum bubble diameter increases with increasing particle diameter d_p. Figures 14 and 15 both show that for a given (dimensionless) initial disturbance, the minimum bubble diameter should increase, for glass/air systems, with d_p.

Apart from the difficulties in comparing a theory for the initial motion of infinitesimal disturbances with experimental data, a further problem must be pointed out. The theory has been developed for systems containing uniformly sized particles. On the other hand, in any practical situation, even a laboratory experiment of the type carried

* See page 87a

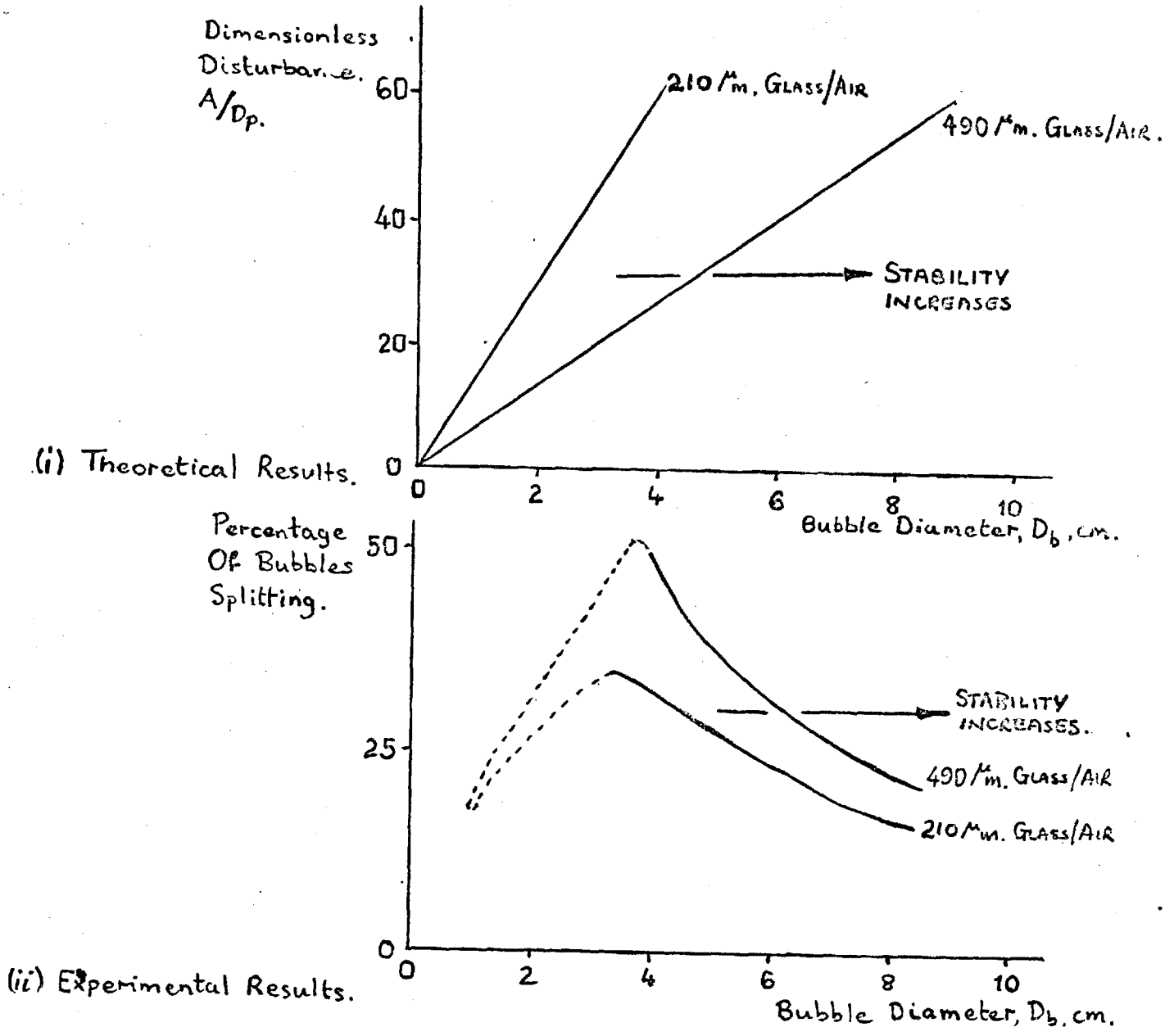

Figure 21a: Comparison of experimental and theoretical bubble stability in air fluidised systems

In the experimental results, Figure 21a (ii), the initial section of the graph is shown as a broken line; here, the bubble behaviour is governed by coalescence. That is, the bubbles are so small and numerous, and coalesce so readily that disturbances on their boundaries do not have time to develop fully.

Once the bubble behaviour ceases to be dominated by coalescence (full line, Figure 21a (ii)), it can be seen that the tendency to split decreases with bubble diameter. This is in complete agreement with the theoretical predictions, Figure 21a (i) (see also Figures 14 and 15) where the bubble stability can be seen to increase with the bubble diameter.

out here, there will be present a distribution of particle sizes. The results in Figure 21 for the non-spherical sand mixture of wide particle size range show that the minimum bubble diameter is decreased by the non-ideality of the system, but it is not known to what extent each of the two factors operate.

It can be seen in Figure 21 that the minimum stable bubble diameter with respect to splitting is between 3 and 5 cm. The experimental results of Godard and Richardson (1969) show that the minimum bubble diameter is 0.5 cm, but, as pointed out in section 3.2, the Godard and Richardson analysis predicts the bubble diameter below which a bubble cannot exist, whereas the present work predicts the diameter below which a bubble tends to split. The two results are not therefore contradictory.

CHAPTER 4: STABILITY OF VERTICAL CHANNELS IN FLUIDISED BEDS

4.1 Introduction

Another interface between the particle free 'support' fluid and the homogeneous fluidised bed phase of great interest is the vertical interface, say the wall of a channel or spout.

Channelling, on a large scale, is an abnormality in the behaviour of a fluidised system, characterised by the establishment of flow paths in the bed of solids through which disproportionately large amounts of fluid pass. This can occur in both gas and liquid fluidised systems (see Hasset (1961)). It is particularly important in industrial fluidisation, where the fluid distribution is usually through a small number of geometrically spaced holes, so that preferential fluid flow paths are common. As this leads to poor fluid-solids contacting and mixing, it is undesirable in most situations, and so a greater understanding of the factors affecting the stability of these channels should help in the design of more efficient fluidised beds.

It is also thought that channelling may be responsible for the initiation of bubbles in fluidised beds. Particularly with a distributor of the sieve-plate type, the fluid will enter the bed as jets (or in channels) which penetrate the dense phase, breaking up to form bubbles. (Zenz (1968); Fakhimi and Harrison (1970); Chiba, Terashima and Kobayashi (1972)).

There are many physical factors which seem to effect the formation of channels in fluidised systems, for example, the shape, density and size of the particles, the fluidising velocity and the bed history.

Matheson, Herbst and Holt (1949) reported channelling behaviour for beds of synthetic cracking catalyst of 10 microns diameter when aerated at velocities up to 1 fps. For the same material of 40 microns diameter, no channelling was observed for fluidising velocities as low as 0.01 fps.

Leva (1959) reported that the tendency towards channelling increases as the sphericity factor decreases, ie non-spherical particles are more susceptible to channelling.

Godard and Richardson (1969) reported that severe channelling in air fluidised beds of fine solids could be overcome by the rotation of a paddle within 1 cm of the distributor. Withdrawal of the paddle does not then return the bed to its former channelling state.

In some cases, a vertical channel is deliberately induced in a fluidised system, in fact, the spouted bed technique often permits fluidisation of solids that are too coarse for normal fluidisation. Spouting is achieved by forcing the fluid through one channel (spout) and, by using a conical based vessel, a cyclic particle movement is achieved.

Once again, the stability of the spout depends on the physical parameters of the system (namely, spout and bed diameter, cone angle, fluid velocity, particle size and distribution and bed depth). These are well reviewed by Mathur (1971). The main parameter of interest here is the maximum stable spout height (or the maximum spoutable bed depth), for which many correlations have been presented (again see Mathur (1971)). If the bed depth is greater than this, the spouted bed changes into the normal fluidised state, and it

appears that this occurs when the interstitial fluid velocity near the spout wall approaches the minimum fluidising velocity (Lefroy and Davidson (1969)).

It is hoped that the analysis presented here will explain some of these phenomena.

4.2 Equations of Motion for Channelling and Their Solution

If the wall of a (2-dimensional) channel is considered to be a plane vertical interface between the 'support' fluid (particle free fluid in the channel) and the two interacting fluidised bed phases, all three phases being assumed of infinite extent (see Figure 22b), the analysis will be similar to that already presented for a plane horizontal interface.

The equations of motion governing the behaviour of the three phases are not altered; that is, the two interacting bed phases are governed by the equations based on those of Jackson (1963) and the 'support' fluid governed by the Navier-Stokes equations (equations (2A.1) to (2A.9), see section 2A.1).

The stability of the vertical interface to small wave-like disturbances may then be studied; a major difference from the earlier analysis is that in linearising the equations of motion (2A.1) to (2A.9) the steady state vertical velocity in the support fluid, W_y, is taken to be some (variable) ratio of the incipient fluidisation velocity, so that

$$W_y = \phi U_o \qquad (4.1)$$

where ϕ is a constant.

The use of equation (4.1) allows the effect of variations in the steady state velocity in the channel to be calculated. This is necessary, as the channel velocity may be many orders of magnitude greater

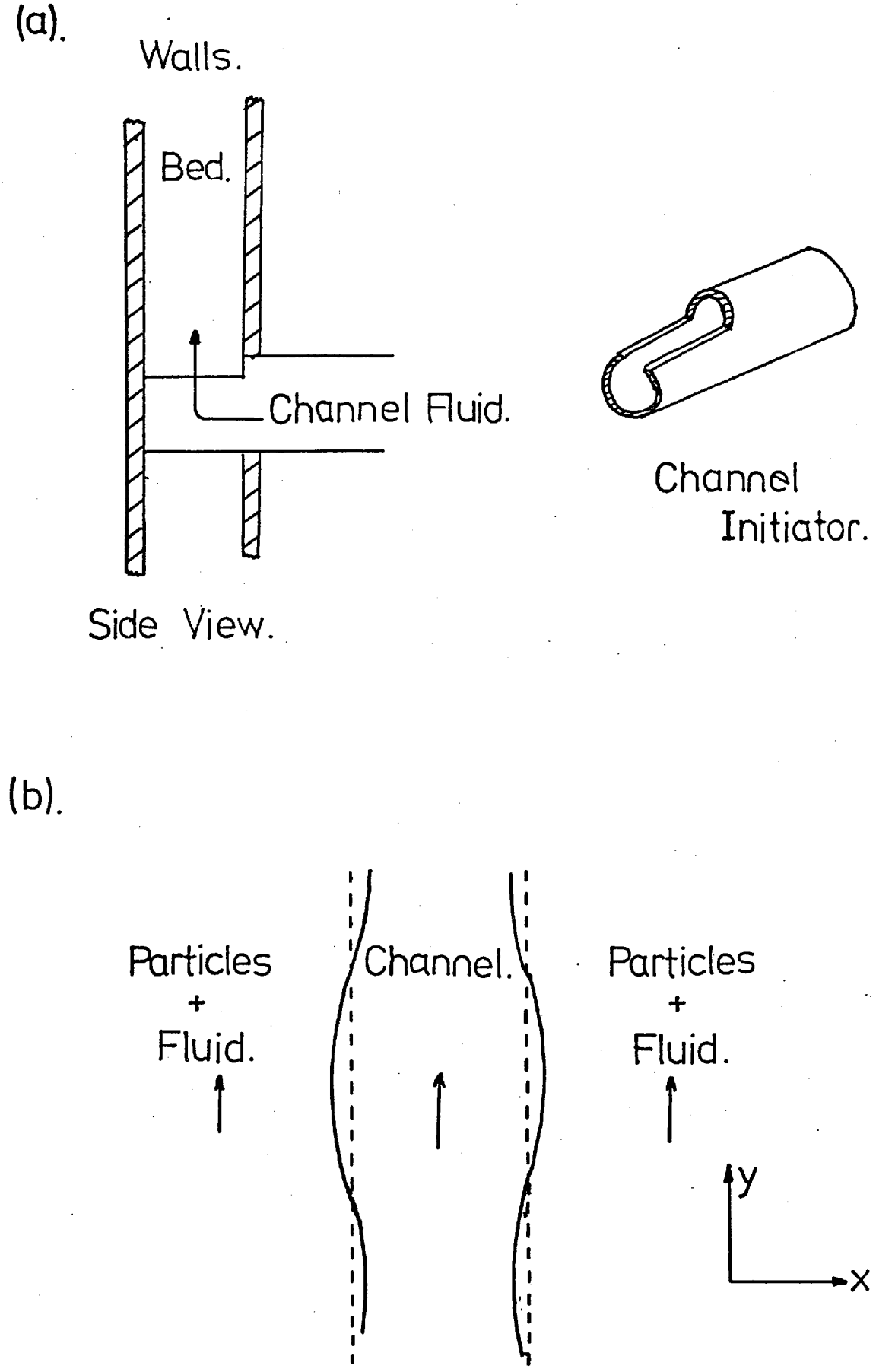

Figure 22: Channel initiator and wavelike disturbance on a plane vertical boundary

than the minimum fluidising velocity.

Using the same techniques as in section 2A.1, the equations of motion are cast into the linearised and dimensionless form; equations (2A.21) to (2A.25) and (2A.27) to (2A.28) continue to hold and equation (2A.26) is replaced by:-

$$\rho\left[\frac{dW_x}{dt} + \phi\frac{dW_x}{dy}\right] + \frac{1}{Fr}\frac{dP_3}{dx} - \frac{1}{R_{ep}}\left[\frac{d^2W_x}{dx^2} + \frac{d^2W_x}{dy^2}\right] = 0 \quad ---- \quad (4.2)$$

Whilst (2A.29) is replaced by:-

$$\rho\left[\frac{dW_y}{dt} + \phi\frac{dW_y}{dy}\right] + \frac{1}{Fr}\frac{dP_3}{dy} - \frac{1}{R_{ep}}\left[\frac{d^2W_y}{dx^2} + \frac{d^2W_y}{dy^2}\right] = 0 \quad ---- \quad (4.3)$$

Where the dimensionless groups are as defined in section 2A.1.

A particular solution to these perturbed, dimensionless equations is then, as in section 2A.2, with the equation (2A.38) for the support fluid pressure replaced by:-

$$P_3 = \frac{Fr\,\rho}{K}(n + \phi K).F.\ \exp(Ky + nt)\ \text{Cos}\ Kx \quad ---------- \quad (4.4)$$

and m_3 given by:

$$m_3^2 - \phi R_{eF} m_3 - R_{eF} n - K^2 = 0 \quad ---------- \quad (4.5)$$

The solution to the equations of motion is then equations (2A.30) to (2A.37) with (4.4) and (4.5). Complete details are given in Appendix 2, section A2.2.

4.3 Boundary Conditions and the Solution Using These Boundary Conditions

Again, as in section 2A.3, six independent and consistent boundary conditions are required.

The boundary is now defined at $x = 0$, the perturbed boundary being $x = \eta(y, t)$. By definition, the boundary is the limit of the particle

phase, thus, the rate of change of the boundary with time,

$$\frac{d\eta}{dt} = V_x \qquad \text{- -} \quad (4.6)$$

Integration of (4.6) gives:

$$\eta = \frac{V_x}{n} = \frac{B}{n} \exp(-Ky + nt) \sin Kx; \quad \text{for } V_x = 0 \text{ at } t = 0 \quad \text{- -} \quad (4.7)$$

The boundary conditions are derived as before by taking material balances across the (slightly) deformed interface and by equating normal and tangential stresses on either side of the surface.

All the arguments put forward in 2A.3 regarding the boundary conditions for the horizontal boundary still hold true for the vertical boundary, so that once again, the six sets of boundary conditions equivalent to those proposed in section 2A.3 could be derived. However, the results for the horizontal boundary show that the two sets of boundary conditions of most interest are sets 2 and 6; it will be recalled that set 2 is derived from the assumption that the interstitial fluid momentum is large and set 6 is derived from the assumption that it is negligible. Thus, only the two sets of boundary conditions equivalent to sets 2 and 6 are derived here for the vertical boundary.

Set 2 gives, on derivation in the same manner as in section 2A.3, the same results, viz, equations (2A.42a), (2A.43) and (2A.50).

Set 6 gives as before, equations (2A.42), (2A.43), (2A.47) combined with (2A.54) together with (2A.48) combined with (2A.55). As this would give an indefinite result, the solution of Clift, Grace and Weber (1973) is re-calculated for the vertical boundary with these boundary conditions, with their equivalent solution to equations

(2A.30) to (2A.37), (4.4) and (4.5) for the solution to their simplified equations of motion.

Substitution of the solution into these boundary conditions gives the general solution:-

$$[M]\,[A\ B\ C\ D\ E\ F]^T = 0 \qquad \text{- - - - - - - - - - - - - - - - - - - -} \qquad (4.6)$$

Where M is a 6 x 6 matrix, for boundary condition set 2 and

$$[M']\,[A'\ B'\ C'\ D']^T = 0 \qquad \text{- - - - - - - - - - - - - - - - - - - -} \qquad (4.6a)$$

Where M is a 4 x 4 matrix for set 6.

The non-trivial solution is then: $\det [M] = 0$ - - - - - - - (4.7)

which degenerates to:

$$n^3 (a) + n^2 (b) + n (c) + d = 0 \qquad \text{- - - - - - - - - - - - - - -} \qquad (4.8)$$

M, M', a, b, c and d are given in Appendix 2, section A2.2, for both sets of boundary conditions.

Equation (4.8) has been solved by digital computer for several known physical systems, with the constant $\emptyset$ as a parameter.

4.4 Predictions from the Theory

The solutions to the theory described above have been found for two different cases:

a The spouting situation, where the gas all flows through the channel, that is, the particle phase is not properly fluidised. Under these conditions, the particle phase viscosity ~~tends to~~ becomes large (see Schugerl et al (1961); as the fluidising velocity approaches the minimum from above, μ_b increases rapidly). In a spouted bed the interstitial gas velocity outside the spout is zero at the foot of the bed and increases up the bed as gas percolates into the bed from the spout.

This situation proved to be always stable for all values of the channel fluid velocity, for both sets of boundary conditions.

b The channelling situation, where the homogeneous phase close to the channel wall is well fluidised. For this situation, the normal particulate phase viscosity values were used.

For the channelling situation, Figure 23 shows a typical solution using the boundary condition set 2. The solution was found for all the systems recorded in Table 4, and all showed the same basic trends. That is, for any given value of the fluid velocity in the channel (ie $\emptyset$ U_o), the channel wall is unstable to small wave-like disturbances; the magnitude of the growth rate of the instability decreasing with increasing channel velocity. At a given channel velocity, the magnitude of the growth rate of the instability also decreases with increasing particle size.

This does explain the presence of a maximum spoutable bed depth in spouted beds; the spout wall remains stable until the height where the particles close to the spout wall become fluidised, at which point the wall becomes unstable. Once the top of the spout breaks up and disturbs the circulatory particle movement, the whole spout collapses. However, none of the other trends of channelling seem to be explained by these results.

Figure 24 shows a typical solution using boundary condition set 6. This solution was investigated for four of the systems presented in Table 4 and for cracking catalyst of 55 micron diameter fluidised with air. The other water fluidised systems given in Table 4 were investigated but found to have only stable solutions for all channel velocities down to 0.1 U_o.

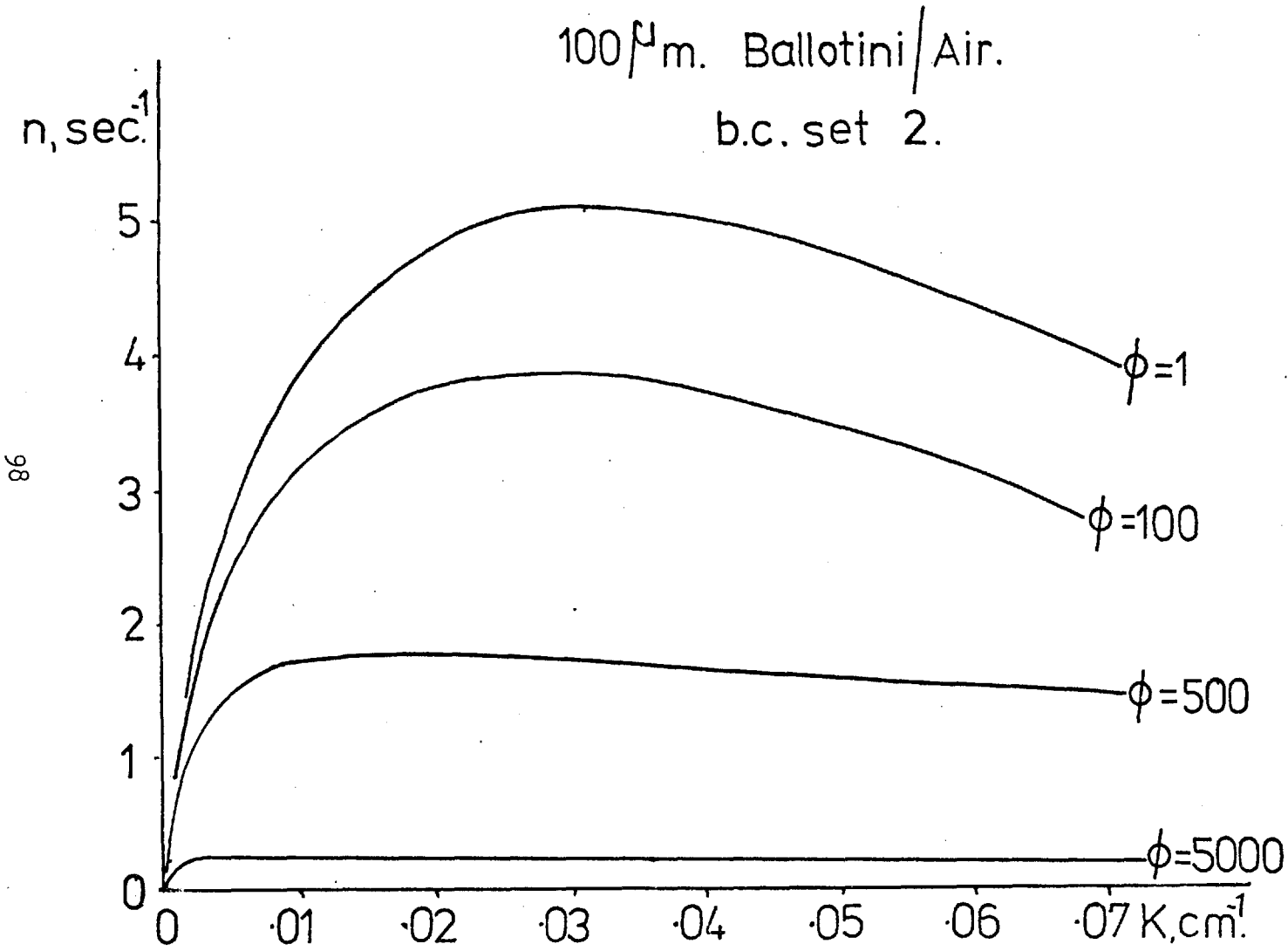

Figure 23: Growth rate of a surface disturbance on a vertical boundary as a function of wave number

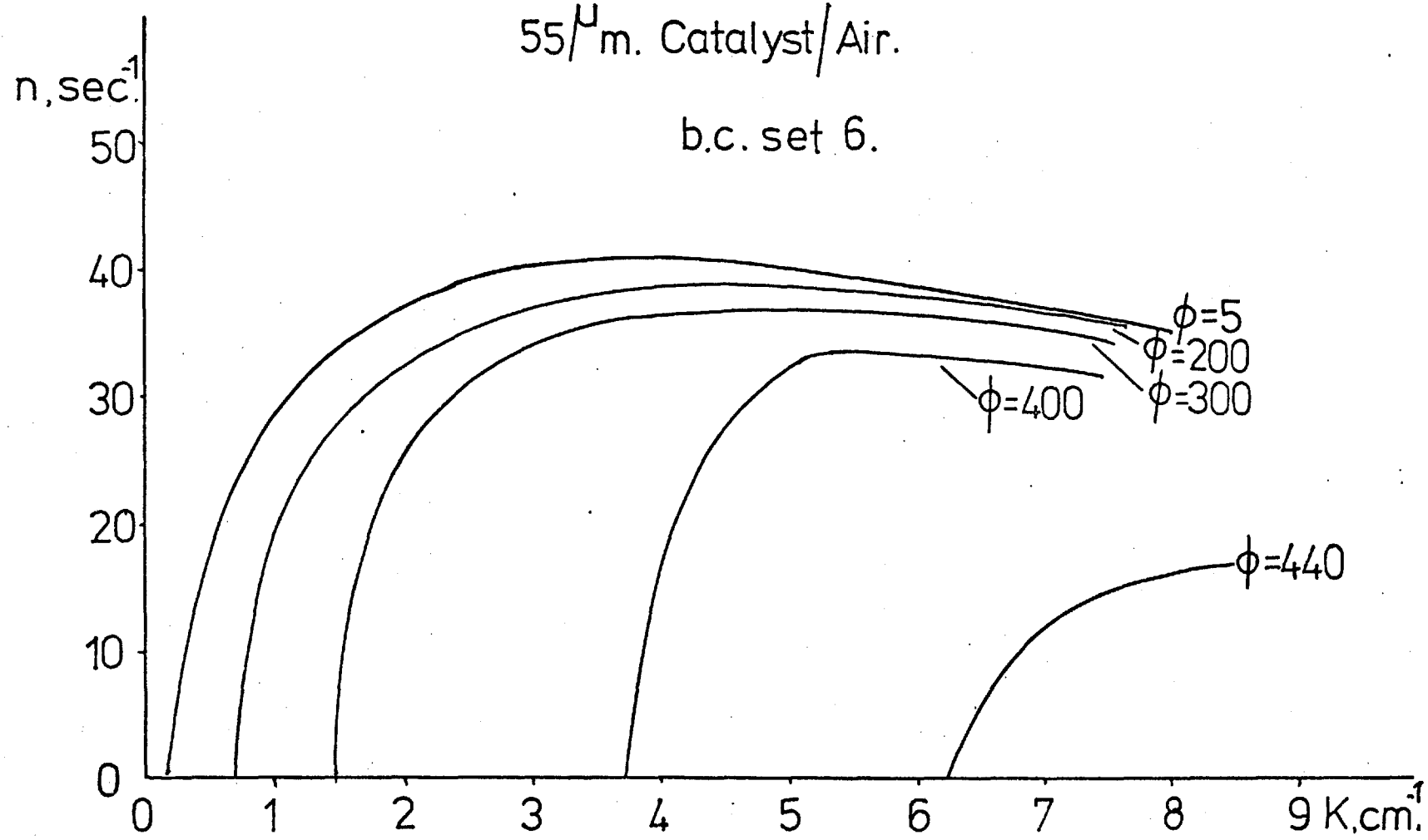

Figure 24: Growth rate of a surface disturbance on a vertical boundary as a function of wave number

It can be seen that increasing the channel velocity makes the boundary stable to large wavelength disturbances (small wave number, K) until a given limit is reached, above which the boundary is stable to all disturbances. These limiting values are given in Table 8.

It can be seen that the limiting channel velocity decreases with particle size for gas fluidisation, and is much smaller for water fluidisation. It must be pointed out, for the water fluidised systems, that a channel velocity of less than the minimum fluidising velocity has no physical meaning. It would not be possible to maintain a channel at a velocity lower than that in the surrounding fluidised phase.

The results from boundary condition set 6 explain the maximum spoutable bed depth in the same way as do those from set 2. Spouting is usually carried out with coarse particles, which, according to Table 8, would have a very high limiting channel velocity, and the spout will become unstable as soon as the particles become fluidised. The results here indicate that a bed spouted with water would not be limited by a maximum spoutable bed depth, as the spout will still be stable, even when the particles become fluidised. This has not been reported by other workers, but little work has been done with liquid spouted beds, possibly because they do not offer any obvious advantages over particulate fluidisation, which, unlike aggregative fluidisation, is as effective for coarse solids as for fine material.

The results from the solution of boundary condition set 6 are consistent with the known trends in channelling behaviour. Channelling is to be expected for small particle diameters in gas fluidised beds, as the channel walls are stable at lower (and therefore experimentally

attainable) channel velocities. For larger particles, the channel walls are stable only for very high channel fluid velocities, which are not likely in a normal physical situation.

The effect noted by Godard and Richardson (1969), that channels broken up by a paddle rotated close to the distributor did not re-appear, is also accounted for by this theory. The severe channelling (spouting) at the base of the bed occurs as the fluidising fluid is unevenly distributed. The particles close to the channel wall are therefore poorly fluidised so that the wall is always stable, no matter what the channel velocity is. The paddle will break up the channels and ensure good fluidisation, so that, at the low gas velocities used by Godard and Richardson, any channel that reforms is now unstable.

The non-bubbling behaviour of most water fluidised systems is also accounted for. The fluid enters the dense phase in the form of small jets, the particle phase being, close to the distributor, poorly fluidised. As the fluid seeps into the particle phase through the walls of these jets, the particles close to the jet walls become more uniformly fluidised. Thus in gas (air) fluidised beds, the jets become unstable and break up forming small bubbles which then coalesce. However, in (most) water fluidised beds, the jets will remain stable, so that no bubbles form.

It is not possible to compare this channel break up with that proposed by other authors (see Levich (1962a)) for liquid jet break up, as it is shown that this is wholly dependent on the surface tension, which is non-existent in fluidised beds.

TABLE 8

Limiting Values of the Superficial Channel Velocity Above Which the Channel Wall is Stable
(Theoretical and Experimental)

System	Minimum Superficial Fluidising Velocity U_o cm/sec	Theoretical ϕ_{max}	Limiting Theoretical Superficial Channel Velocity $= \phi_{max} U_o$ cm/sec	Limiting Experimental Superficial Channel Velocity cm/sec
490 micron diam Glass/air	30.0	24.0	720.0	Not measured
100 micron diam Glass/air	1.5	200.0	300.0	270.0
55 micron diam Catalyst/air	0.5	440.0	220.0	250.0
1280 micron diam Lead/water	4.0	2.8	11.2	Not measured
5180 micron diam Glass/water	4.3	0.7	3.4	Not measured
All other glass/water systems from Table 4	U_o	< 0.1	< 0.1 x U_o	0

4.5 Experimental Study of Channelling Behaviour

The behaviour of a channel in a two-dimensional fluidised bed was observed using cine-photography at a frame speed of 64 frames/sec with angled back illumination. The film was then observed at slow speed to determine the stability of the channel wall. The bed had the dimensions 30 cm x 120 cm x 1.5 cm and was fitted with either a porous plastic (Vyon) distributor for air fluidisation, or a fine filter cloth distributor for water fluidisation. The channel was initiated approximately 10 cm above the distributor, so that the bed on either side of the channel would be well fluidised, using the system illustrated in Figure 22a.

These experiments were carried out for several different particle sizes fluidised by both air and water with many different fluidising and channel velocities. Figure 25 shows a typical photographic sequence for an unstable channel in air fluidisation. It can be seen that a channel as such, did not form completely through the bed, but tended more towards bubbling. This is to be expected; if the channel wall is inherently unstable, any channel will break down, and once bubble formation at the orifice (channel initiation point) commences in this way, the forced oscillations that this sets up in the bed oppose any further attempt at channel formation. Zenz (1968) reports that jets of gas in fluidised beds break away to form bubbles in the above manner, but did not record the jet velocity.

It was found that this bubbling behaviour could be characterised by a constant bubble frequency at any given air flow rate. Davidson and Harrison (1963) derived a theory for bubble formation from an orifice in inviscid liquids and showed that it also applied for fluidised

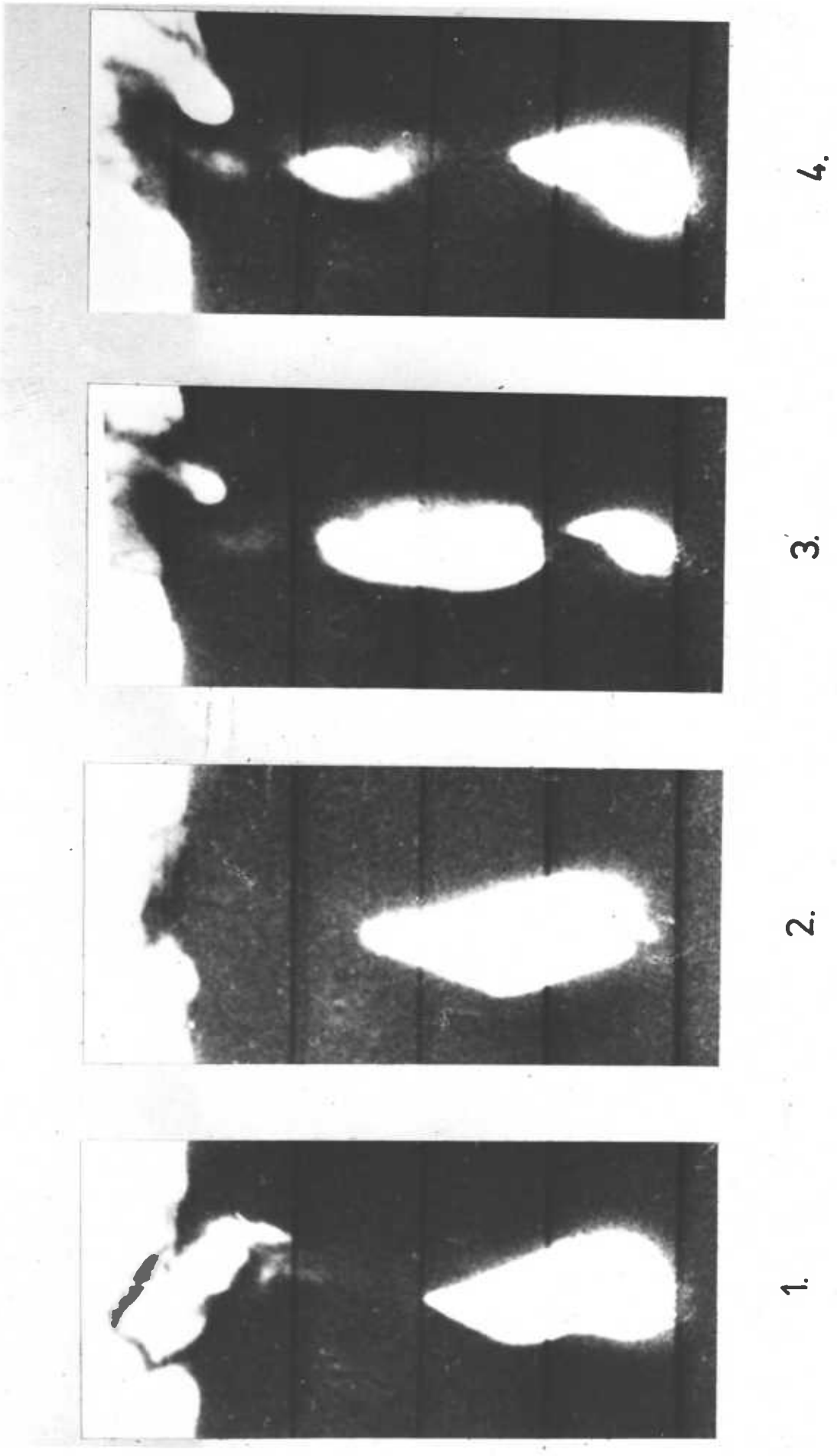

Figure 25: Behaviour of an unstable channel in a gas fluidised bed

beds. However, their derivation was for three-dimensional spherical bubbles and not therefore applicable here. Their analysis is repeated in Appendix 4 for two-dimensional circular bubbles and the results, together with the experimentally measured frequencies for 100 micron diameter glass particles, and the theoretical frequencies of oscillation of the expected dominant disturbance, are given in Table 9. Although the basic trends are similar, the agreement seems to be poor, but it should be remembered that the bubbles produced experimentally are, as can be seen in Figure 25, far from circular.

As the film shows, the system is bubbling from a point source rather than channelling with disturbances growing on the wall breaking up the channel. The results in Table 9 bear this out, as the frequency of the expected dominant wavelength on the channel wall ($n_{max/2\pi}$) shows very poor agreement with the experimentally measured frequencies.

Figure 26a shows a typically stable channel in air fluidisation. Any disturbance on the wall is damped out. Occasionally, very large disturbances occur but these are quickly swept aside and the stable channel reformed.

Figure 26b shows a stable channel produced in a water fluidised bed. It can be seen that the channel wall is stable, but that the channel loses its identity higher up the bed, as the channel fluid velocity falls below the surrounding interstitial fluid velocity.

The experimental results confirm the theoretical predictions obtained from boundary condition set 6. That is: for the range of particles studied here, for air and water fluidisation, the channel is stable

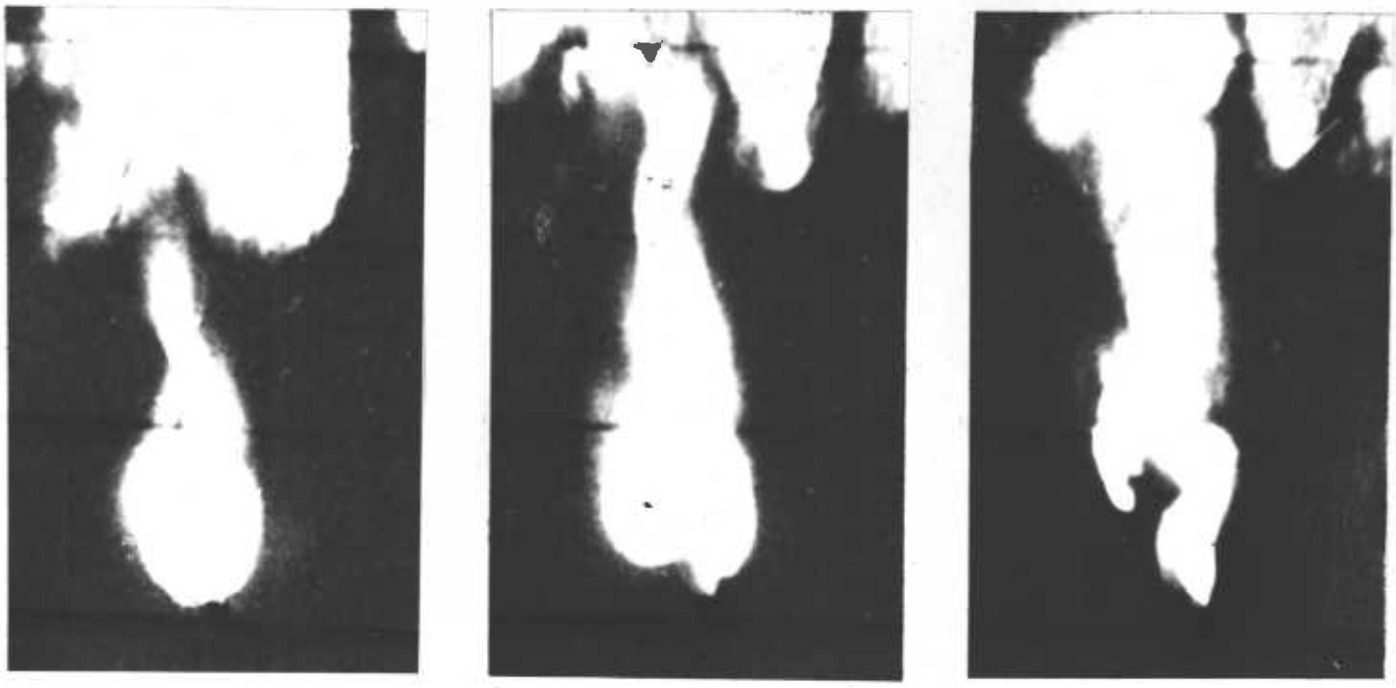

(a). 1. 2. 3.

(b).

Figure 26: Behaviour of a stable channel in gas and water fluidised beds

(as in Figure 26a, b) when the background fluidising velocity is zero, for all channel fluid velocities.

For all the water fluidised systems investigated, the channel remains stable with the bed phases well fluidised, providing the channel velocity is greater than that in the surrounding fluid.

For gas fluidisation, the channel is unstable (as in Figure 25) with the bed well fluidised, until the channel velocity exceeds a given limit, when it stabilises (as in Figure 26a). These experimentally measured limiting channel velocities are recorded in Table 8, and it can be seen that they agree well with the theoretically predicted values.

It is to be expected that the results from boundary condition set 6 adequately describe this physical situation whilst those from set 2 do not, as the assumption made in their derivation is more applicable here. The fluid velocity in the channel is very large whilst in the interstitial fluid it is assumed to be the minimum fluidising velocity. It is therefore quite reasonable that the interstitial fluid momentum should be ignored in comparison. It seems then, that the boundary condition set 6 is approximately true for the case of a vertical channel, and the experimental results do bear this out.

TABLE 9

Frequency of Bubble Formation for 100 Micron Diameter Particles Fluidised With Air

Gas Flow Rate G cc/sec	ϕ	Theoretical Bubbling Frequency.f. sec^{-1} (equation (A4.6))	Experimental Bubbling Frequency sec^{-1}	Theoretical Frequency of Oscillation of Dominant Disturbance Sec^{-1} $(= n_{max/2\pi})$	Description of Channel Behaviour
333.0	92	17.3	10.5	4.7	Bubbling ie unstable
542	100	14.6	10.0	4.7	Bubbling ie unstable
750	119	13.1	9.5	4.6	Bubbling ie unstable
1230	160	11.1	9.0	4.3	Bubbling ie unstable
1580	180	10.2	8.5	4.1	Transitional
> 1580	> 180	-	Non-bubbling	-	Non-bubbling ie stable

NB: ϕ is obtained by calculating the superficial channel velocity

ie $\phi \times U_o$ = superficial channel velocity = $\frac{G}{\text{channel width x bed width}}$

CHAPTER 5: THE BEHAVIOUR OF LIQUID FLUIDISED BEDS FOLLOWING STEPWISE CHANGES IN FLOW RATE

5.1 Introduction

During the particulate fluidisation of mono-sized particles the particles are uniformly dispersed throughout the expanded solid-fluid mixture. Most liquid fluidised systems fall into the range of particulate behaviour, and generally expand smoothly as the velocity is increased from the minimum fluidisation velocity. The steady state relation between expansion, or voidage fraction, and fluidising velocity is well correlated by the relationships due to Richardson and Zaki (1954). Slis, Willemse and Kramers (1959) studied the transient effects on the bed height of step changes in the fluidising flow rate using a water fluidised bed. They developed a theory for the propagation of 'continuity waves' through the system which satisfactorily accounts for the observations following a decrease in flow rate: rather similar arguments have been developed by Wallis (1969) to account for the behaviour of other two-phase systems. Following a step increase in flow rate, however, Slis et al found that the bed height increased uniformly at first, followed by a fall in the rate of increase. The explanation for this curious behaviour which is proposed by Slis et al was that the boundary between the regions of constant voidage fraction corresponding to the two levels of fluidising velocity spreads out rather than propagates as a sharp interface. They argue that this should happen since the lower region, which has a higher voidage fraction, also has a higher velocity, and this overtakes the region of lower voidage.

There may however, be another explanation for this behaviour since following a stepwise change in liquid flow rate there exist two

regions of different density with the lower density zone underneath. This would apparently be an unstable situation and the horizontal interface might be expected to break up due to the formation of two- or three-dimensional disturbances (Taylor (1959); Bellman and Pennington (1954)). Such a possibility has been noted by Wallis (1969) and Volpicelli (1967) has observed apparent unstable behaviour in liquid fluidised beds.

In this work, some simple experimental studies of this situation following step increases in fluidising velocity are reported and the applicability of the analyses of Taylor instabilities to this problem are discussed.

5.2 Theory

Taylor's classical analysis of the instability of superposed fluids of different densities was pursued further by Bellman and Pennington, who investigated the stabilising influences of viscosity and density. Rice and Wilhelm's (1958) analysis of fluidised bed instabilities follows a very similar path to Bellman and Pennington's analysis. These theories all relate to the initial motion and growth of an unstable interface and allow one to predict growth rates and 'most dangerous' wavelengths for infinitesimal disturbances, (see section 1.3).

Layzer (1955) produced an elegant theory which includes both the initial growth of a two dimensional disturbance and its final developed steady movement when the flow is confined within a cylindrical region or between two parallel walls. Initially a number of small wavelike disturbances develop on the horizontal interface: the movement should be quickly dominated by the most rapidly growing -

most dangerous - wavelengths; finally the movement of the lower density region will have the form of a single tongue or slug, essentially filling the confining region. The steady movement of a gas slug in a liquid of low viscosity has been analysed by Dumitrescu (1943), Davies and Taylor (1950) and other workers. Stewart and Davidson (1967) summarise these studies which predict that the slug velocity should depend only on the tube diameter, 2R, or the distance (2R) between the parallel walls: they show that the Froude Number $(\frac{V}{(gR)^{\frac{1}{2}}})$ is 0.326 in the two-dimensional case, and 0.511 in three dimensions.

Layzer adopted a suggestion due to Fermi (1951) to connect the two regions where a solution is available: the initial region of exponential growth, which results from the linearised theory, and the final steady motion of the vertex of the developed slug-like disturbance. Layzer's solution for the rising velocity of the leading vertex of the disturbance is:

a In three dimensions:

$$V = \left[\frac{e^{2\xi} - 2\xi - 1}{3.83(e^{2\xi} + 1)} \right]^{\frac{1}{2}} (gR)^{\frac{1}{2}} \text{ - - - - - - - - - - - - } \quad (5.1)$$

b In two dimensions:

$$V = \left[\frac{e^{3\eta} - 3\eta - 1}{3\pi(e^{3\eta} + 0.5)} \right]^{\frac{1}{2}} (gR)^{\frac{1}{2}} \text{ - - - - - - - - - - - - } \quad (5.2)$$

which reduce, in the steady state, ξ and η ---> ∞, to the results quoted above for the slug velocity.

In this analysis, ξ and η are as defined by Layzer from the dimensionless equations for the free surface between the two fluids: in 2-dimensions $\eta = y/_{(\pi)}^{(R)}$ - - - - - - - - - - - - - - - - - - (5.3)

Where the reference variables are, Length = $\frac{R}{\pi}$; velocity = $\frac{(gR)^{\frac{1}{2}}}{(\pi)}$

in 3-dimensions; $= y/\frac{(R)}{(3.83)}$ .....(5.4)

where reference variables are, Length = $\frac{R}{3.83}$; velocity = $\frac{(gR)^{\frac{1}{2}}}{3.83}$

y is the vertical coordinate of the slug nose, where y = 0 corresponds to the height at which the slug is initiated.

The theory is strictly applicable only to situations where the density difference between the two phases is very large (eg the interface between air and water). Dimensional analysis (Wallis (1969); Davidson and Harrison (1963a); Stewart and Davidson (1967)) suggests that when viscous and surface tension forces are negligible the Froude number relating to the final steady motion should be corrected by $(1 - \rho_{S/\rho_F})^{\frac{1}{2}}$ where ρ_S is the density of the fluid within the slug, and ρ_F is the density of the surrounding (ie initially uppermost) fluid. Stewart and Davidson's experimental results correlated well when this factor was introduced.

A further complication arises in the case of two-dimensional disturbances. Considering a typical 'two-dimensional' apparatus where the depth of the apparatus is perhaps one or two orders of magnitude less than its width (R) it will be clear that:

a the initial movement of the disturbance will probably be three-dimensional and,

b that three-dimensional effects will persit until the width of the disturbance is much greater than the depth of the apparatus.

Griffith (1963) suggests a corrected Froude number of the form:

$$F_1 = 0.326 + 0.185\ D_{s/D_b} \quad \text{- - - - - - - - - - - - - - - - - - - -} \quad (5.5)$$

Where D_s is the depth of the slug and D_b its width.

This appears to correlate results for the rising velocities of slugs in tubes of rectangular cross-section. Including these two corrections a modified version of Layzer's two-dimensional theory has the form:

$$V = F_2 \, (gR)^{\frac{1}{2}} \, (1 - \rho_{S/\rho_F})^{\frac{1}{2}} \qquad \text{- (5.6)}$$

$$\text{with } F_2 = (1.0 + 0.568 \frac{D_s}{D_b}) \left[\frac{e^{3\eta} - 3\eta - 1}{3\pi(e^{3\eta} + 0.5)} \right]^{\frac{1}{2}} \qquad \text{- - - - - - - - (5.7)}$$

NB: F_2 is derived from Layzer's 2-dimensional solution with F_1 from equation (5.5) included, and defined to give the correct results for the steady state for both 3 and 2-dimensions.

$$\text{ie } F_2 = \frac{F_1}{\lim. \xi \dashrightarrow \infty \left[\frac{e^{2\xi} - 2\xi - 1}{3.83(e^{2\xi} + 1)} \right]^{\frac{1}{2}}} \left[\frac{e^{3\eta} - 3\eta - 1}{3\pi(e^{3\eta} + 0.5)} \right]^{\frac{1}{2}} \qquad \text{- - - - - - - - (5.8)}$$

$$\text{or } F_2 = \frac{F_1}{0.326} \left[\frac{e^{3\eta} - 3\eta - 1}{3\pi(e^{3\eta} + 0.5)} \right]^{\frac{1}{2}}$$

It should be possible to define the behaviour of the interface by an analysis similar to that presented in section 2A. This would involve an assumption similar to that made in sextion 2C, that is, the region of lower density would become the support fluid, with mean viscosity and density, whilst the region of higher density would be described as two interacting phases. However, as before, this approach would only be applicable to infinitesimally small disturbances; once the disturbance has grown to finite proportions the analysis would become invalid. Thus, an approach similar to that due to Layzer presented here would still be necessary.

5.3 Experimental

The behaviour of a two-dimensional bed fluidised with water following step changes in water flow rate was observed, using glass ballotini particles of nominal diameter 100; 280 and 490 micron respectively. The bed, with dimensions 120 cm x 30 cm x 1.5 cm was illuminated by high intensity angled back lighting. The fluid distributor was a fine filter cloth. It was found possible to follow clearly by eye the movement of the interface separating regions of different density following a step change in flow rate. The movement of the interface was recorded on cine film; some measurements of the velocity of the developed disturbance were taken by measuring with a stopwatch the time to travel 20 cms.

5.4 Observations, Results and Comparison with Theory

The development and motion of an unstable interface in a bed of 490 micron particles is hown in Figure 27. The sequence shows the initial formation and rapid growth of a number of small wavelength disturbances along the horizontal interface; the initial wavelength is in the region of 1.5 - 2 cms. The growing disturbances begin to interact and are gradually taken over by one dominant disturbance. In the relatively shallow beds used in these experiments the dominant disturbance never increased to completely fill the bed, although it seems likely that this would occur, given sufficient time. Figure 27 appears to give a convincing qualitative demonstration of the role of Taylor instabilities in the movement of interfaces between regions of different voidage fraction.

In order to compare the results with the theory of equations (5.6) and (5.7) it was necessary to calculate the voidage fraction of the two regions. It was assumed that each region was homogeneous with

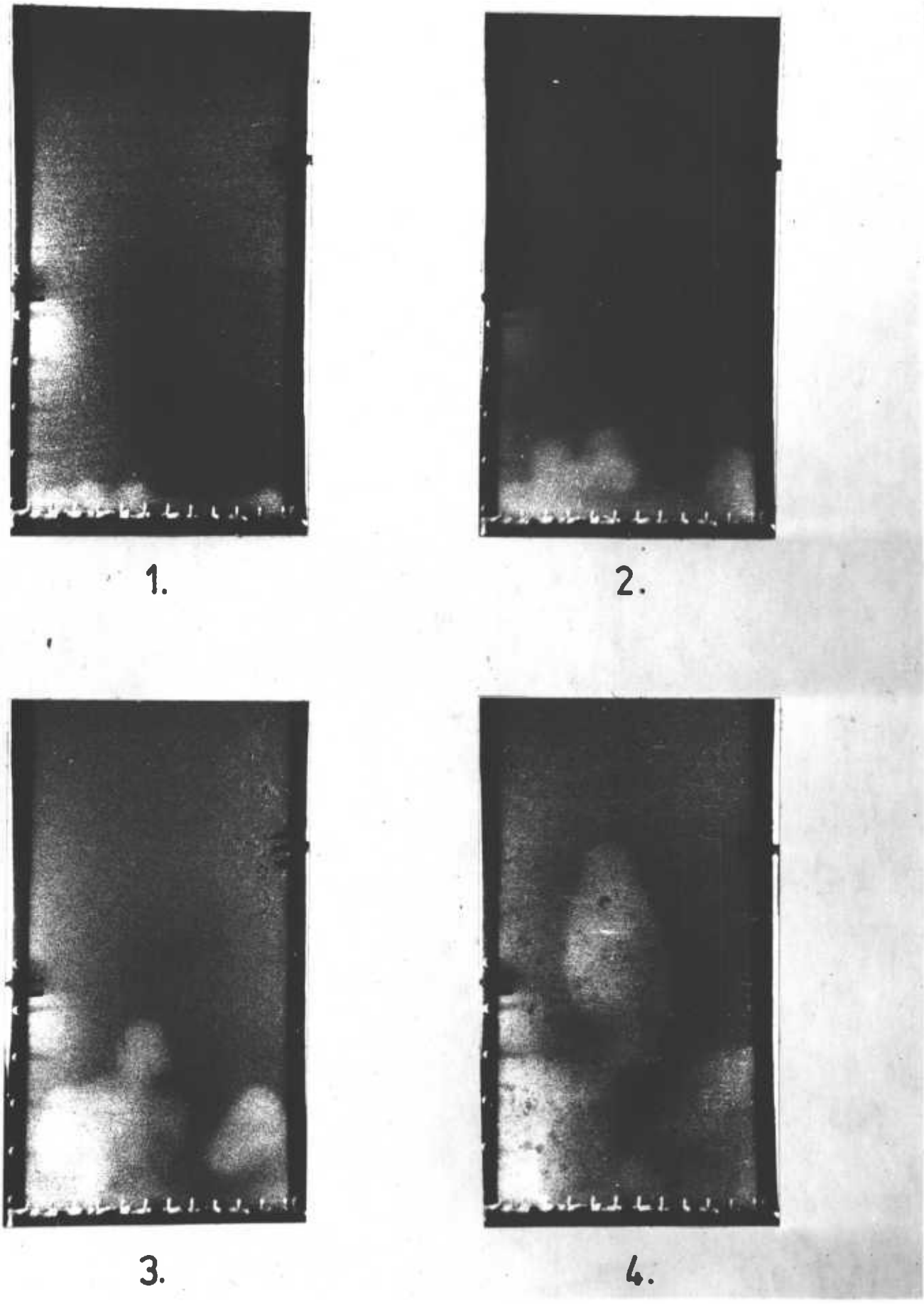

Figure 27: Formation and growth of a voidage fraction disturbance in a liquid fluidised bed following a step increase in flow rate

constant voidage fraction which was related to the liquid velocity by the appropriate form of Richardson and Zaki's (1954) relation, which is $\frac{U}{U_t} = e^N$ where U_t is the particle terminal velocity and the exponent, N, depends on the Reynold's number (N = 4.65 in the experiments reported here). Given the initial steady voidage fraction before the step change in flow rate, it is a straightforward matter to calculate the density ratio between the two regions.

It was found that the light transmission through the bed as measured by the reading on a light meter, calibrated against beds of known voidage fraction, gave a good check on these results.

From cine film of the movement of the interface, and given the densities ρ_S and ρ_F of the lower and upper regions, F_2, as defined by equation (5.6) was calculated. These values are compared with the theoretical values from equation (5.7) in Figures 28-30. The limiting width of the slug, 2R, was measured from the film, taking the measurement away from the slug vertex.

The agreement between the theoretical predictions and the experimental results is encouragingly close. The deviation as time increases is probably due to the assumption of constant voidage fraction, since there must be some local variations, especially around the interface between the two regions. In some cases there was a certain amount of channelling near the base of the bed. This probably explains the deviations between theory and experiment near the origin in some of the curves.

The widest range of voidage fraction (and, thus, density) changes were achieved with the smallest (100 micron) particles, where the

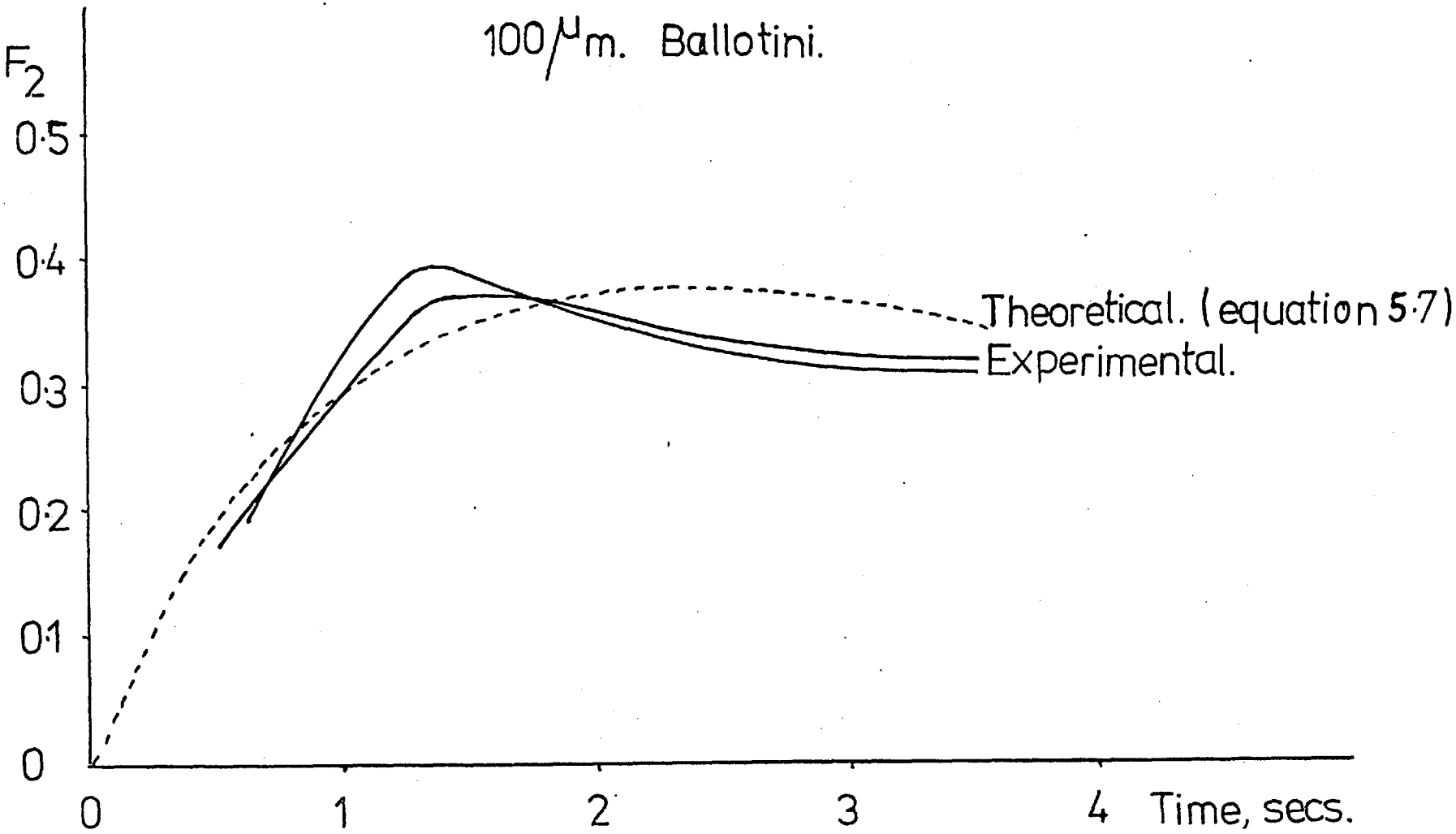

Figure 28: Growth of voidage fraction disturbance: comparison of experimental and theoretical Froude number

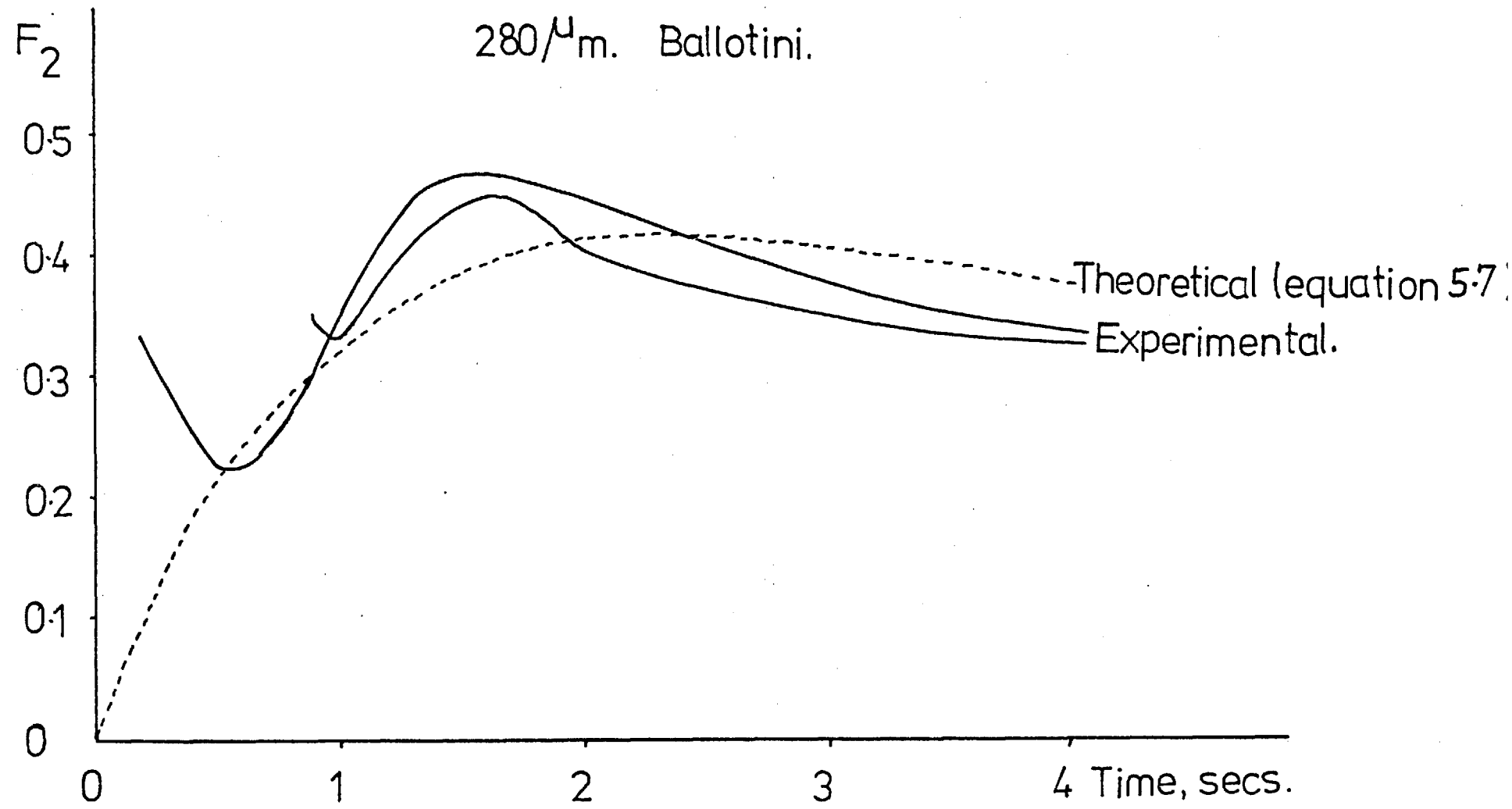

Figure 29: Growth of voidage fraction disturbance: comparison of experimental and theoretical Froude number

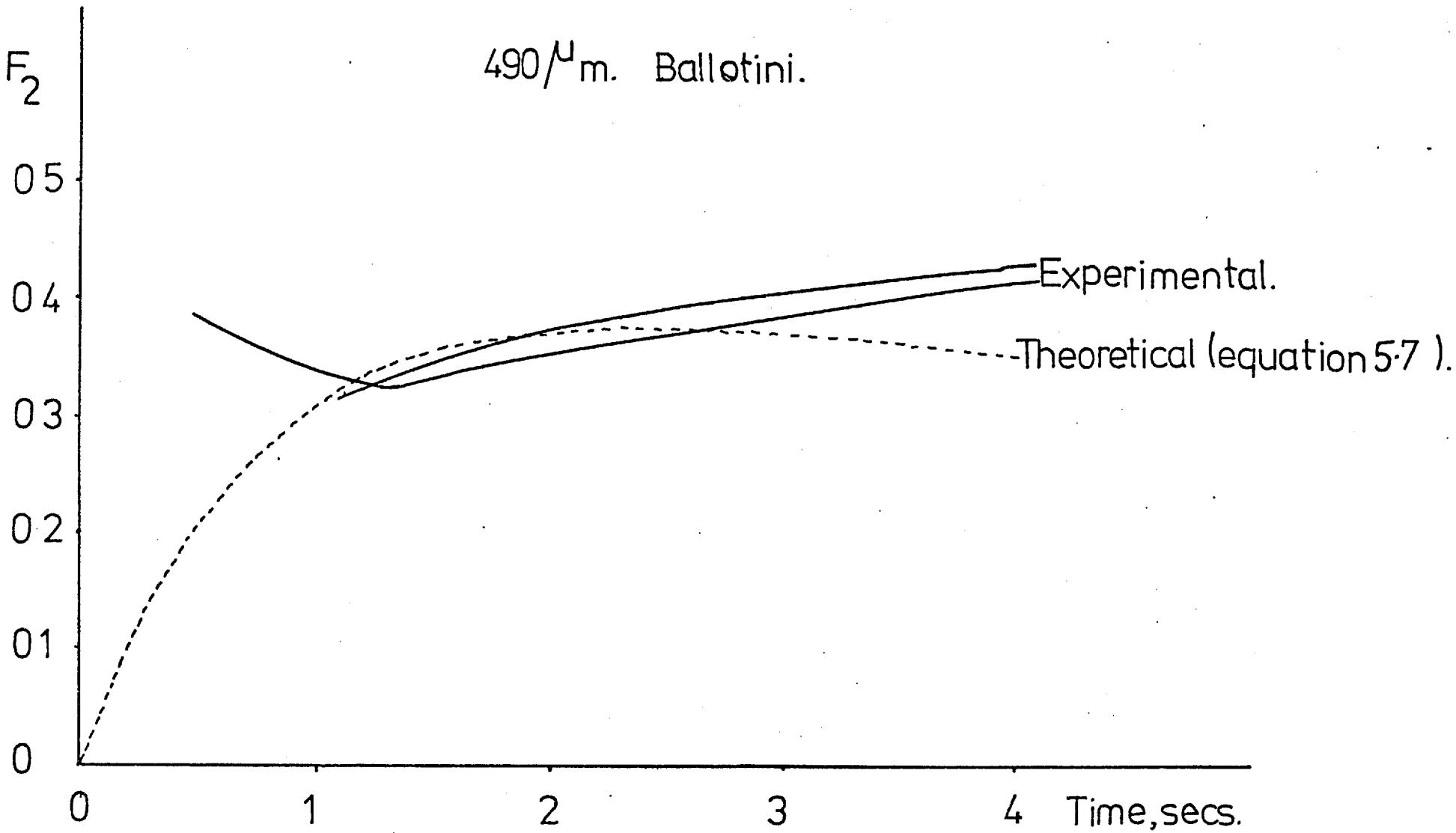

Figure 30: Growth of voidage fraction disturbance: comparison of experimental and theoretical Froude number

voidage fraction was doubled from its initial state. Inaccuracies and small fluctuations in voidage fraction would thus be most important in the case of the larger particles and this, too, may explain the better agreement found with the smaller particles.

Figure 31 shows a typical set of the measurements obtained by using direct observation and employing a stopwatch. It can be seen that all the measurements lie below those from the cine film (and thus below the theoretical results); the time-averaging method is not sufficiently accurate in this case because the steady state was only achieved near the top of the bed.

The initial wavelength, λ, of the disturbance is difficult to estimate with accuracy because of the design of the bed used. Measurements suggest that for the 100 micron particles, λ is 1.0-1.5 cm and for the 490 micron particles, λ is 1.5-2.0 cm. These may be compared with Rice and Wilhelm's (1958) predictions of the 'most dangerous' wavelength of 1.25 cm and 1.55 cm respectively, for conditions comparable to those studied here.

5.5 Conclusions

It has been shown experimentally that following a step increase in liquid flow rate in a particulate fluidised bed the two regions of different voidage fraction behave qualitatively and quantitatively like a denser fluid superposed over a lighter fluid. The boundary between these two regions is thus unstable and the theory developed by Layzer to describe the development of a slug from an initially horizontal interface, when suitably modified for density and geometrical effects, satisfactorily describes the motion of the interface.

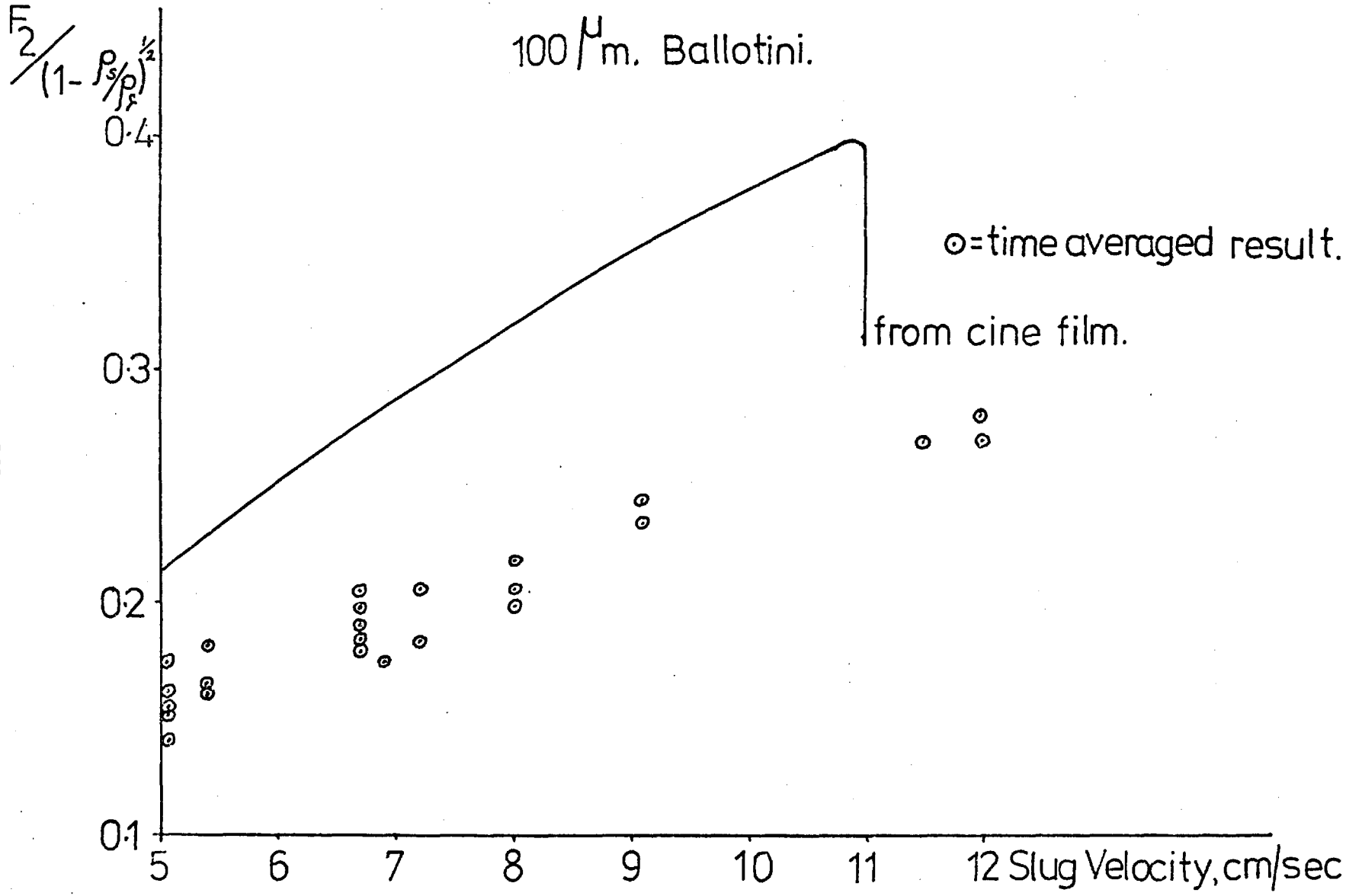

Figure 31: Slug velocity: comparison of time averaged results from cine film

A stepwise decrease in fluidising velocity leads to a hydrodynamically stable situation which is well described by the theory developed by Slis et al. Their conjecture that, following an increase in flow rate, the interface broadens out appears to be incorrect, as the interface is in fact unstable. Although the results here were taken in a two-dimensional apparatus, they seem to confirm Volpicelli's (1967) observation of particle movement at the wall of a three-dimensional bed which also indicate the unstable behaviour of such an interface leading to slugging.

Finally, it may be noted that these results should also apply to other equivalent situations involving two-phase flows (eg sedimentation, bubble columns) where density driven instabilities may exist.

CHAPTER 6: CONCLUSIONS

The stability of plane horizontal boundaries within a fluidised bed has been analysed. The theory indicates that such boundaries, with the fluidised phase uppermost, are always unstable to small two-dimensional disturbances. The experimental results suggest that the momentum of the interstitial fluid lies somewhere between the two proposed extremes; viz very large as in boundary condition set 2, or negligible as in set 6.

A mechanism of bubble splitting, based on the preceding stability analysis, has been proposed. This leads to the prediction of a maximum and a minimum stable bubble diameter. The theory shows that bubbles in gas fluidised beds are much more stable than those in liquid fluidised systems and this is supported by experimental evidence taken from the observation of bubble behaviour in a freely bubbling gas fluidised bed and of injected bubbles in a water fluidised bed. The agreement between the predicted and measured growth rates of the disturbances is poor, but measured frequencies of bubble splitting agree semi-quantitatively with the theory.

The stability of plane vertical boundaries within a fluidised bed has been analysed. The theory indicates that the boundary is stable for all fluid velocities in the particle-free channel when the homogeneous phase is not fluidised (spouting), and that the boundary is stable only when the fluid velocity in the channel exceeds a given limit when the homogeneous phase is well fluidised (channelling). The theoretical predictions agree qualitatively and quantitatively with known channelling behaviour and with experimental results.

It has been shown experimentally that, following a step increase in liquid flowrate in a particulate fluidised bed, the two regions of different voidage fraction behave qualitatively and quantitatively like a denser fluid

superposed over a lighter fluid. The boundary between these two regions is thus unstable and the theory developed by Layzer to describe the development of a slug from an initially horizontal interface, when suitably modified for density and geometrical effects, satisfactorily describes the motion of the interface.

Suggestions for Further Work:

Research work tends, by nature, to be self-perpetuating. The work described here is no exception and raises a number of points on which further clarification should be of value.

The experimental results on bubble splitting could be refined to eliminate the influence of factors not included in the theoretical analysis, for example, observations of single injected bubbles should eliminate the influence of coallescence on bubble splitting in gas fluidised systems. More pwerful and accurate filming techniques would enable the frequency and growth rate of instabilities on bubbles in water fluidised beds to be measured.

The theoretical study on channel stability could be tested further by observing systems of larger particles. This would involve more refined equipment than that employed here, as very high channel velocities would be necessary. Experimental observations on the spouting of particles with water would also be useful to check the hypothesis put forward here that spouting with water would not be limited by a maximum spoutable bed depth.

Further experimental studies to verify the analysis of the stability of the horizontal boundary would not be particularly informative. As mentioned earlier, experimental work in this field cannot really be expected to correlate well with the theory due to the practical difficulties in observing situations where the theory remains valid.

APPENDIX 1: GENERAL SOLUTION TO THE EQUATIONS OF MOTION

A general solution to the equations of motion (2A.21) to (2A.29) is sought to a small initial sinusoidal disturbance of the plane horizontal interface with wave number K.

A solution is therefore defined to allow each variable a voidage and pressure dependence where appropriate and its own individual term. Thus:

$$\epsilon = A \exp(- Ky + nt) \text{ Cos } Kx$$

$$V_x = B \exp(- m_1 y + nt) \text{ Sin } Kx + a_1 A \exp(- Ky + nt) \text{ Sin } Kx$$

$$V_y = b_1 B \exp(- m_1 y + nt) \text{ Cos } Kx + a_2 A \exp(- Ky + nt) \text{ Cos } Kx$$

$$U_x = C \exp(- m_2 y + nt) \text{ Sin } Kx + D \exp(- Ky + nt) \text{ Sin } Kx +$$

$$+ a_3 A \exp(- Ky + nt) \text{ Sin } Kx$$

$$U_y = c_1 C \exp(- m_2 y + nt) \text{ Cos } Kx + d_1 D \exp(- Ky + nt) \text{ Cos } Kx +$$

$$+ a_4 A \exp(- Ky + nt) \text{ Cos } Kx$$

$$P_2 = d_2 D \exp(- Ky + nt) \text{ Cos } Kx$$

$$W_x = E \exp(m_3 y + nt) \text{ Sin } Kx + F \exp(Ky + nt) \text{ Sin } Kx$$

$$W_y = e_1 E \exp(m_3 y + nt) \text{ Cos } Kx + f_1 F \exp(Ky + nt) \text{ Cos } Kx$$

$$P_3 = f_2 F \exp(Ky + nt) \text{ Cos } Kx \qquad \text{- - - - - - - (A1.1)}$$

Where m_1, m_2, m_3 are all positive by definition.

The unknown coefficients, a_1, a_2, b_1, etc are then defined to allow solution of the continuity equations, (2A.21) to (2A.23).

Then substitution of equations (A1.1) into the momentum equations (2A.24) to (2A.29) reveals the solution for variables m_1, m_2 and m_3;

$$m_1 = m_2 = K \quad \text{------------------------------} \quad (A1.2)$$

and m_3 from $m_3^2 - R_{eF}\, m_3 - R_{eF}\, n - K^2 = 0$ -------------- (A1.3)

NB (A1.2) is only one of the solutions for m_1 and m_2. However, other possible solutions for m_1 and m_2 are very complex functions of the dimensionless groups defined in (2A.21) to (2A.29), K and n, and are therefore mathematically prohibitive.

The particular solution found in this way is then as given by equations (2A.30) to (2A.39).

APPENDIX 2: SOLUTION USING THE PROPOSED SETS OF BOUNDARY CONDITIONS

A2.1 Horizontal Interface Between the Phases

The complete solution is given here for boundary condition set 1 only, but the same procedure also applies for all the other proposed sets.

Set 1: The boundary conditions in this set are:

Material balance:

$$W_y = \epsilon_o U_y + \frac{\epsilon}{\epsilon_o} + V_y (1 - \epsilon_o) \quad \text{- - - - - - - - - - - - - - - - - -} \quad (2A.42)$$

$$W_x = \epsilon_o U_x \quad \text{- -} \quad (2A.43)$$

Tangential Stress:

$$\frac{dW_x}{dy} + \frac{dW_y}{dx} = \frac{dU_x}{dy} + \frac{dU_y}{dx}$$

$$\frac{dW_x}{dy} + \frac{dW_y}{dx} = \mu \left[\frac{dV_x}{dy} + \frac{dV_y}{dx} \right]$$

Normal Stress:

$$\frac{R_{ep}}{Fr} P_3 - \frac{R_{eF}}{Fr} \eta (1 - \epsilon_o) + \frac{4}{3} \frac{dW_y}{dy} - \frac{2}{3} \frac{dW_x}{dx} = \frac{R_{ep}}{Fr} P_2 + \frac{4}{3} \frac{dU_y}{dy} - \frac{2}{3} \frac{dU_x}{dx}$$

$$\frac{R_{ep}}{Fr} P_3 - \frac{R_{eF}}{Fr} \eta + \frac{4}{3} \frac{dW_y}{dy} - \frac{2}{3} \frac{dW_x}{dx} = \frac{4}{3} \mu \frac{dV_y}{dy} - \frac{2}{3} \mu \frac{dV_x}{dx}$$

- - - from (2A.50)

Substitution of the assumed solution of the equations of motion, (2A.30) to (2A.39), into the above boundary conditions gives:

from equation (2A.42):

$$\epsilon_o C \exp(- Ky + nt) \operatorname{Cos} Kx + \epsilon_o D \exp(- Ky + nt) \operatorname{Cos} Kx -$$

$$- E \exp(Ky + nt) \operatorname{Cos} Kx - F \exp(Ky \div nt) \operatorname{Cos} Kx = 0 \quad \text{- - - - -} \quad (A2.1)$$

with equivalent equations from the other five boundary conditions.

These can be written in the form:

$$[M]\begin{bmatrix} A\exp(-Ky+nt) \\ B\exp(-Ky+nt) \\ C\exp(-Ky+nt) \\ D\exp(-Ky+nt) \\ E\exp(Ky+nt) \\ F\exp(Ky+nt) \end{bmatrix} = 0 \qquad \text{(A2.2)}$$

Where M is a 6 x 6 matrix, given in this case by:

$$[M] = \begin{bmatrix} 0 & 0 & (\epsilon_o) & (\epsilon_o) & -1 & -1 \\ 0 & (1-\epsilon_o) & (\epsilon_o) & (\epsilon_o) & (\frac{K}{m_3}) & +1 \\ -\frac{\mu n}{(1-\epsilon_o)} & (2\mu K) & 0 & 0 & (m_3+\frac{K^2}{m_3}) & (2K) \\ \frac{\epsilon_o n - K}{\epsilon_o^2} & 0 & (2K) & (2K) & (m_3+\frac{K^2}{m_3}) & (2K) \\ a_1 & b_1 & 0 & 0 & (2K) & c_1 \\ d_1 & R_{eF}\frac{(1-\epsilon_o)}{F_r n} & (-2K) & (-2K+R_{ep}\frac{n}{K}) & (2K) & c_1 \end{bmatrix}$$

Where $a_1 = \frac{4}{3}\frac{\mu n}{(1-\epsilon_o)} - \frac{R_{eF}}{Fr}\frac{1}{K(1-\epsilon_o)}$ ---------- (A2.3)

$$b_1 = -2\mu K + \frac{R_{eF}}{Fr}\frac{1}{n} \qquad \text{----------} \qquad \text{(A2.4)}$$

$$c_1 = 2K - R_{eF}\frac{(n+K)}{K} \qquad \text{----------} \qquad \text{(A2.5)}$$

$$d_1 = -\frac{4}{3}\frac{(\epsilon_o n - K)}{\epsilon_o^2} - \frac{R_{eF}}{Fr}\frac{1}{K} \qquad \text{----------} \qquad \text{(A2.6)}$$

The non-trivial solution to (A2.2) thus being: det [M] = 0

- - - - - (2A.57)

Expanding the determinant leads to:-

$$n^3(a) + n^2(b + c) + n\,(d + e) + f = 0 \qquad \text{- - - - - - - - -} \quad (2A.58)$$

for the configuration, fluidised phase uppermost, or

$$n^3(a) + n^2(- b + c) + n(- d + e) + f = 0 \qquad \text{- - - - - - - - -} \quad (2A.58a)$$

for the configuration, support fluid uppermost.

Where:

$$a = R_{eF}\left[\frac{m_3}{K}\,\frac{(1-\epsilon_o + \epsilon_o\mu)}{\epsilon_o} + \frac{K}{\epsilon_o m_3}\,((1-\epsilon_o) - \mu\,(2-\epsilon_o))\right] \quad \text{- - - -} \quad (A2.7)$$

$$b = \frac{4}{3}\,\frac{\mu^2 K}{(1-\epsilon_o)}\left[m_3 + \frac{K(1-\epsilon_o)}{\epsilon_o} - \frac{K^2}{\epsilon_o m_3}\right] - \frac{\mu K}{\epsilon_o}\left[\left(\frac{4}{3} + 2\epsilon_o\right)m_3 + 4K\left(\frac{4}{3} - \epsilon_o\right) + \right.$$

$$\left. + \frac{K^2}{m_3}\left(2\epsilon_o - \frac{20}{3}\right)\right] + - \frac{2K(1-\epsilon_o)}{\epsilon_o}\left[m_3 - 2K + \frac{1}{m_3}\right] \quad \text{- - - - - - - -} \quad (A2.8)$$

$$c = R_{eF}\left[\mu\left(m_3 + \frac{2K}{\epsilon_o^2} + \frac{K^2}{m_3}\,\frac{(2-2\epsilon_o + \epsilon_o^2)}{\epsilon_o^2}\right) - \frac{(1 - 2\epsilon_o + \epsilon_o^2)}{\epsilon_o^2}\left(m_3 + \frac{1}{m_3}\right)\right]$$

$$\text{- - - - - - - -} \quad (A2.9)$$

$$d = \frac{4\mu K^2}{\epsilon_o^2}\left(m_3 - \frac{K^2}{m_3}\right) + 2K^2\frac{(1-\epsilon_o)}{\epsilon_o^2}\left(m_3 - 2K + \frac{K^2}{m_3}\right) \quad \text{- - - - - - - -} \quad (A2.10)$$

$$e = R_{eF}\left[\frac{1}{Fr}\left[-\frac{m_3 2\mu}{(1-\epsilon_o)} + \frac{2K(1-\mu)}{\epsilon_o} + \frac{2K^2}{\epsilon_o m_3}\left[\frac{\mu}{(1-\epsilon_o)} - 1\right]\right]\right.$$

$$\left. - m_3\,\frac{K(1-\epsilon_o)}{\epsilon_o^2} + \frac{2\mu K^2}{\epsilon_o^2} + \frac{K^3}{\epsilon_o^2 m_3}\,(-1 + \epsilon_o + 2\mu)\right] \quad \text{- - - - - - - -} \quad (A2.11)$$

$$f = \frac{R_{eF}}{Fr}\,\frac{2K}{\epsilon_o^2}\,(K - m_3) \quad \text{- - - - - - - - - - - - - - - - - - -} \quad (A2.12)$$

Set 2: ie Equations (2A.42a); (2A.43) and (2A.50)

These give:

$$[M] = \begin{bmatrix} 0 & 0 & (\epsilon_o) & (\epsilon_o) & -1 & -1 \\ (\frac{n}{K}) & 0 & (\epsilon_o) & (\epsilon_o) & (\frac{K}{m_3}) & +1 \\ -(\frac{\mu n}{(1-\epsilon_o)}) & (2\mu K) & 0 & 0 & (m_3 + \frac{K^2}{m_3}) & (2K) \\ \frac{(\epsilon_o n - K)}{\epsilon_o^2} & 0 & (2K) & (2K) & (m_3 + \frac{K^2}{m_3}) & (2K) \\ a_1 & b_1 & 0 & 0 & (2K) & c_1 \\ d_1 & \frac{(R_{eF}(1-\epsilon_o))}{Fr\ n} & (-2K) & (-2K + R_{ep}\frac{n}{K}) & (2K) & c_1 \end{bmatrix}$$

- - - - - - - - (A2.13)

Where a_1 to d_1 are as given by equations (A2.3) to (A2.6).

This leads to (2A.58), where:-

$$a = R_{eF}\left[\frac{m_3}{K^2} + \frac{1}{\epsilon_o K} - \frac{(1-\epsilon_o)}{\epsilon_o m_3}\right] \quad \text{- - - - - - - - - - - - - - - - - (A2.14)}$$

$$b = -2m_3 - 4\frac{(1+\epsilon_o)K}{\epsilon_o} + \frac{2K^2(2-\epsilon_o)}{m_3\epsilon_o} + \frac{2\mu}{3(1-\epsilon_o)}\left[m_3 + K\frac{(1-\epsilon_o)}{\epsilon_o} - \frac{K^2}{\epsilon_o m_3}\right]$$

- - - - - - (A2.15)

$$c = R_{eF}\left[\frac{m_3}{K} + \frac{(1+\epsilon_o)}{\epsilon_o^2} + \frac{K}{m_3}\frac{(1+\epsilon_o^2-\epsilon_o)}{\epsilon_o^2}\right] \quad \text{- - - - - - - - - - (A2.16)}$$

$$d = \frac{2m_3 K}{\epsilon_o^2} - \frac{2K^3}{\epsilon_o^2 m_3} \quad \text{- (A2.17)}$$

$$e = R_{eF}\left[\frac{K^2}{\epsilon_o^2 m_3} + \frac{K}{\epsilon_o^2} + \frac{1}{F_r(1-\epsilon_o)}\left[-\frac{m_3}{K} - \frac{(1-\epsilon_o)}{\epsilon_o} + \frac{K}{\epsilon_o m_3}\right] + \right.$$

$$\left. + \frac{1}{\mu Fr}\left[\frac{1}{\epsilon_o} - \frac{K}{\epsilon_o m_3}\right]\right] \quad \text{- -} \quad \text{(A2.18)}$$

$$f = \frac{R_{eF}}{Fr}\ \frac{2}{\epsilon_o^2}\ (K - m_3) \quad \text{- -} \quad \text{(A2.19)}$$

Set 3: ie Equations (2A.42a), (2A.43), (2A.50) for normal stress, (2A.47) and (2A.52) for tangential stress. These give:-

$$[M] = \begin{bmatrix} 0 & 0 & (\epsilon_o) & (\epsilon_o) & -1 & -1 \\ (\frac{n}{K}) & 0 & (\epsilon_o) & (\epsilon_o) & (\frac{K}{m_3}) & 1 \\ \frac{-n(1+\mu)}{(1-\epsilon_o)} & (2K(1+\mu)) & 0 & 0 & (m_3 + \frac{K^2}{m_3}) & (2K) \\ \left[\frac{n}{\epsilon_o(1-\epsilon_o)} - \frac{K}{\epsilon_o^2}\right] & (-2K) & (2K) & (2K) & 0 & 0 \\ a_1 & b_1 & 0 & 0 & (2K) & c_1 \\ d_1 & \frac{R_{eF}(1-\epsilon_o)}{Fr.n} & (-2K) & (-2K + \frac{R_{ep}n}{K}) & (2K) & c_1 \end{bmatrix}$$

$$\text{- - - - - - - -} \quad \text{(A2.20)}$$

Where a_1 to d_1 are given by equations (A2.3) to (A2.6).

This leads to (2A.58), where:-

$$a = R_{eF}\left[\frac{m_3}{K} + \frac{(1+\mu)}{\epsilon_o} - \frac{K}{m_3}\ \frac{(1-\epsilon_o+\mu)}{\epsilon_o}\right] \quad \text{- - - - - - - - -} \quad \text{(A2.21)}$$

$$b = \frac{2}{3}\frac{\mu^2K^2}{\epsilon_o(1-\epsilon_o)}\left(1 - \frac{K}{m_3}\right) + \frac{2}{3}\mu K\left[\frac{m_3}{(1-\epsilon_o)} - \frac{5K}{\epsilon_o} - \frac{K^2}{m_3}\frac{(6\epsilon_o-5)}{\epsilon_o(1-\epsilon_o)}\right] -$$

$$-2K\left(m_3 + \frac{K(1-2\epsilon_o)}{\epsilon_o} - \frac{K^2}{\epsilon_o m_3}(1-\epsilon_o)\right) \quad \text{----------} \quad \text{(A2.22)}$$

$$c = R_{eF}\left[m_3 + K(1+\mu)\frac{(1+\epsilon_o)}{\epsilon_o^2} + \frac{K^2}{m_3}(1+\mu)\frac{(1-\epsilon_o)}{\epsilon_o^2} + \frac{K^2}{m_3}\right] \text{---} \quad \text{(A2.23)}$$

$$d = \frac{2K^2}{\epsilon_o^2}\left(m_3\mu + K - \frac{K^2(1+\mu)}{m_3}\right) \quad \text{----------} \quad \text{(A2.24)}$$

$$e = R_{eF}\left[\frac{1}{Fr}\left[\frac{-m_3}{(1-\epsilon_o)} - \frac{K\mu}{\epsilon_o(1-\epsilon_o)} + \frac{K^2(\mu+\epsilon_o)}{m_3\epsilon_o(1-\epsilon_o)}\right] + \frac{(1+\mu)K^2}{\epsilon_o^2}\left(1+\frac{K}{m_3}\right)\right]$$

$$\text{----------} \quad \text{(A2.25)}$$

$$f = \frac{R_{eF}}{Fr}\frac{K}{\epsilon_o^2}(K - m_3) \quad \text{----------} \quad \text{(A2.26)}$$

Set 4: ie Equations (2A42a); (2A.43); (2A.50) for tangential stress, (2A.48) and (2A.53) for normal stress. These give:-

$$[M] = \begin{bmatrix} 0 & 0 & (\epsilon_o) & (\epsilon_o) & -1 & -1 \\ (\frac{n}{K}) & 0 & (\epsilon_o) & (\epsilon_o) & (\frac{K}{m_3}) & 1 \\ -(\frac{\mu n}{(1-\epsilon_o)}) & (2\mu K) & 0 & 0 & (m_3 + \frac{K^2}{m_3}) & (2K) \\ \left[\frac{\epsilon_o n - K}{\epsilon_o^2}\right] & 0 & (2K) & (2K) & (m_3 + \frac{K^2}{m_3}) & (2K) \\ a_1 & b_1 & 0 & (R_{ep}\frac{n}{K}) & (2K) & c_1 \\ d_1 & (-2K) & (2K) & (2K) & 0 & 0 \end{bmatrix}$$

- - - - - - - - - - - - (A2.27)

Where $a_1 = \frac{4}{3}\frac{(1+\mu)n}{(1-\epsilon_o)} - \frac{R_{eF}}{Fr}\frac{1}{K}$ - - - - - - - - - - - - (A2.28)

$$b_1 = \frac{R_{eF}}{Fr}\frac{(1-\epsilon_o)}{n} - 2(1+\mu)K \quad \text{- - - - - - - - - - - -} \quad \text{(A2.29)}$$

$c_1 = 2K - R_{eF}\frac{(n+K)}{K}$ as given by (A2.5)

$$d_1 = \frac{4}{3}\frac{n}{\epsilon_o(1-\epsilon_o)} - \frac{4K}{3\epsilon_o^2} \quad \text{- - - - - - - - - - - -} \quad \text{(A2.30)}$$

This leads to (2A.58), where:-

$a = b = c = e = 0$ - (A2.31)

$$d = \frac{-m_3\mu}{3\epsilon_o(1-\epsilon_o)} + \frac{K}{\epsilon_o} + \frac{K\mu(-\frac{1}{3} - \frac{2}{3}\epsilon_o + \epsilon_o^2)}{\epsilon_o^2(1-\epsilon_o)} - \frac{K^2}{\epsilon_o m_3} +$$

$$+ \frac{K^2\mu(\frac{1}{3} + \epsilon_o - \epsilon_o^2)}{m_3\epsilon_o^2(1-\epsilon_o)} \quad \text{- -} \quad \text{(A2.32)}$$

$$f = \frac{-Km_3}{\epsilon_o^2} + \frac{4}{3}\frac{\mu Km_3}{\epsilon_o^2} + \frac{K^2}{\epsilon_o} + \frac{K^2\mu(1-4\epsilon_o)}{3\epsilon_o^3} - \frac{K^3\mu}{3m_3\epsilon_o^3} \quad \text{------} \quad \text{(A2.33)}$$

Set 5: ie Equations (2A.42), (2A.43), (2A.50) for tangential stress, (2A.48) and (2A.53) for normal stress. These give:-

$$[M] = \begin{bmatrix} 0 & 0 & (\epsilon_o) & (\epsilon_o) & -1 & -1 \\ 0 & (1-\epsilon_o) & (\epsilon_o) & (\epsilon_o) & (\frac{K}{m_3}) & 1 \\ -(\frac{\mu n}{(1-\epsilon_o)}) & (2\mu K) & 0 & 0 & (m_3 + \frac{K^2}{m_3}) & (2K) \\ \frac{\epsilon_o n - K}{\epsilon_o^2} & 0 & (2K) & (2K) & (m_3 + \frac{K^2}{m_3}) & (2K) \\ a_1 & b_1 & 0 & (R_{epK}\frac{n}{}) & (2K) & c_1 \\ d_1 & (-2K) & (2K) & (2K) & 0 & 0 \end{bmatrix}$$

$$\text{---------- (A2.34)}$$

Where a_1, b_1, c_1 and d_1 are given by equations (A2.28), (A2.29), (A2.5) and (A2.30). This leads to (2A.58) where:-

$$a = b = c = e = 0 \quad \text{---------- (A2.31)}$$

$$d = \frac{Km_3}{\epsilon_o^2}(-\frac{2}{3} + 2\epsilon_o) + \frac{Km_3\mu(-10 + 6\epsilon_o)}{3\epsilon_o(1-\epsilon_o)} - \frac{4K^2(\mu-1)}{3\epsilon_o^2} - \frac{K^3}{3\epsilon_o^2 m_3}(2 + 6\epsilon_o) +$$

$$+\frac{K^3\mu}{m_3\epsilon_o^2}\frac{(\frac{4}{3} + 2\epsilon_o - 2\epsilon_o^2)}{(1-\epsilon_o)} \quad \text{---------- (A2.35)}$$

$$f = \frac{2K^2 m_3}{3\epsilon_o^3}(1-7\epsilon_o) + \frac{16\mu K^2 m_3}{3\epsilon_o^2} + \frac{4K^3(1-4\epsilon_o)(\mu-1)}{3\epsilon_o^3} - \frac{4}{3}\frac{K^4\mu}{m_3\epsilon_o^3} +$$

$$+\frac{2}{3}\frac{K^4(1-\epsilon_o)}{m_3\epsilon_o^3} \qquad \text{- - - - - - - - - - - - - - - - -} \quad \text{(A2.36)}$$

Set 6: The solution of Clift, Grace and Weber (1973) reduces to the simplified form (cast into the dimensionless form used in this analysis):

$$\det \begin{bmatrix} (2K^2) & (m^2+K^2) \\ \left[\frac{R_{eF}}{Fr}\frac{1}{n} - \frac{R_{eF}n}{K} - \frac{2\rho\mu K}{(1-\epsilon_o)}\right] & \left[\frac{R_{eF}}{Fr}\frac{1}{n} - \frac{2\rho\mu m}{(1-\epsilon_o)}\right] \end{bmatrix} = 0 \qquad \text{- - - - -} \quad \text{(A2.37)}$$

$$\text{Where } m = \sqrt{K^2 + R_{eF}\frac{(1-\epsilon_o)\,n}{\rho\mu}} \qquad \text{- - - - - - - - - - - - -} \quad \text{(A2.38)}$$

This simplification can be made when $\mu \gg 1$ and $\rho \ll 1$, ie in most gas fluidised systems, but, as Clift, Grace and Weber point out 'for liquid fluidised beds, the simplified solution still gives a good indication of the most dangerous wavelength'.

This solution (A2.37, A2.38) is the same as that obtained by Bellman and Pennington (1954) for fluids of zero surface tension, with the upper fluid much more dense and more viscous than the lower fluid, and that obtained by Rice and Wilhelm (1958) for gas fluidised beds.

(A2.36) reduces to:

$$n^2\left(\frac{m^2}{K} + K\right) + n\left[\frac{2K(K-m)^2\rho\mu}{(1-\epsilon_o)R_{eF}}\right] + \frac{(K^2-m^2)}{Fr} = 0 \qquad \text{- - - - - -} \quad \text{(A2.39)}$$

which can then be solved with (A2.38).

(A2.2) Vertical Interface Between the Phases

A similar procedure is followed in the analysis of the stability of a vertical boundary (see section 4.3) and the solution yields: $\det [M] = 0$ - - - - - - - - - - - (4.7)

which leads to: $n^3(a) + n^2(b) + n(c) + d = 0$ - - - (4.8)

Where: 1) for boundary condition set 2;

$$[M] = \begin{bmatrix} 0 & 0 & (\epsilon_o) & (\epsilon_o) & -1 & -1 \\ (\frac{n}{K}) & 0 & (\epsilon_o) & (\epsilon_o) & (\frac{K}{m_3}) & 1 \\ -(\frac{\mu n}{(1-\epsilon_o)}) & (2\mu K) & 0 & 0 & (m_3 + \frac{K^2}{m_3}) & (2K) \\ \frac{\epsilon_o n - K}{\epsilon_o^2} & 0 & (2K) & (2K) & (m_3 + \frac{K^2}{m_3}) & (2K) \\ -\frac{4}{3}(\frac{\mu n}{(1-\epsilon_o)}) & a_1 & 0 & 0 & (-2K) & b_1 \\ \frac{4}{3}\frac{(\epsilon_o n - K)}{\epsilon_o^2} & \frac{R_{eF}(1-\epsilon_o)}{Fr.n} & (2K) & (2K - R_{ep}\frac{n}{K}) & (-2K) & b_1 \end{bmatrix}$$

- - - - - - (A2.40)

Where: $a_1 = 2\mu K + \frac{R_{eF}}{Fr}\frac{1}{n}$

$$b_1 = -2K + R_{eF}\frac{(n + \emptyset K)}{K} \quad \text{- - - - - - - - - - - - - - - (A2.41)}$$

(4.9) gives: $a = R_{eF}\left[\frac{m_3}{K^2} + \frac{1}{K\epsilon_o} - \frac{(1-\epsilon_o)}{m_3\epsilon_o}\right]$ - - - - - - - (A2.42)

$$b = -2m_3 - 4K\frac{(1-\epsilon_o)}{\epsilon_o} + \frac{2K^2(2-\epsilon_o)}{m_3\epsilon_o} + \frac{2}{3}\frac{\mu}{(1-\epsilon_o)}\left(m_3 + K\frac{(1-\epsilon_o)}{\epsilon_o} - \frac{K^2}{m_3\epsilon_o}\right) +$$

$$+ R_{eF}\left[\frac{m_3\phi}{K} + \frac{(1+\phi\epsilon_o)}{\epsilon_o^2} + \frac{K}{m_3}\frac{(1-\phi\epsilon_o+\phi\epsilon_o^2)}{\epsilon_o^2}\right] \quad \text{------} \quad \text{(A2.43)}$$

$$c = \frac{2}{\epsilon_o^2}\left[Km_3 - \frac{K^3}{m_3}\right] + \frac{R_{eF}\phi}{\epsilon_o^2}\left[K + \frac{K^2}{m_3}\right] - \frac{R_{eF}}{Fr(1-\epsilon_o)}\left[\frac{m_3}{K} + \frac{(1-\epsilon_o)}{\epsilon_o} - \frac{K}{\epsilon_o m_3}\right] +$$

$$+ \frac{R_{eF}}{Fr\mu\epsilon_o}\left[\frac{K}{m_3} - 1\right] \quad \text{----------} \quad \text{(A2.44)}$$

$$d = \frac{R_{eF}}{Fr\mu\epsilon_o^2}(m_3 - K) \quad \text{----------} \quad \text{(A2.45)}$$

2) For boundary condition set 6, (4.8) gives (in the dimensionless form used in this analysis):

$$[M] = \begin{bmatrix} (1 + \frac{Frn}{\epsilon_o}) & 1 & -1 & -1 \\ (1 + Frn) & (m) & (K) & (\ell) \\ (2\mu K^2) & (\mu(m^2 + K^2)) & (-2K) & (-K^2 - \ell^2) \\ a_1 & b_1 & c_1 & (-2\ell) \end{bmatrix}$$

$$\text{--------} \quad \text{(A2.46)}$$

Where $a_1 = (\rho + 1)\frac{(1-\epsilon_o)}{n}\frac{R_{eF}}{Fr} - (1-\epsilon_o)\frac{n}{K}R_{ep} - 2\mu K$ --- (A2.47)

$$b_1 = (\rho + \frac{m}{K})\frac{(1-\epsilon_o)}{n}\frac{R_{eF}}{Fr} - 2\mu m \quad \text{---------} \quad \text{(A2.48)}$$

$$c_1 = - R_{eF} \left(1 + \frac{n}{K}\right) - 2K \qquad \text{(A2.49)}$$

and ℓ and m are given by:

$$\ell^2 - \phi R_{eF} \ell - R_{eF} n - K^2 = 0 \qquad \text{(A2.50)}$$

$$m^2 - K^2 - (1-e_o) \frac{R_{ep} n}{\mu} = 0 \qquad \text{(A2.51)}$$

This could, of course, be expanded in the normal manner to give equation (4.8), but this was found to be impractical, as the computer solution did not converge. The determinant was therefore expanded in full and the resulting expression was solved on a digital computer using a minimising routine.

APPENDIX 3: COMPARISON WITH THE STABILITY OF THE STATE OF HOMOGENEOUS FLUIDISATION

To compare the stability of a horizontal interface in a fluidised bed with the stability of the state of homogeneous fluidisation as given by Anderson and Jackson (1967), the general solution to the equations of motion (equations (2A.21) to (2A.20)) is written in the complex form analogous to that used by them. That is:-

$$\epsilon = A \exp(-ikx - iky + nt) \qquad \text{(A3.1)}$$

$$V_x = B \exp(ikx - iky + nt) \qquad \text{(A3.2)}$$

$$V_y = B \exp(-ikx - iky + nt) - \frac{n}{ik(1-\epsilon_o)} A \exp(-ikx - iky + nt) \qquad \text{(A3.3)}$$

$$U_x = C \exp(ikx - iky + nt) + D \exp(ikx - iky + nt) \qquad \text{(A3.4)}$$

$$U_y = C \exp(-ikx - iky + nt) + D \exp(-ikx - iky + nt) + \frac{(\epsilon_o n - ik)}{i\epsilon_o^2 K} A \exp(-ikx - iky + nt) \qquad \text{(A3.5)}$$

$$P_2 = \frac{Frn}{ik} D \exp(-ikx - iky + nt) \qquad \text{(A3.6)}$$

$$W_x = E \exp(ikx + im_3 y + nt) + F \exp(ikx + iky + nt) \qquad \text{(A3.7)}$$

$$W_y = -\frac{K}{m_3} E \exp(-ikx + im_3 y + nt) - F \exp(-ikx + iky + nt) \qquad \text{(A3.8)}$$

$$P_3 = \frac{Fr}{ik}\left(n + ik + \frac{2K^2}{R_{ep}}\right) F \exp(-ikx + iky + nt) \qquad \text{(A3.9)}$$

Where m_3 is given by:

$$m_3^2 + iR_{eF} m_3 + R_{eF} n + K^2 = 0 \qquad \text{(A3.10)}$$

and R_{ep} is now given by: $R_{ep} = \frac{\rho_b d_p U_o}{\mu F}$

with $\rho_b = (1-\epsilon_o)\,\rho_p + \epsilon_o\,\rho_F$, as the support fluid now has the parameters of the generalised homogeneous fluidised phase.

n is the complex growth rate, $n = \xi - i\eta$

This particular solution to the dimensionless, perturbed equations of motion is derived from a general solution in the same way as in the simpler solution (see Appendix 1), and is valid only at x = 0. However, as the solution is sinusoidal in x, it is assumed that the solution at x = 0 is also approximately valid for all other x.

This solution is then substituted into the boundary conditions (set 2 is used, that is, equations (2A.42a), (2A.43) and (2A.50) for the 'unstable' configuration; support fluid below the fluidised phases, seetion 2A.3), where in equation (2A.50), the stress defined for the support fluid now has the physical parameters of the generalised homogeneous phase.

This gives: $[M]\,[A\ B\ C\ D\ E\ F]^T = 0$ - - - - - - - - - - - - - - - - (A3.11)

Where M is a 6 x 6 matrix of coefficients.

The non-trivial solution is then: $\det [M] = 0$ --- - - - - - - (A3.12)

which leads to:

$n^3(a) + n^2(b + ic) + n(d + ie + if) + g = 0$ --- - - - - - - (A3.13)

[Note the 'stable' configuration, support fluid uppermost, reduced to

$n^3(a) + n^2(-\,b + ic) + n(d + ie - if) + g = 0$ - - - - - - - - - (A3.13a)

and although this has not been solved, one would expect similar results, as both configurations should be the same].

Where:

$$[M] = \begin{bmatrix} 0 & 0 & (\epsilon_o) & (\epsilon_o) & -1 & -1 \\ (\frac{n}{ik}) & 0 & (\epsilon_o) & (\epsilon_o) & (\frac{K}{m_3}) & 1 \\ -(\frac{\mu n}{(1-\epsilon_o)}) & (2\mu iK) & 0 & 0 & (im_3+\frac{iK^2}{m_3}) & (2iK) \\ \frac{(\epsilon_o n-iK)}{\epsilon_o^2} & 0 & (2iK) & (2iK) & (im_3+\frac{iK^2}{m_3}) & (2iK) \\ a_1 & b_1 & 0 & 0 & (2iK) & c_1 \\ d_1 & \frac{R_{ep}(1-\epsilon_o)}{Fr\ n} & (-2iK) & \frac{(-2iK+R_{ep}n)}{iK} & (2iK) & c_1 \end{bmatrix}$$

---------- (A3.14)

Where: $a_1 = \frac{4}{3}\frac{\mu n}{(1-\epsilon_o)} - \frac{R_{ep}}{Fr}\frac{1}{iK(1-\epsilon_o)}$ ---------- (A3.15)

$$b_1 = -2\mu iK + \frac{R_{ep}}{Fr}\frac{1}{n} \quad \text{---------- (A3.16)}$$

$$c_1 = 2iK - \frac{R_{ep}}{iK}\left(n + iK + \frac{2K^2}{R_{ep}}\right) \quad \text{---------- (A3.17)}$$

$$d_1 = \frac{-R_{ep}}{Fr\ iK} - \frac{4}{3}\frac{(\epsilon_o n - iK)}{\epsilon_o^2} \quad \text{---------- (A3.18)}$$

and in (A3.13):-

$$a = R_{ep}\left[\frac{m_3}{K^2} + \frac{1}{\epsilon_o K} - \frac{(1-\epsilon_o)}{\epsilon_o m_3}\right] \quad \text{---------- (A3.19)}$$

$$b = \frac{2K(1-2\epsilon_o)}{\epsilon_o} - \frac{2K^2}{\epsilon_o m_3} + \frac{2}{3}\frac{\mu}{(1-\epsilon_o)}\left[- m_3 - K(1-\epsilon_o) + \frac{K^2}{\epsilon_o m_3}\right]$$

---------- (A3.20)

$$c = R_{ep}\left[\frac{m_3}{K} + \frac{(1+\epsilon_o)}{\epsilon_o^2} + \frac{K}{m_3}\frac{(1-\epsilon_o+\epsilon_o^2)}{\epsilon_o^2}\right] \quad ---------- \quad (A3.21)$$

$$d = R_{ep}\left[- \frac{K}{\epsilon_o^2} - \frac{K^2}{\epsilon_o^2 m_3}\right] \quad ---------- \quad (A3.22)$$

$$e = \frac{R_{ep}}{Fr}\left[\frac{- m_3}{K(1-\epsilon_o)} - \frac{1}{\epsilon_o} + \frac{K}{m_3\epsilon_o(1-\epsilon_o)} + \frac{1}{\mu}\left[\frac{1}{\epsilon_o} - \frac{K}{\epsilon_o m_3}\right]\right] \quad --- \quad (A3.23)$$

$$f = - \frac{2Km_3}{\epsilon_o^2} - \frac{2K^2}{\epsilon_o^2} \quad ---------- \quad (A3.24)$$

$$g = \frac{R_{ep}}{Fr\mu\epsilon_o^2}(m_3 - K) \quad ---------- \quad (A3.25)$$

The solution of equation (A3.13) with equation (A3.10) gives the characteristic form of the growth rate vrs wave number curve, that is, there is a maximum of ξ (real n) corresponding to the most rapidly growing or 'most dangerous' wavelength.

Values of ξ max with their corresponding η and K are given in Table 5, with the equivalent solutions due to Anderson and Jackson (1967), 1968), for different physical systems.

APPENDIX 4: FREQUENCY OF TWO-DIMENSIONAL BUBBLE FORMATION FROM AN ORIFICE

Repeating the theory of Davidson and Harrison (1963) in two dimensions.

The bubble is initially centred at the orifice, but because of bouyancy, tends to rise, so that at any instant the centre has risen a distance, s. It is assumed that the bubble detaches when the base reaches the orifice, ie when bubble radius r = s.

For a constant gas flow rate, G, the bubble volume at time, t, is

$$V_b = \pi r^2 \delta = Gt \qquad \text{(A4.1)}$$

Where δ = the two dimensional bubble thickness.

For the forming bubble, the rate of change of upward momentum is equal to the bouyancy force, thus

$$\rho_F \cdot V_b \cdot g = \frac{d}{dt}\left(\tfrac{1}{2} \rho_F V_b \frac{ds}{dt}\right) \qquad \text{(A4.2)}$$

Substitution of (A4.1) into (A4.2) and integrating twice gives:

$$s = \tfrac{1}{2} g t^2 \qquad \text{(A4.3)}$$

with $\frac{ds}{dt} = s = 0$ at $t = 0$.

At detachment, r = s, (A4.1) and (A4.3) give:

$$\text{time of formation, } t, = \left(\frac{1}{g}\right)^{2/3} \left[\frac{4G}{\pi\delta}\right]^{1/3} \qquad \text{(A4.4)}$$

$$\text{Volume at formation, } V_b = \left(\frac{1}{g}\right)^{2/3} \left(\frac{4}{\pi\delta}\right)^{1/3} G^{4/3} \qquad \text{(A4.5)}$$

$$\text{Frequency of formation, } f = \frac{G}{V_b} = g^{2/3} \left(\frac{\pi\delta}{4}\right)^{1/3} \frac{1}{G}1/3 \qquad \text{(A4.6)}$$

In the case under consideration, the bed thickness, and thus the bubble thickness, δ = 1.5 cm.

NOTATION

A, B, C, D, E, F - constants in the wavelike solution to the equations of motion.

a, b, c, d, e, f - coefficients in the solution of det M = 0 given in Appendix 2.

a_1, b_1, c_1, d_1 - terms of the matrix M, given in Appendix 2.

A^1 - initial disturbance on the boundary.

d_b - bubble diameter.

d_p - particle diameter.

D_b - slug width (asymptotic).

D_s - slug depth.

$F_{x,y}$ - general force term in equations (2A.6) (2A.9).

F - Froude number, $\frac{V}{(gR)^{\frac{1}{2}}}$

F_1 - corrected Froude number.

F_2 - corrected Froude number (equation 5.7).

Fr - Froude number, $\frac{U_o^2}{gdp}$

f - frequency of bubble formation.

g - acceleration due to gravity.

G - flow rate of injected gas.

i - $\sqrt{-1}$

K - wave number of the disturbance.

m - exponent in the solution to the equations of motion.

M - matrix in the solution using the boundary conditions. Given in Appendix 2.

N - exponent in the drag coefficient relationship.

N_f - criterion due to Doitchev, defined by equation (2D.4).

n - growth rate of the disturbance.

P - pressure.

r - bubble radius.

R - half width of the slug.

R_{ef} - Reynold's number, $\frac{\rho_F . d_p . U_o}{\mu_F}$

R_{ep} - Reynold's number, $\frac{\rho_p . d_p . U_o}{\mu_F}$

s - height of bubble centre above orifice.

t - time.

U_b - bubble velocity.

U_o - minimum fluidising velocity.

U_t - particle terminal velocity.

$U_{x,y}$ - interstitial fluid superficial velocity.

V - instantaneous velocity of vertex of disturbance.

V_b - bubble volume.

$V_{x,y}$ - particle phase superficial velocity.

$W_{x,y}$ - support fluid superficial velocity.

x - horizontal direction.

y - vertical direction.

$\beta(\epsilon)$ - drag coefficient.

Υ - dimensionless time ratio, τ_2/τ_1

δ - thickness of two dimensional bed.

ϵ - voidage fraction.

η - the perturbed boundary.

or η - imaginary part of complex growth rate, as defined by Anderson and Jackson. Equation (2C.2).

or η - as defined by the dimensionless equations of Layzer. Equation (5.4).

λ - wavelength of the disturbance.

μ - dimensionless viscosity group, μ_P/μ_F.

μ_F - viscosity of the fluid phases.

μ_P - viscosity of the particulate phase.

ξ - real part of complex growth rate as defined by Anderson and Jackson. Equations (2C.1).

or ξ - as defined by the dimensionless equations of Layzer. Equation (5.3).

ρ - dimensionless density, ρ_F/ρ_P.

ρ_F - density of the fluid.

ρ_P - density of the particles.

σ - normal and tangential stress.

σ_T - surface tension.

τ_1 - time for the disturbance to grow through the bubble.

τ_2 - time for the disturbance to be swept around the bubble.

ϕ - ratio of the superficial fluid velocity in the channel to the minimum fluidising velocity.

Subscripts

0 - at the minimum fluidising velocity.

1 - particle phase.

2 - interstitial fluid phase.

3 - support fluid phase.

F - interstitial fluid phase.

P - particle phase.

SF - support fluid phase.

x - in the x (horizontal) direction.

y - in the y (vertical) direction.

REFERENCES

ANDERSON, T B; BRYDEN, J O
(1965) 'Viscosity of a liquid fluidised bed'.
Dept of C E Report. University of Edinburgh.

ANDERSON, T B; JACKSON, R
(1967) Ind and Eng Chem (Fund) 6, 527.

ANDERSON, T B; JACKSON, R
(1968) ibid 7, 12.

ANDERSON, T B; JACKSON, R
(1969) ibid 8, 137.

BELLMAN, R; PENNINGTON, R H
(1954) Quart Appl Math 12, 151

CHIBA, T; TERASHIMA, K; KOBAYASHI, H
(1972) Chem Eng Sci 27, 965

CLIFT, R; GRACE, J R
(1972) Chem Eng Sci 27, 2309

CLIFT, R; GRACE, J R; WEBER, M E
(1973) Unpublished work

DAVIDSON, J F
(1961) Trans Inst Chem Eng 39, 230

DAVIDSON, J F; HARRISON, D
(1963) 'Fluidised Particles'.
Cambridge University Press, p50

DAVIDSON, J F; HARRISON, D
(1963a) ibid p26

DAVIDSON, J F; HARRISON, D; de KOCK, J W
(1961) Trans Inst Chem Eng 39, 202

DAVIES, R M; TAYLOR, G I
(1950) Proc Roy Soc A200, 375

van DEEMTER, J J; van der LAAN, E T
(1961) App Sci Res A10, 102

DOITCHEV, K
(1973) Unpublished Work.

DUMITRESCU, D T
(1943) Z Angew Math Mech 23, 139

FAKHIMI, S; HARRISON, D
(1970) Proc of 'Chemica '70' Butterworths of Australia, p29

FERMI, E
(1951) Doc No AECU 2979; paper no 244 in collected works. Univ of Chicago Press

FURUKAWA, J; OHMAE, T
(1958) Ind Eng Chem 50, 821

GODARD, K; RICHARDSON, J F
(1969) Can Jrnl Chem Eng 47, 350

GODARD, K; RICHARDSON, J F
(1969a) Chem Eng Sci 24, 194

GRIFFITH, P
(1963) ASME Paper 63-HT-20. Natl Ht Trans Conf Boston, Mass

HAGYARD, T; SACERDOTE, A M
(1966) Ind Eng Chem Fund 5, 500

HARGREAVES, J; PYLE, D L
(1972) Chem Eng Sci 27, 433

HASSET, N J
(1961) Brit Chem Eng 6, 777

HETZLER, R; WILLIAMS, M C
(1969) Ind Eng Chem Fund 8, 668

HINZE, J O
(1962) App Sci Res A11, 33

JACKSON, R
(1963) Trans Inst Chem Eng 41, 13

JACKSON, R
(1963a) ibid 41, p 22

JACKSON, R
(1969) Chem Eng Prog Symp series 66, no 105, p3

JONES, B R E
(1970) PhD Thesis, University of London

LEFROY, G A; DAVIDSON, J F
(1969) Trans Inst Chem Eng 47, 120

LEVA, M
(1959) 'Fluidisation' McGraw Hill, NY p24

LEVICH, V G
(1962) 'Physicochemical Hydrodynamics' Prentice Hall p453

LEVICH, V G
(1962a) ibid p630

LAYZER, D (1955) The Astrophysical Jrnl. 122, 1

MATHESON, G L; HERBST, W A; HOLT, P H
(1949) Ind Eng Chem 41, 1099

MATHUR, K B
(1971) In 'Fluidisation' ed J F Davidson and D Harrison. Academic Press ch 17

MOLERUS, O
(1967) 'Int Symp on Fluidisation' ed A A H Drinkenburg Netherlands Univ press p 134

MURRAY, J D
(1965) Jrnl Fluid Mech 21, 465

MURRAY, J D
(1965a) ibid 22, 57

MURRAY, J D
(1966) US Public Health Service Grant AP00455-01. Report No 1

PIGFORD, R L; BARON, T
(1965) Ind Eng Chem Fund 4, 81

PYLE, D L; ROSE, PL
(1965) Chem Eng Sci 20, 25

RICE, W J; WILHELM, R H
(1958) Ame Inst Chem Eng Jrnl 4, 423

RICHARDSON, J F; ZAKI, W N
(1954) Trans Inst Chem Eng 32, 35

ROMERO, J B; JOHANSON, L N
(1962) Chem Eng Prog Symp Series 58, (38), 28

ROWE, P N
(1971) in 'Fluidisation' ed J F Davidson and D Harrison, Academic Press ch 4

RUCKENSTEIN, E; TZECULESCU, M
(1967) 'Int Symp on Fluidisation' ed A A H Drinkenburg, Netherlands Univ Press p180

SCHUGERL, K
(1971) in 'Fluidisation' ed J F Davidson and D Harrison Academic Press ch 6.

SCHUGERL, K; MERZ, M; FETTING, F
(1961) Chem Eng Sci 15, 1

SLIS, P L; WILLEMSE, Th W; KRAMERS, H
(1959) Appl Sci Res A8, 209

STEWART, P S B; DAVIDSON, J F
(1967) Powder Tech 1, 61

TAYLOR, G I
(1950) Proc Roy Soc (London) A201, 192

VOLPICELLI, G
(1967) 'Int Symp on Fluidisation'. ed A A H Drinkenburg, Netherlands Univ Press p 189

WALLIS, G B
(1969) 'One-dimensional two-phase flow' McGraw Hill NY

WILHELM, R H; KWAUK, M
(1948) Chem Eng Prog 44, 201

ZENZ, F A
(1968) Proc of Symp at Tripartite Chem Eng Conf, Inst Ch E Symp Series p136